CaviTAU®

TRANSALVEOLAR ULTRASOUND SONOGRAPHY

www.cavitau.de

1. Ist CaviTAU® validiert?

Dieser QR-Code öffnet 2 Publikationen zur wissenschaftlichen Validierung von CaviTAU® in deutschen Abtracts und freien PDF-Downloads.

2. Bringt CaviTAU® Patientennutzen in der Praxis?

Dieser QR-Code öffnet 2 Publikationen zur wissenschaftlichen Falldarstellung von CaviTAU®.

3. Sind die Untersuchungen zu RANTES/CCL5 in Knochenmarksdefekten im Kiefer validiert?

Dieser QR-Code öffnet alle 15 wissenschaftlichen Publikationen von Dr.Dr. (PhD-UCN) J. Lechner in deutschen Abtracts und freien PDF-Downloads.

4. Gibt es wissenschaftliche Publikationen zur Toxizität von endodontisch behandelten Zähnen?

Dieser QR-Code öffnet 2 Publikationen zur wissenschaftlichen Validierung von OroTox®.

CaviTAU® | Grünwalder Str. 1 | 81547 München | Fon: +49 89 244 15 44 60 | Fax: +49 89 244 15 44 69
E-Mail: office@cavitau.de | www.cavitau.de

Clinical, Cosmetic and Investigational Dentistry

Dovepress

open access to scientific and medical research

Open Access Full Text Article

ORIGINAL RESEARCH

Ultrasound Sonography to Detect Focal Osteoporotic Jawbone Marrow Defects: Clinical Comparative Study with Corresponding Hounsfield Units and RANTES/CCL5 Expression

This article was published in the following Dove Press journal:
Clinical, Cosmetic and Investigational Dentistry

Johann Lechner[1]
Bernd Zimmermann[2]
Marlene Schmidt[3]
Volker von Baehr[4]

[1]Department of Clinical Research, Clinic Integrative Dentistry, Munich, Germany; [2]Medical Devices, QINNO, Wessling, Germany; [3]Department of Statistics, STEYR Motorenwerke, Steyr, Austria; [4]Department of Immunology and Allergology, Institute for Medical Diagnostics Berlin, Germany

Introduction: The presently used impulse echo ultrasound examination is not suitable to provide relevant and reliable information about the jawbone, because ultrasound (US) almost completely reflects from the hard cortical jawbone. At the same time, "focal osteoporotic bone marrow defects" (BoneMarrowDefects = BMD) in jawbone are the subject of scientific presentations and discussions.

Purpose: Can a newly developed trans-alveolar ultrasonic sonography (TAU-n) device locate and ascertain BMD?

Patients and Methods: TAU-n consists of a two-part handpiece with an extraoral ultrasound transmitter and an intraoral ultrasound receiver. The TAU-n computer display shows the different jawbone densities with corresponding colour coding. The changes in jawbone density are also displayed numerically. The validation of TAU-n readings: A usual orthopantomogram (2D-OPG) on its own is not suitable for unequivocally determining jawbone density and has to be excluded from this validation. For validation, a 3D-digital volume tomogram/cone beam computer tomogram (DVT/CBCT) with the capacity to measure Hounsfield units (HU) and a TAU-n are used to determine the presence of preoperative BMD in 82 patient cases. Postoperatively, histology samples and multiplex analysis of RANTES/CCL5 (R/C) expression derived from surgically cleaned BMD areas are evaluated.

Results: In all 82 bone samples, DVT-HU, TAU-n values and R/C expressions show the presence of BMD with chronic inflammatory character. However, five histology samples showed no evidence of BMD. All four evaluation criteria (DVT-HU, TAU-n, R/C, histology) confirm the presence of BMD in each of the 82 samples.

Conclusion: The TAU-n method almost completely matches the diagnostic reliability of the other methods. The newly developed TAU-n scanner is a reliable and radiation-free option to detect BMD.

Keywords: trans-alveolar ultrasonography, cone beam computed tomography, RANTES/CCL5, Hounsfield units, cavitational osteonecrosis of jawbone

Introduction

In medicine, impulse echo ultrasound is generally used for all kinds of tissue imaging. In principle, body structure images are generated by analyzing the reflection of ultrasound waves. In a recent systematic review and meta-analysis, the possible use of ultrasonography for evaluating masseter muscles in orthodontic or functional orthopedic treatment was published.[1] However, this method is not suitable to provide

Correspondence: Johann Lechner
Tel +49-89-6970129
Fax +49-89-6925830
Email drlechner@aol.com

submit your manuscript | www.dovepress.com
DovePress
http://doi.org/10.2147/CCIDE.S247345

medically relevant information about the status of jawbone, because ultrasound is almost completely reflected at the border between bone and soft tissue. In particular, the cancellous part of the jawbone cannot be examined with a commonly used ultrasound. Therefore, ultrasound is only of limited use in dentistry despite "focal osteoporotic bone marrow defects (BMD)" being the subject of scientific papers and discussion.[2,3] Why is their detection necessary for dentists and doctors alike? The condition of the cancellous jawbone can be of great clinical importance. Bouquot has proven that cancellous bone can be largely degenerated. A phenomenon he calls "aseptic ischemic osteonecrosis of jawbone" (AIOJ), which leads to "cavitations". He relates this osteonecrosis of the jawbone to neuralgic pain and defines a disease called "neuralgia inducing cavitation osteonecrosis (NICO)."[4] For the first time, the authors recommend the use of an ultrasound device[5] to detect these lesions. With respect to the conspicuous morphology, we proposed the term "fatty-degenerative osteonecrosis/osteolysis of jawbone" (FDOJ) for this cavitational osteonecrosis,[6,7] additionally to the term of AIOJ. According to publications by AI-Nawas, the status of the cancellous jawbone is of utmost importance for the success of dental implants.[8,9] A major problem, however, is that jawbone with BMD/AIOJ/FDOJ often appears without abnormal findings in x-rays.[10]

Objectives and Questions

This paper presents the latest diagnostic possibilities to measure jawbone density with a new device used in dentistry for trans-alveolar ultrasound sonography (TAU). The new equipment TAU-n calls for clarification whether the measured TAU-n values are reliable and if they correctly reflect clinical states of focal bone marrow defects (AIOJ/BMD/FDOJ). Is TAU-n outcome prediction performance enough?

Materials and Methods

A New Trans-Alveolar Ultrasonography Device

To overcome the previously mentioned challenges, a different approach was necessary. Using innovative trans-alveolar ultrasonic pulses (TAU), the newly developed TAU-n is capable of detecting and locating these cavitations up to the fatty-degenerative dissolution of the medullary trabecular structures in jawbone. The TAU-n device generates an ultrasonic pulse and guides the pulse through the entire jawbone. The pulse is then recorded and measured by an ultrasound receiver. This pulse is generated by an extraoral transmitter and detected and measured by a receiving unit positioned intraorally. Both parts (ie transmitter and receiver) are parallel fixed in a single handpiece. The size of the TAU-n receiver unit is designed for easy insertion into the patient's mouth. The jawbone must be positioned between the two parts of the measuring unit. The acoustic coupling between transmitter and receiver and the alveolar ridge is achieved using a semi-solid gel. The contact between the extraoral transmitter and the intraoral receiver (Figure 1) is optimized by the use of a special ultrasound gel pad specially developed for this purpose. The results are displayed on a color screen, which shows different colors depending on the degree of attenuation of the ultrasound pulse. Attenuation of the pulse amplitude indicates pathological changes in the jawbone. Each organ and each organ structure show a highly individual attenuation behavior depending on its physiological state. Corresponding values are based on the published data by Wells[11] and Njeh.[12] They are only guiding values due to biological fluctuation.

Display of TAU-n

The TAU-n display can detect the following physical structures in the dentoalveolar and maxillary sinus region, with corresponding color codes from 91 color columns per cm2. Figure 2 assigns the coloring of TAU-n in a left lower jaw area (area 37, 38 and 39/European coding).

- Green or white/light blue = extremely dense and hard structures such as teeth, implants and crowns; solid bone in marginal cortical region; = healthy medullar spongial bone; air components in oral and maxillary sinuses
- Yellow/blue = fatty nerve structures

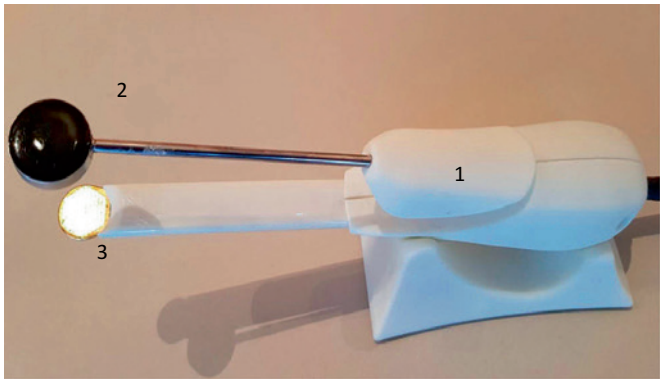

Figure 1 (1) Handpiece with ultrasonic transmitter and receiver unit. (2) Ultrasonic transmitter, (3) Ultrasonic receiver with coplanar and fixed arrangement of transmitter and receiver.

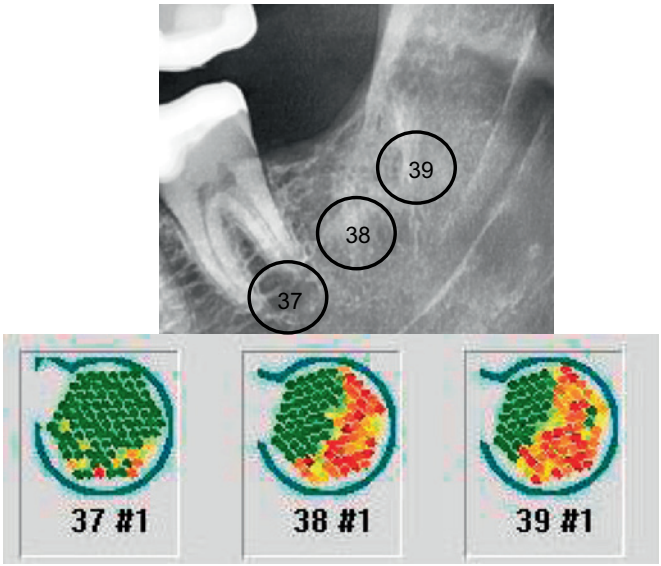

Figure 2 Example of 2D coloring in TAU-n in area 37 = GREEN = solid bone. Area 38 = RED = reduced bone density = fatty-degenerative parts. Retromolar area 39 = RED= decreased bone density = fatty-degenerative parts.

- Red or black/dark blue = chronically inflammatory medullary-spongial bone with fatty-degenerative components

Numerical Bone Density Determination with TAU-n

The TAU-n software numerically displays the attenuation coefficients of the TAU-n measuring range. By clicking on one of the 91 sensor fields the software marks the field and displays the measured value in a logarithmic evaluation. The cells to be evaluated are selected and highlighted with a mouse click. The display shows the number of marked cells, the resulting mean value and the corresponding color. TAU-n calculates the logarithmic mean value of the sum of the lowest sensor elements as "mean value (log)" in RED. The logarithmic mean value of the highest sensor elements is also displayed in GREEN – corresponding to the reduced attenuation by a fixed structure (see Figures 3, 4 and 5).

The TAU-n software thus allows the mean value to be calculated over a freely selectable cell range of the 91 piezoelectric sensors. The averaging is logarithmic: The meaning of logarithmic averaging is that the color change to green already occurs at relatively small values (eg 3); however, the value range goes up to a total of 100. This means that green fields are much more important than red fields with linear averaging. Example: A green field with value 100 and 10 red fields with value 1 are marked. The linear average results in (100 + 10*1)/11 = 10, which averages the colour green. With logarithmic averaging, the logarithms of the values are averaged and the exponential value shown: log10(100) = 2, log10(1) = 0 would be the average value of the logarithms (2 + 10*0)/11 = 0.18. The exponential value is then 10^0.18 = 1.52. This would show red to orange.

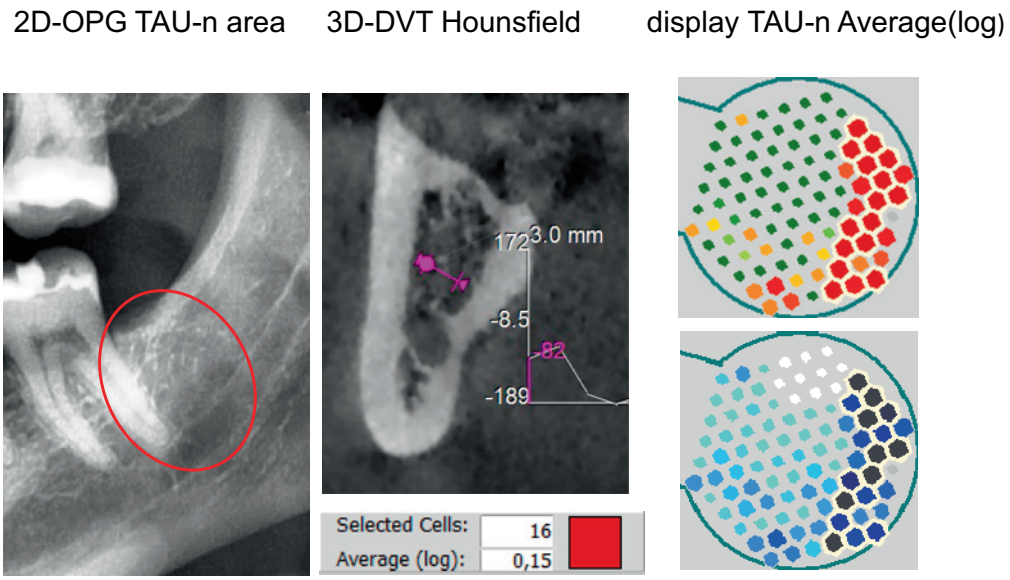

Figure 3 The top right picture shows a clear division into two parts: The right part, which points distally when the TAU sensor is inserted, corresponds with the strong red coloration to a high attenuation and thus reduced bone density with possible osteolysis. The clear distinction from red to green shows that the distal root of tooth 37 was detected in the mesial part of the sensor. In TAU-n, hard substance with low attenuation is marked with green or light-blue to white. The sensor fields marked white-blue to black in the lower right image allow an even more detailed interpretation of the attenuation. Both TAU-n measurement images correspond with the HU value of −8.5 in the edentulous are of 38 shown in the center part of Figure 3.

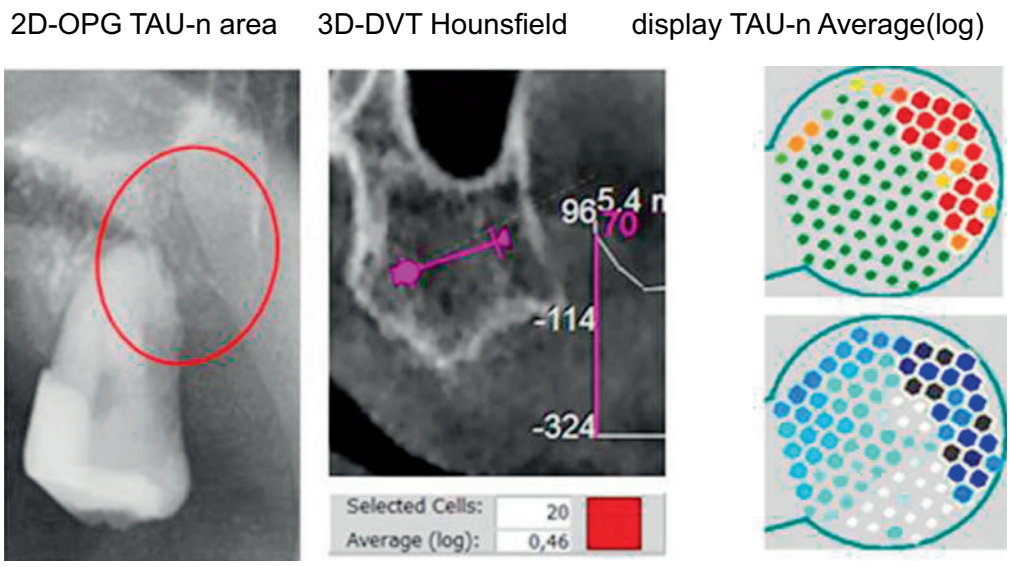

Figure 4 Reduced bone density in HU and TAU-n in the maxillary area 28 corresponding to the area of BMD/AIOJ/FDOJ.

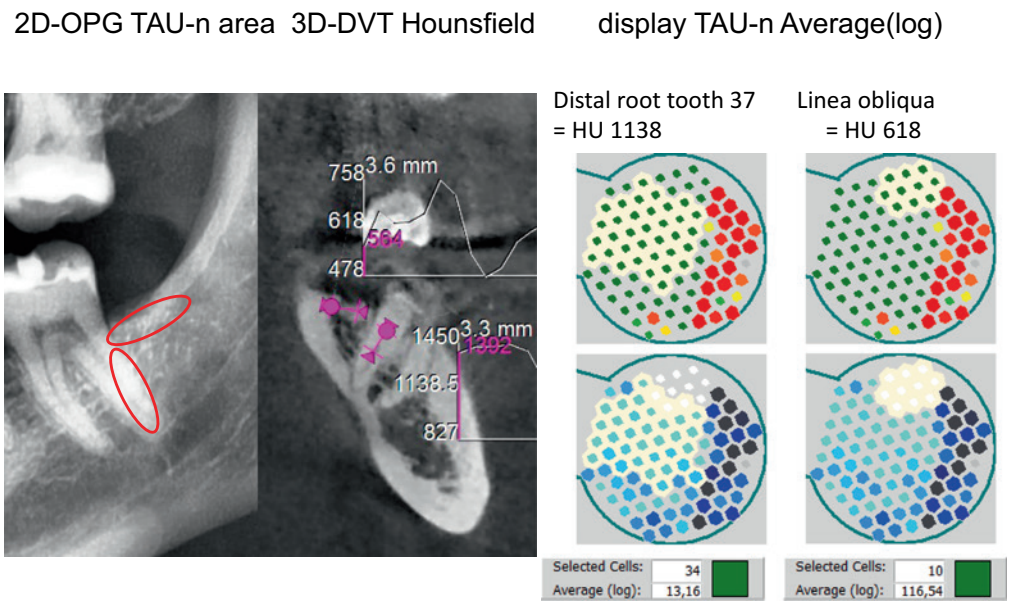

Figure 5 Two areas of increased density: The distal root of tooth 37 and the cortical density of oblique line as the upper rim of area 38. The left image marks the two measuring areas with red circles and with HU values of +1138 for the root portion and +618 for the oblique line. Average(log) of these two very radiopaque areas are in TAU-n 13 and 116 and thus in green.

Methods for Validation of TAU-n Measurements

How reliable are these measurements? To answer this question, we compare four parameters. Two options for the pre-operative diagnosis of AIOJ/BMD/FDOJ:

1. Digital Volume Tomography (DVT)/CBCT (Cone beam computed tomography/CBCT) with the option of HU measurement.

2. Use of TAU-n as a novel radiation-free option for bone density measurement

Two options for post-op confirmation or failure of pre-operative 1) and 2):

3. Histology findings of operated jawbone samples.

4. Multiplex analysis of the RANTESS/CCL5 (R/C) expression of operated jawbone samples as proof or disprove of inflammation.

Two-Dimensional X-Ray with Orthopantomogram

Since the occurrence and phenomena of AIOJ, FDOJ and BMD are practically undetectable in any type of X-ray

examination, they are largely unknown, widely controversial or even disputed.[10] The existence of BMD/AIOJ/FDOJ has been predominantly ignored in mainstream dentistry. The reason is that conventional two-dimensional X-ray techniques with orthopantomograms (OPG) are only able to visualize areas affected by BMD/AIOJ/FDOJ to a limited extent.[11] 2D-OPG is then useful when there is a mix of osteolysis and osteosclerosis apparent.[12] At the same time, a significant loss of bone mineral (30–50%) is required before it becomes visual on the OPG.[13,14] In view of these diagnostic difficulties, BMD/AIOJ/FDOJ is often underdiagnosed by dentists.[14] In 2D-OPG pathological changes can be completely absent without pathognomonic radiological findings pointing to AIOJ/BMD/FDOJ. The same applies to the reduced mineralization of BMD/AIOJ/FDOJ.[15] Even months after tooth removal or spontaneous tooth loss, the cortical walls of the alveoli remain intact without showing progressive destruction due to progressive osteolysis.[16] Consequently, we did not integrate the use of 2D-OPG in the pre-operative diagnosis of BMD/AIOJ/FDOJ.

Three-Dimensional X-Ray with Digital Volume Tomography

Modern X-ray methods like DVT/CBCT allow the clinician to perform a three-dimensional assessment of the jawbone with the determination of X-ray attenuation coefficients expressed in Hounsfield units (HU).[17,18] SimPlant software bone density measurements performed in the posterior mandible (3D Diagnostix, Boston, MA, USA) showed a mean CT value of 669.6 HU.[19] Further investigations classified the cancellous bone density of the jaw bone into five categories, with the worst bone density for a normal jaw bone being <150 HU (Class 5). Therefore, the HU values generated in our study (range: <150 to −370) show osteolysis of the jawbone for Class 5 cases.[20] The device used by our team for DVT diagnosis was an orange 3D PaX-i3D Duo Multi X-ray, which displays HU values over a freely selectable jaw distance. In X-ray technology, the HU scale is generally scientifically recognized for assessing bone density.[17–20] The values are assigned to physical states and tissues. The HU scale starts at −1000 for the damping coefficient of air, for fat it is −120, for healthy cancellous bone at +300 to +400 and for cortical bone at +1800 to over +2000. By definition the HU for water = 0.

For HU measurement we have a DVT from Orangedental PaX-i3D Duo 3D Multi X-ray unit 3D with corresponding software for evaluation of HU at our disposal. In accordance with DIN 6868–57, the availability of the viewing monitors with a contrast of >40:1, a brightness of at least 120 cd/m2 and a DICOM characteristic was maintained. Our device displays the mean value of an optically freely selected measurement path with the maximum and minimum values as a curve (see Figures 3, 4 and 5).

Bone Density Comparison: Hounsfield Units versus TAU-n

Example 1: Measuring Reduced Bone Density with HU and TAU-n in Mandible

Figure 3 shows in the left picture the TAU-n measuring range of area 38 with inconspicuous X-ray structure in 2D-OPG; the picture in the center shows in cross-section the DVT at this point with the HU attenuation coefficient at a level of −8.5. According to the HU scale, the HU attenuation coefficient is below that of water (= 0 HU). Thus, a reduced bone density in this area can be concluded with suspicion of osteolysis (AIOJ/BMD//FDOJ).

Example 2: Measurement of Reduced Bone Density with DVT/HU and TAU-n in the Maxilla

Figure 4 shows a HU value of −114 in the retromolar area 19 and thus reduced bone density. As shown in Figure 4, the distal part of the root tooth 28 is also visible here with contrasting green and white-light blue staining in TAU-n. The toothless alveolar ridge disto-cranial of tooth 28 shows the strongly reduced bone density with intensive red and blue-black colouring, presumably osteolysis/osteonecrosis of jawbone. HU and TAU-n attenuation coefficients fully correspond with each other.

Example: Measuring High Bone Density with DVT/HU and TAU-n

Show examples of TAU-n measurements with maximum attenuation. compares ranges of minimum attenuation in HU and TAU-n and the corresponding attenuation coefficients. For this purpose, the sensor elements are marked which show green colors in TAU-n (top right) or white/light blue (bottom right). In the bottom center, the logarithmic mean value of the measurement of the "best" sensor elements (= minimum attenuation) is displayed (Average(log)).

Figure 5 (left 2D-OPG) shows two areas of increased bone density: the distal root of tooth 37 and the cortical density of the oblique line on the cranial rim of area 38.

The red circles mark the two measuring areas with HU values of 1138 for the root portion and 618 for the oblique line (3D-DVT). The corresponding measuring points in TAU-n are marked (right part of Figure 5) and output is shown as logarithmic average values. The HU of 1138 corresponds to the TAU-n value of 13.16 and the HU of 618 corresponds to a TAU-n value of 116.54.

Comparison: TAU-n Vs Histology of BMD/FDOJ

Each BMD/AIOJ/FDOJ sample was histologically examined (1). Almost all showed the following typical finding:

> Chronic degenerative changes mix with non-reactive adipocyte necrosis. The amount of fat cells is significantly increased. There are no typical signs of inflammation, in particular no inflammatory cell reaction. The fatty-degenerative and osteolytic aspect predominates due to an insufficient metabolic supply (trophic disorder). Bone marrow shows enlarged intertrabecular spaces, often small necrotic bone fragments, fatty micro-vesicles and pools of liquefied fat similar to oil cysts. Small nerve fibers are a prominent feature of most BMD/AIOJ/FDOJ fibroses.

Based on the results of several hundred histological BMD/AIOJ/FDOJ samples, we defined five different characteristics to build up statistics: "FDOJ" (how far does pathology confirm the presence of FDOJ), "fibrosis", "necrotic adipocytes", "trophic disorder" and "no inflammatory cells". For evaluation purposes, we defined these five terms and assigned them to a number from 0 to 4, depending on their strength or presence. Regarding the histological results, if none of these five characteristics in total would give a value of "0" in grading intensity, this would indicate that the preoperative diagnosis of BMD/AIOJ/FDOJ in this jaw area was proven wrong. At the end of the evaluation (see Chapter 7 Results) the grading intensity is the sum of the individual evaluations of FDOJ, fibrosis, necrosis, trophic disorder and inflammatory cells. The higher the grading intensity values (maximum = 20), the more reliable was the preoperative evaluation by DVT and TAU-n. Values <4 correspond to a misdiagnosis under histological criteria.

(1 Institute for Pathology & Cytology Dr. Zwicknagel/Assmus (Freising, Germany))

Comparison: TAU-n in Fatty-Degenerative Osteolysis (in Jawbone with Reduced Bone Density) versus Local RANTES/CCL5 Overexpression

Morphology of BMD/AIOJ/FDOJ and Local RANTES/CCL5 Expression

What does BMD/AIOJ/FDOJ look like clinically? The histologically defined main components of BMD/AIOJ/FDOJ are necrotic adipocytes (Figure 6)

The authors examined in detail the tissue in such jaw lesions that appears as fatty lumps inside an intact cortical bone.[6,7] They showed that the fatty lumps found are biochemically extremely active and produce certain cytokines in large quantities, in particular the chemokine RANTES/CCL-5 (R/C). The expression levels of these cytokines are also elevated in a number of systemic diseases such as cancer, dementia, multiple sclerosis or arthritis. There is strong evidence that the development and persistence of a variety of systemic diseases may be associated with R/C overexpression by BMD/AIOJ/FDOJ. However, in most of these cases, the local effect of neuralgic pain is missing.[6,7,21,22] It has also been plausibly shown that AIOJ/BMD/FDOJ describes the pathological condition of the jawbone, which is listed in code M87.0 of the ICD-10 (International Code of Diseases, Tenth Revision (ICD-10)).

Comparison in FDOJ: DVT/HU Vs RANTES/CCL5 Expression

Figure 7 on the right shows the typical fatty-degenerative morphology of a BMD/AIOJ/FDOJ sample. Which clinical parameters correspond with this reduced HU- and TAU-n bone density values of this area? In addition to the histological findings, we can determine the R/C expression of the BMD/

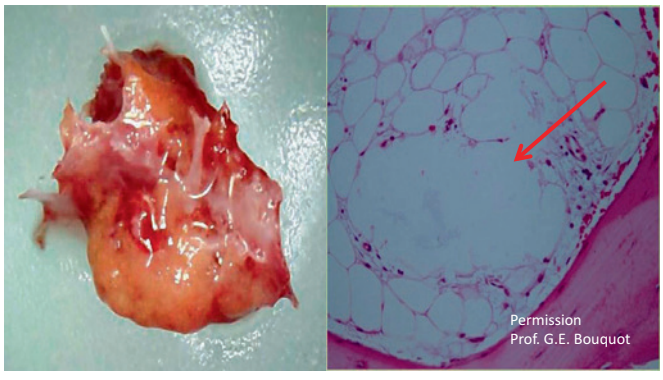

Figure 6 Left picture: Preparation of intraoperatively removed fatty-degenerative osteonecrosis from BMD/AIOJ/FDOJ; Right picture: Necrotic adipocytes confluent to so-called "oil cysts" with high-fat content (arrow points to such a big "oil cyst").

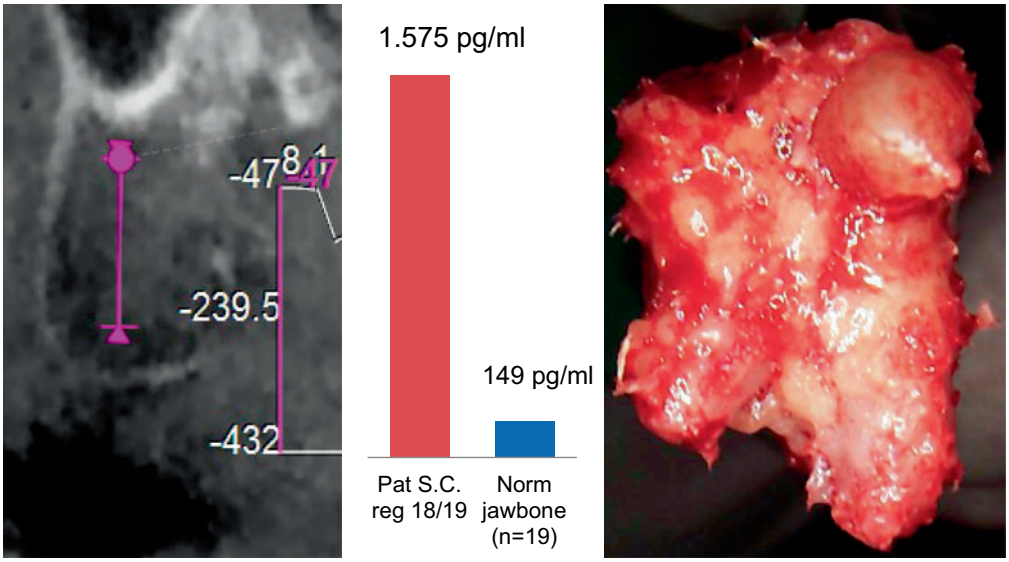

Figure 7 Left image shows DVT/HU of the retromolar area 18/19 with −239,5 Center image shows the R/C expression of the intraoperatively taken bone sample, which is about ten-fold higher than healthy jawbone. Thus, a chronic inflammatory process in the area of 18/19 has been confirmed by multiplex laboratory analysis. Right picture shows the fatty-degenerated cancellous bone from area 18/19, which structurally corresponds to the HU attenuation coefficient of −239. Related histologic findings in area 18/19 are: internal medullary spaces with myxoid or fibrillar degeneration of fatty tissue; trophic disorders.

AIOJ/FDOJ samples postoperatively. The example of BMD/AIOJ/FDOJ in Figure 7 compares the preoperatively determined HU values of a right upper wisdom tooth area with the fatty-degenerated cancellous bone, the postoperative histological findings and the multiplex analysis of the local R/C expression. The relationship between reduced medullary bone density, BMD/AIOJ/FDOJ and R/C overexpression with detection of R/C expression was discussed by the authors in previous publications.[6,7,21,22] Figure 7 deliberately omits the corresponding 2D-OPG.[9] In accordance with earlier publications,[6,7,21,22] this example demonstrates the morphology, the elevated R/C level (= red column; healthy jawbone shows 149.9 pg/mL R/C= blue column) and histology of the suitability of HU attenuation coefficients to assess BMD/AIOJ/FDOJ.

Summary of the Pre- and Post-Operative Presentation of an FDOJ

In summary, we use preoperative and postoperative diagnostic means in a BMD/AIOJ/FDOJ area for comparison: preoperative DVT/HU and bone density measurement with TAU-n. Postoperatively, histology examines fibrillary and fatty degeneration without inflammatory signs[25] and multiplex analysis shows the extent of R/C expression.

Results

Table 1A and B show the results of the preoperative determination of DVT/HU and TAU-n attenuation coefficients as "CavLog" numbers and postoperatively the R/C expression in pg/mL as well as the histological findings, presented numerically as "gradings" in 82 BMD/AIOJ/FDOJ cases.

Discussion

The presented study is patient-centered. Samples and data of all 82 patients are taken directly from day-today practice (2). The data were collected as part of the normal everyday medical care of the patients and evaluated retrospectively. In the context of clinically necessary surgical treatment of AIOJ/BMD/FDOJ, we examined removed BMD/AIOJ/FDOJ samples postoperatively histologically and for the content of R/C inflammatory messengers. The medical indication for BMD/AIOJ/FDOJ surgery in these patients was given by 2D-OPG and additional DVT/CBCT to determine bone density radiographically. This indication was supplemented by the measurement of bone density using TAU-n. The average age of the investigated group was 56.4 in a gender ratio of 59w/23m. The clinical case studies presented herein were performed as part of a case–control study and were deemed to be retrospective in nature. Approval was granted by IMD-Berlin forensic accredited Institute DIN EN 15189/DIN EN 17025. All patients provided their written informed consent (as outlined in the PLOS consent form) to participate in the studies,

(2 Clinic for Integrative Dentistry Gruenwalder Str. 10A 81547 Munich)

Table 1 The Results of the Preoperative Determination of DVT/HU and TAU-n Attenuation Coefficients

A									
Nr	**RANTES**	**HU**	**CavLg**	**FDOJ**	**Fibr**	**Necr**	**TroDi**	**Infla**	**Grad**
1	1.787.50	−211.0	0.32	2	2	3	2	0	9
2	9.899.32	−299.0	0.86	1	4	4	0	0	9
3	776.25	−328.0	0.21	3	0	0	1	1	5
4	820.00	−221.0	1.81	4	2	0	3	1	10
5	3.937.50	−230.0	0.42	4	3	0	0	0	7
6	1.987.50	−344.0	0.47	3	3	3	3	0	12
7	123.75	−293.0	1.18	3	4	2	2	0	11
8	5.700.00	−533.0	0.42	3	3	0	4	0	10
9	933.75	−290.0	3.18	3	1	3	3	0	10
10	706.25	−447.0	0.19	2	4	4	3	1	14
11	1.750.00	−390.0	0.82	4	4	4	3	0	15
12	775.00	−201.0	4.25	3	4	4	2	0	13
13	5.712.50	−350.0	0.80	4	4	2	3	1	14
14	4.325.00	−201.0	3.54	4	2	4	2	0	12
15	3.762.50	−291.0	0.37	2	4	4	4	1	15
16	1.825.00	−263.0	0.72	4	4	3	4	0	15
17	992.50	−340.0	0.41	4	4	4	0	0	12
18	557.50	−304.0	2.08	3	2	2	2	0	9
19	2.825.00	−431.0	0.71	3	2	2	3	0	10
20	873.75	−359.0	0.55	3	0	0	1	0	4
21	2.050.00	−280.0	0.23	3	3	0	0	2	8
22	5.412.50	−287.0	4.25	3	2	3	1	0	9
23	722.50	−345.0	1.25	2	3	0	0	2	7
24	3.250.00	−326.0	2.04	2	0	4	1	1	8
25	2.850.00	−250.0	0.21	0	0	0	0	0	0
26	3.162.50	−327.0	1.84	2	1	4	3	0	10
27	2.187.50	−93.0	0.47	3	2	2	2	0	9
28	902.50	−346.0	3.95	4	4	4	1	0	13
29	8.212.50	−298.0	1.06	4	3	2	3	0	12
30	1.675.00	−400.0	1.19	3	4	4	0	0	11
31	865.00	−502.0	0.53	4	4	0	3	0	11
32	767.50	−471.0	0.26	3	3	0	0	0	6
33	2.262.50	−334.0	1.22	3	1	3	2	0	9
34	1.400.00	−208.0	2.06	0	3	2	2	1	8
35	1.875.00	−200.0	0.77	2	4	0	2	0	8
36	1.575.00	518.0	0.65	4	4	3	4	0	15
37	9.998.15	−268.0	0.85	2	1	4	0	0	7
38	1.400.00	−213.0	0.74	4	1	4	4	0	13
39	495.00	−333.0	1.12	3	4	4	4	0	15
40	2.737.50	−379.0	1.21	4	1	4	4	0	13
41	3.725.00	−335.0	0.87	0	0	0	0	0	0
42	1.712.50	−235.0	0.69	4	4	1	4	0	13
B									
Nr	**RANTES**	**HU**	**CavLg**	**FDOJ**	**Fibr**	**Necr**	**TroDi**	**Infla**	**Grad**
43	2.962.50	−452.0	1.12	4	3	3	3	0	13
44	9.965.88	−322.0	0.54	4	1	4	0	0	9
45	5.362.50	−418.0	0.51	4	1	4	4	0	13
46	2.100.00	−301.0	0.33	4	3	3	3	0	13

(*Continued*)

Table 1 (Continued).

B									
Nr	**RANTES**	**HU**	**CavLg**	**FDOJ**	**Fibr**	**Necr**	**TroDi**	**Infla**	**Grad**
47	4.562.50	−186.0	1.59	4	3	4	3	0	14
48	2.425.00	−349.0	1.70	4	4	4	1	0	13
49	702.50	−376.0	0.15	4	2	2	4	2	14
50	2.425.00	−228.0	0.20	3	1	4	2	0	10
51	3.950.00	−261.0	0.30	4	4	4	4	1	17
52	2.000.00	−463.0	0.57	2	4	0	0	0	6
53	1.612.50	−345.0	0.71	4	3	4	3	0	14
54	527.50	−438.0	0.29	3	1	4	0	1	9
55	1.275.00	−363.0	1.06	0	0	0	0	0	0
56	1.700.00	−432.0	0.76	4	2	4	3	1	14
57	1.587.50	−198.0	0.51	4	2	4	3	0	13
58	486.25	−260.0	0.47	4	1	4	1	0	10
59	518.75	−294.0	0.90	4	1	3	4	0	12
60	1.337.50	−373.0	0.47	3	4	1	2	0	10
61	2.112.50	−249.0	0.50	4	4	0	4	0	12
62	810.00	−243.0	0.41	4	3	3	3	0	13
63	1.078.75	−440.0	0.60	4	4	4	3	0	15
65	863.75	−227.0	0.81	0	0	0	0	0	0
67	405.00	−450.0	1.11	4	3	4	1	2	14
68	2.875.00	−387.0	0.26	4	1	4	0	0	9
70	1.800.00	−308.0	0.41	1	4	0	0	0	5
72	1.337.50	−248.0	1.77	1	4	0	0	0	5
73	6.512.50	−348.0	0.23	4	2	3	3	0	12
74	893.75	−264.0	2.73	3	4	4	3	0	14
75	1.775.00	−168.0	1.58	4	2	4	3	0	13
76	146.25	−265.0	0.20	2	3	1	0	0	6
77	8.062.50	−373.0	1.02	3	1	2	3	0	9
80	1.875.00	−173.0	1.95	4	2	3	3	0	12
81	910.00	−454.0	0.77	0	0	0	0	0	0
82	645.00	−189.0	2.29	3	3	1	0	1	8
MV	2.459.37	−303.7	0.9	3.01	3	2.4	1.99	0.3	10.2

Notes: Table 1 a and Table 1 b: Nr = number of patient in 82 BMD/AIOJ/FDOJ cases; RANTES = multiplex value of RANTES/CCL5 expression in pg/mL of jawbone sample; HU = Hounsfield units of CBCT of corresponding area of jawbone surgery, CavLg = TAU-n value; FDOJ = fatty-degenerative osteonecrosis of jawbone in histological findings from 0 to 4 in intensity or obvious presence; Fibr = presence of fibrosis; Necr = presence of necrosis; TroDi = presence of a trophic disorder; Inflam = no inflammatory cells are present; Grade = sum of five upper characteristics as grading intensity. Samples marked in yellow and graded in 0 show no histological evidence for BMD/AIOJ/FDOJ.

Discussion of the Hounsfield Units

With a mean value of –303 HU, the BMD/AIOJ/FDOJ sites diagnosed with DVT/HU are clearly below the minimum value for healthy jawbone of +300 HU.[23,24] The bone density is therefore clearly below normal.

Discussion of the TAU-n Average(Log) Values

The limit value of TAU-n Average(log) is 100: high-density areas (average[log] ≥100) are indicated in TAU-n by the color green and low-density areas by red (average[log] <100). With the mean value of 0.9 [log], the areas examined with TAU-n are preoperatively well within the display range red of BMD/AIOJ/FDOJ typical reduction of bone density.

Discussion of Histology

From 82 histological findings, five parameters were defined for the evaluation of a BMD/AIOJ/FDOJ. Depending on intensity or obvious presence, a number from 0 to 4 was assigned to the finding. Table reading:

a) "FDOJ": Pathology confirms the presence of BMD/AIOJ/FDOJ. The mean value of 3.01 in Table 1A and B confirms on average the presence of BMD/AIOJ/FDOJ in almost all 82 BMD/AIOJ/FDOJ samples.
b) "Fibr": presence of fibrosis. The mean value of 2.47 confirms fibrosis in all BMD/AIOJ/FDOJ samples.
c) "Necr": presence of necrosis. The mean value of 2434 confirms on average the necrosis of the adipocytes in the 82 BMD/AIOJ/FDOJ samples.
d) "TroDi": presence of a trophic disorder. The mean value of 2 confirms on average the trophic disturbances in the 82 BMD/AIOJ/FDOJ samples.
e) "Inflam": No inflammatory cells are present (free from acute inflammatory reactions). The mean value of 0.25 confirms on average the absence of inflammatory cells in the 82 BMD/AIOJ/FDOJ samples.
f) "Grade": sum of these five characteristics as "grading intensity". The mean value of 10.2 confirms on average the presence of a histologically defined BMD/AIOJ/FDOJ in the 82 BMD/AIOJ/FDOJ samples.

Nevertheless, there are five samples (marked yellow in Table 1and b and consistently graded in 0) in which the pathologist cannot find histological evidence for BMD/AIOJ/FDOJ. A contradiction of these negative histological findings is shown.

a) To the positive results of BMD/AIOJ/FDOJ in these five cases with overexpressed R/C of 2.850, 3.725, 1.275, 863 and 910 pg/mL, respectively, at a normal healthy bone value of 149.90 pg/mL.
b) To the positive results of BMD/AIOJ/FDOJ in these five cases, each with strongly negative HUs with −250.0, −335.0, −363.0, −227.0 and −454.0 at a standard value of >300.
c) On the positive findings of BMD/AIOJ/FDOJ in these five cases with very low Cav [log] values of 0.21, 0.87, 1.06, 0.81 and 0.77 with a healthy limit of >100.

Therefore, it can be concluded that the BMD/AIOJ/FDOJ findings were correct preoperatively by DVT/HU and TAU-n. However, the light microscopically histology performed postoperatively shows the highest failure rate, whilst all R/C expression values proved the existence of BMD/AIOJ/FDOJ.

Discussion of the RANTES/CCL5 Expression

The normal range of R/C expression in the healthy jawbone is 149 pg/mL In our cohort of 82 patients, the mean value of 2459.37 pg/mL is approximately 15 times higher than in healthy bone marrow areas and thus confirms the preoperative TAU-n values postoperatively.

Summary

In summary, all four evaluation criteria predominantly confirm the presence of BMD/AIOJ/FDOJ in each of the 82 samples. Validation of the TAU-n method in comparison to the other methods was thereby confirmed. TAU-n fits seamlessly into the reliability of the other methods.

Conclusion

The data and procedures presented show that the TAU-n device provides reliable bone density data. Thus, it is a metrologically unbiased alternative to the increasingly critically assessed X-ray radiation[26,27] and the more stringent radiation protection laws.[28] This work is at the interface of morphology and immunology of chronic osteolytic changes in the jawbone. The presented medullary mineralization and ossification disorder of BMD/AIOJ/FDOJ is not an isolated clinical picture as it is often presented in clinical research on osteoporosis or bisphosphonate-induced osteonecrosis. Rather, it is a chronic osteo-immunologically derailed condition that can be regarded as an additional stress factor in immune and inflammatory diseases. Its character of a "silent inflammation" with proinflammatory chemokine expression, especially of R/C, shows itself as a common stress factor or possibly even a common trigger of numerous immunological systemic diseases.[29,30] For their simple detection, the reliable, unstressed and easy-to-use TAU-n device is available.

Abbreviations

AIOJ, Aseptic-Ischemic Osteonecrosis of Jawbone; BMD, Bone Marrow Defects; CBCT, Cone Beam Computed Tomography; CCL5, Chemokine (C-C motif) ligand 5; DVT, Digital Volume Tomography; FDOJ, Fatty-Degenerative Osteonecrosis/Osteolysis of Jawbone; HU, Hounsfield Units; Log, logarithmic; OPG, Orthopantomogram; R/C, RANTES/CCL5; RANTES, Regulated on Activation, Normal T cell Expressed and Secreted; TAU, Trans-Alveolar Ultrasonogra-

phy; TAU-n, New Trans-Alveolar Ultrasonography Device; US, Ultrasound.

Acknowledgments

English-language editing of this manuscript was provided by Journal Prep and Dr. Elmar Jung.

Disclosure

CaviTAU® (Munich, Germany), the company that designed the new TAU-n apparatus and associated software, provided these tools without charge for the purposes of this study. The ultrasonography procedure was carried out at the Clinic for Integrative Dentistry Munich. CaviTAU® and the Clinic for Integrative Dentistry are in ongoing discussions regarding numerous collaborative arrangements to further improve and verify the new TAU apparatus, CaviTAU®, as it is introduced to the market. Dr. Johann Lechner is the holder of a patent PCT/EP2018/084199 used in CaviTAU®. The authors report no other conflicts of interest in this work.

References

1. Patini R, Gallenzi P, Lione R, Cozza P, Cordaro M, et al. Ultrasonographic evaluation of the effects of orthodontic or functional orthopaedic treatment on masseter muscles: a systematic review and meta-analysis. *Medicina*. 2019;55(6):256.
2. Lipani CS, Natiella JR, Greene GW Jr. The hematopoietic defect of the jaws: a report of sixteen cases. *J Oral Pathol*. 1982;11(6):411–416. doi:10.1111/j.1600-0714.1982.tb00184.x
3. Lee S-C, Jeong CH, Im HY, et al. Displacement of dental implants into the focal osteoporotic bone marrow defect: a report of three cases. *J Korean Assoc Oral Maxillofacial Surgeons*. 2013;2(94):39.
4. Bouquot JE, Roberts AM, Person P, Christian J. Neuralgia-inducing cavitational osteonecrosis (NICO). Osteomyelitis in 224 jawbone samples from patients with facial neuralgia. *Oral Surg Oral Med Oral Pathol*. 1992;73(3):307–319. doi:10.1016/0030-4220(92)90127-C
5. Bouquot J, Martin W, Wrobleski G. Computer-based thru-transmission sonography (CTS) imaging of ischemic osteonecrosis of the jaws – a preliminary investigation of 6 cadaver jaws and 15 pain patients. *Oral Surg Oral Med Oral Pathol Oral Radiol Endod*. 2001;92:550.
6. Lechner J, von Baehr V. RANTES and fibroblast growth factor 2 in jawbone cavitations: triggers for systemic disease? *Int J Gen Med*. 2013;6:277–290. doi:10.2147/IJGM.S43852
7. Lechner J, Schuett S, von Baehr V. Aseptic-avascular osteonecrosis: local `silent inflammation` in the jawbone and RANTES/CCL5 overexpression. *Clin Cosmet Investig Dent*. 2017;9:99–109. doi:10.2147/CCIDE.S149545
8. Al-Nawas B, Grotz KA, Kann P. Ultrasound transmission velocity of the irradiated jaw bone in vivo. *Clin Oral Invest*. 2001;5(4):266–268. doi:10.1007/s00784-001-0133-4
9. Klein MO, Grotz KA, Manefeld B, Kann PH, Al-Nawas B. Ultrasound transmission velocity for non-invasive evaluation of jaw bone quality in vivo prior to dental implantation. *Ultrasound Med Biol*. 2008;34(12):1966–1971. doi:10.1016/j.ultrasmedbio.2008.04.016
10. Lechner J. Validation of dental X-ray by cytokine RANTES - comparison of X-ray findings with cytokine overexpression in jawbone. *Clin Cosmet Investig Dent*. 2014;6:71–79. doi:10.2147/CCIDE.S69807
11. Wells PNT. Ultrasonic imaging of the human body. *Rep Prog Phys*. 1999;62(5):676. doi:10.1088/0034-4885/62/5/201
12. Njeh C, Hans D, Fuerst C, Gluer C, Genant HK. *Quantitative Ultrasound. Assessment of Osteoporosis and Bone Status*. United Kingdom: Martin Dunitz. Ltd; 1999.
13. Chiandussi S, Biasotto M, Dore F, Cavalli F, Cova M, Lenarda R. Clinical and diagnostic imaging of bisphosphonate- associated osteonecrosis of the jaws. *Dentomaxillofac Radiol*. 2006;35(4):236–243. doi:10.1259/dmfr/27458726
14. Store G, Boysen M. Mandibular osteoradionecrosis: clinical behaviour and diagnostic aspects. *Clin Otolaryngol*. 2000;25(5):378–384. doi:10.1046/j.1365-2273.2000.00367.x
15. Stockmann P, Hinkmann FM, Lell MM, et al. Panoramic radiograph computed tomography or magnetic resonance imaging. Which imaging technique should be preferred in bisphosphonate-associated osteonecrosis of the jaw? A prospective clinical study. *ClinOralInvestig*. 2010;14(3):311–317.
16. Grötz KA, Al-Nawas B. Persisting alveolar sockets–a radiologic symptom of BP-ONJ? *J Oral Maxillofac Surg*. 2006;64(10):1571–1572. doi:10.1016/j.joms.2006.05.041
17. Swennen GR, Schutyser F. Three-dimensional cephalometry: spiral multi-slice vs cone-beam computed tomography. *Am J Orthodontics Dentofacial Orthopedics*. 2006;130(3):410–416. doi:10.1016/j.ajodo.2005.11.035
18. Mah P, Reeves TE, McDavid WD. Deriving Hounsfield units using grey levels in cone beam computed tomography. *Dentomaxillofacial Radiol*. 2010;39(6):323–335. doi:10.1259/dmfr/19603304
19. Norton MR, Gamble C. Bone classification: an objective scale of bone density using the computerized tomography scan. *Clin Oral Implants Res*. 2001;12(1):79–84. doi:10.1034/j.1600-0501.2001.012001079.x
20. Misch CE. Bone density: a key determinant for clinical success. In: Misch CE, editor. *Contemporary Implant Dentistry*. 2nd ed. St Louis: CV Mosby Company; 1999:109–118.
21. Lechner J, von Baehr V. Hyperactivated signaling pathways of chemokine RANTES/CCL5 in osteopathies of jawbone in breast cancer patients—case report and research. *Breast Cancer*. 2014;8:89–96. doi:10.4137/BCBCR.S15119
22. Lechner J, Rudi T, von Baehr V. Osteoimmunology of tumor necrosis factor-alpha, IL-6, and RANTES/CCL5: a review of known and poorly understood inflammatory patterns in osteonecrosis. *Clin Cosmet Investig Dent*. 2018;10:251–262. doi:10.2147/CCIDE.S184498
23. Ganz SD. Conventional CT and cone beam CT for improved dental diagnostics and implant planning. *Dent Implantol Update*. 2005;16(12):89–95.
24. Lee S, Gantes B, Riggs M, Crigger M. Bone density assessments of dental implant sites: 3. Bone quality evaluation during osteotomy and implant placement. *Int J Oral Maxillofac Implants*. 2007;22(2):208–212.
25. Lechner J, Noumbissi S, von Baehr V. Titanium implants and silent inflammation in jawbone – a critical interplay of dissolved titanium particles and cytokines TNF-a and RANTES/CCL5 on overall health? *EPMA J*. 2018;9(3):331–343. doi:10.1007/s13167-018-0138-6
26. Brenner DJ, Elliston CD, Hall EJ, Berdon WE. Estimated risks of radiation induced fatal cancer from pediatric CT. *AJR*. 2001;176(2):289–296. doi:10.2214/ajr.176.2.1760289
27. Vañó E, Miller DL, Martin CJ, et al.; ICRP- International Commission on Radiological Protection. Diagnostic reference levels in medical imaging. ICRP Publication 135. *Ann ICRP*. 2017;46(1):1–144. doi:10.1177/0146645317717209

28. Strahlenschutzgesetz (StrlSchG) Artikel 1 G. v. 27.06.2017 BGBl. I S. 1966; Strahlenschutzverordnung (StrlSchV) Artikel 1 V. v. 29.11.2018BGBl. I S. 2034, 2036; Gesetz zur Neuordnung des Rechts zum Schutz vor der schädlichen Wirkung ionisierender Strahlung (StrlSchGEG) G. v. 27. 06.2017BGBl. I S. 1966.
29. von Luettichau I, NELSON P, PATTISON J, et al. RANTES chemokine expression in diseased and normal human tissues. *Cytokine*. 1996;8(1):89–98. doi:10.1006/cyto.1996.0012
30. Tsukishiro S, Suzumori N, Nishikawa H, Arakawa A, Suzumori K. Elevated serum RANTES levels in patients with ovarian cancer correlate with the extent of the disorder. *Gynecol Oncol*. 2006;102(3):542–545. doi:10.1016/j.ygyno.2006.01.029

Ultrasound in Med. & Biol., Vol. 00, No. 00, pp. 1–12, 2021

0301-5629/$ - see front matter

https://doi.org/10.1016/j.ultrasmedbio.2021.07.012

● *Original Contribution*

FOCAL BONE-MARROW DEFECTS IN THE JAWBONE DETERMINED BY ULTRASONOGRAPHY—VALIDATION OF NEW TRANS-ALVEOLAR ULTRASOUND TECHNIQUE FOR MEASURING JAWBONE DENSITY IN 210 PARTICIPANTS

JOHANN LECHNER,* BERND ZIMMERMANN,† and MARLENE SCHMIDT‡

* Clinic for Integrative Dentistry, Munich, Germany; † Qinno, Wessling, Germany; and ‡ STEYR Motorenwerke, Ramingdorf, Austria

(*Received* 5 *May* 2020; *revised* 1 *July* 2021; *in final form* 13 *July* 2021)

Abstract—Ultrasound imaging of the jawbone is not currently used in dental medicine to determine bone density. Bone-marrow defects in the human jawbone (BMDJ/FDOJ) are widely discussed in dentistry owing to their role in implant failures and as sources of inflammation in various immune diseases. The use of through-transmission alveolar ultrasonography (TAU) to locate BMDJ/FDOJ was evaluated in this study using a new TAU apparatus (TAU-n). The objective was to determine whether TAU-n readings accurately indicate the clinical parameters to detect BMDJ/FDOJ. Three parameters were compared with TAU-n measurements: 2-D orthopantomogram, Hounsfield units using digital volume tomography and post-operatively measured levels of RANTES/CCL5 expression in BMDJ/FDOJ samples. Based on the available clinical data, Hounsfield units, RANTES/CCL5 expression and TAU-n color codes yielded consistent results with respect to bone mineral density. Thus, ultrasonography with TAU-n is a reliable and efficient diagnostic method to screen for BMDJ/FDOJ in dentistry. (E-mail: drlechner@aol.com) **© 2021 The Author(s). Published by Elsevier Inc. on behalf of World Federation for Ultrasound in Medicine & Biology. This is an open access article under the CC BY-NC-ND license (http://creativecommons.org/licenses/by-nc-nd/4.0/).**

Key Words: **Bone marrow defects of the jaw, Digital volume tomography, Fatty-degenerative osteolysis/osteonecrosis of the jaw, Orthopantomogram, RANTES/CCL5, TAU-n device, Transalveolar ultrasonography.**

INTRODUCTION

In the medical field, ultrasonography is widely used to image various types of soft tissues. In principle, images of structures in the body are generated by analyzing the reflection of ultrasound waves. To derive useful information concerning the status of the jawbone, different ultrasound techniques must be used, because the ultrasound waves are almost completely reflected at the interface between bone and soft tissue. *In vivo* measurement of ultrasound velocity in human cortical bone was introduced as a rapid, reliable and non-invasive method which could be used to analyze the mechanical properties of bone (Greenfield et al. 1981). Cortical bone samples show the highest values, followed by mixed bone samples and cancellous bone samples, with the latter showing the lowest values (Kumar et al. 2012). Thus, guided ultrasound waves are able to detect ischemic bone-marrow diseases—that is, focal osteoporotic defects or cavitations in the jawbone (Al-Nawas et al. 2001). Intra-oral equipment used in guided ultrasound must be minimized, however, as the area cannot be examined with commonly used ultrasound apparatus. Until now, ultrasound examinations have thus been of limited use in dental medicine, although they have been used to detect "focal" bone defects of the jawbone (focal osteoporotic marrow defects), as described in previous scientific research (Lipani et al. 1982; Kaufman and Einhorn 1993). The status of cancellous bone in the jaws may be of great clinical importance. Researchers have provided anatomical evidence that cancellous bone may be significantly degenerated, a phenomenon described as ischemic osteonecrosis leading to cavitational lesions (Bouquot et al. 1992).

We conducted an in-depth investigation of the tissue in such lesions, which appeared as clumps of fat within intact cortical bone. This tissue was in an ischemic, fatty-degenerative state. The observed bone marrow defects of the jaw (BMDJ) were thus defined as fatty-

Correspondence to: Johann Lechner, Clinic for Integrative Dentistry, Gruenwalder Str. 10A, 81547 Munich, Germany E-mail: drlechner@aol.com

degenerative osteolysis/osteonecrosis of the jawbone (FDOJ). The clumps of fat found in osteolytic jawbone are extremely biochemically active and produce specific cytokines in high amounts, the most notable of which is the chemokine RANTES (more recently known as CCL5; R/C). This chronic R/C production may influence immunologic patterns and exacerbate systemic immunologic diseases (Lechner and Mayer 2010; Lechner and von Baehr 2013, 2015; Lechner, Huesker et al. 2017; Lechner, Schuett et al. 2017). The status of cancellous bone in the jaw is of great importance with respect to dental implants and the success of implantology, according to previous publications by other authors (Klein et al. 2008; Lee et al. 2013). One of the most significant concerns associated with the treatment of this condition, however, is the fact that jawbone with fatty-degenerated bone marrow does not show signs of abnormal findings on X-ray examination (Lechner 2014). Being virtually undetectable on any type of commonly used 2-D X-ray examination, the occurrence and phenomena of BMDJ/FDOJ remain widely unknown and are even denied. To overcome this challenge, the use of through-transmission alveolar ultrasonography (TAU) was evaluated using a new TAU apparatus (TAU-n; CaviTAU, Qinno GmbH, Wessling, Germany; international patent application PCT/EP2018/084199). The CaviTAU is approved by European Union medical authorities according to MDD 93/42/EWG.

AIM AND OBJECTIVES

The aim of the present study was to evaluate BMDJ/FDOJ using TAU-n and to determine whether TAU-n measurements are practical and capable of promoting quality assurance in assessing BMDJ/FDOJ. Specifically, we aimed to answer the following questions: Are conventional radiographic techniques suitable for detecting osteolytic bone-marrow defects in the jaw (BMDJ/FDOJ), which may display local silent inflammation? Is a newly available ultrasound device (TAU-n) for radiation-free measurement of bone density suitable for visualizing the condition of BMDJ/FDOJ?

MATERIALS AND METHODS

Participant selection

All 210 participants who were enrolled in this study were seeking to uncover the etiology of their respective systemic immunologic diseases, specifically the possibility that BMDJ/FDOJ-induced "silent inflammation" of the jawbone might be involved in the pathogenesis of the disease. The samples and data were taken directly from daily clinical practice at the Clinic for Integrative Dentistry (Munich, Germany). Specifically, the data were obtained in the course of the patients' routine medical care and were retrospectively evaluated. In cases that necessitated surgical treatment, samples of BMDJ/FDOJ were evaluated post-operatively to assess the level of R/C inflammatory markers. Radiographic examinations, namely 2-D orthopantomogram (OPG) and digital volume tomography (DVT)/cone-beam computed tomography, were assessed to determine bone density and provide appropriate medical indications for the surgical treatment of BMDJ/FDOJ in these patients. This indication was supplemented by bone density measurements using TAU-n. The average age of the investigation group was 53.02 y; 129 were women and 81 were men.

The clinical case studies presented here were performed as part of a case-control study and were deemed to be retrospective in nature. Approval was granted by the accredited forensic institute, IMD-Berlin (DIN EN 15189/DIN EN 17025). All participants provided written informed consent (as outlined in the Public Library of Science consent form) to participate in this study. Patients taking bisphosphonates were excluded from the study. All participants reported that they were not taking vitamin D supplements.

PRE-OPERATIVE METHODS TO DETERMINE BONE-MARROW DEFECTS IN JAWBONE (BMDJ/FDOJ)

Determining BMDJ/FDOJ with conventional 2-D OPGs

Panoramic radiographs are routinely used in clinical dentistry. This imaging technique is inexpensive and provides a general overview of the entire jaw and a method of initial assessment of the condition of the jaw. The Orangedental PaX-i3D Duo 3D Multi X-ray unit used in this study displays a measurement of relative bone density of the jawbone (rel-JBD) in the 2-D OGP Panoramix version. A red line shows the measuring range. Figure 1 presents the results of this rel-JBD measurement: The left image shows the relative density of an all-ceramic crown at 0.9. The right image shows the relative density of a healthy area of cancellous bone at 0.49.

Determining BMDJ/FDOJ with 3-D cone-beam computed tomography/DVT

Modern X-ray methods, like DVT, allow the clinician to perform a 3-D assessment of the jawbone using Hounsfield units (HUs), which are generally scientifically recognized as a bone-density assessment tool. HUs are used to describe the attenuation of X-ray radiation in tissues, and this information is displayed in grayscale images. The HU scale ranges from −1000 (attenuation coefficient of air) to −120 (fat), +300 to +400 (healthy cancellous bone) and +1800 to +2200 (cortical bone). Water is defined as 0 HU. Recently, methods to

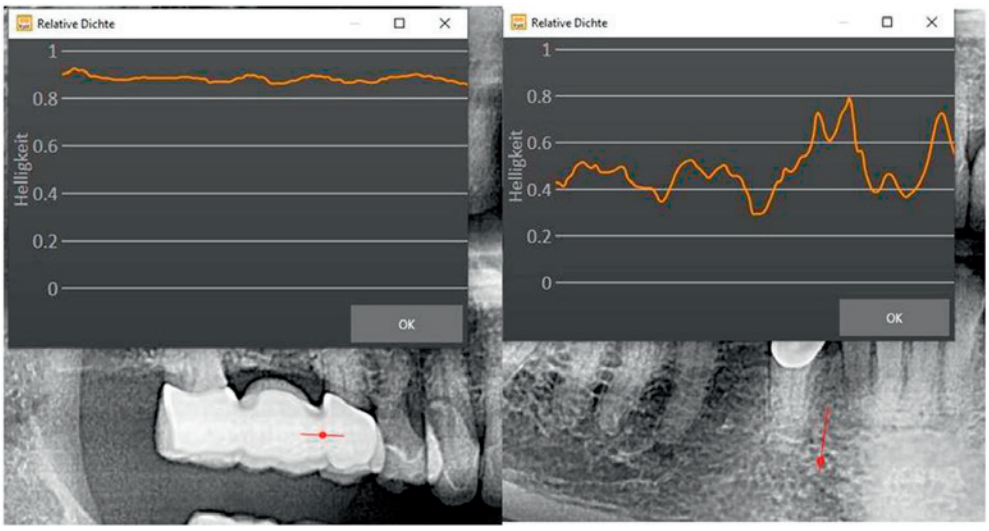

Fig. 1. Example of measurement of relative bone density using OPG. The attenuation coefficients are displayed over the entire test section as a progression curve. In the present validation, only the mean values are used. Measurement of relative jawbone density (rel-JBD) values with an Orangedental PaX-i3D Duo 3D Multi. Legend: Red lines mark the measuring range to display the relative density in the 2-D OPG. OPG = orthopantomogram.

determine HU attenuation coefficients have become available (Norton and Gamble 2001), as actual HU values can be derived using DVT (Misch 1999; Swennen and Schutyser 2006). Further investigations have classified the density of cancellous bone in the jawbone into five categories, with the poorest jawbone density below 150 HU (class 5). In this study, we used specific DVT equipment (PaX-i3D Duo 3D Multi X-ray, Orangedental, Biberach an der Riss, Germany) with the appropriate software to evaluate the density of the jawbone in HUs. In accordance with the DIN 6868-57 standard, the viewing monitors were set with a contrast >40:1 and a brightness ≥120 cd/m^2. The Orangedental PaX-i3D Duo 3D Multi X-ray machine used in this validation study showed the mean value of a randomly selected measurement path, with the maximum and minimum values presented as a progression curve (Fig. 2).

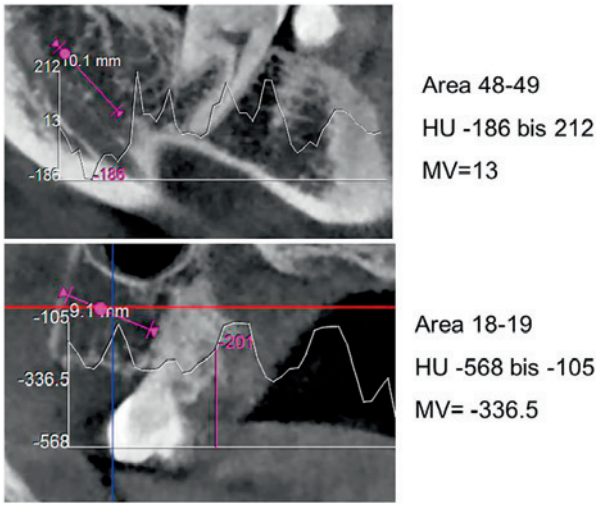

Fig. 2. Example of DVT HU measurement and evaluation of BMDJ/FDOJ. The HU attenuation coefficients are shown as a curve over the measured section. In the present validation study, only the mean values are used. BMDJ/FDOJ = bone-marrow defects of the jaw/fatty-degenerative osteolysis/osteonecrosis of the jaw; DVT = digital volume tomography; HU = Hounsfield units.

Determining BMDJ/FDOJ with TAU-n using ultrasound waves

Attenuation in the amplitude of the ultrasound wave is indicative of pathologic changes in the jawbone and depends on the properties of the medium through which the wave is propagated (Mahmoud et al. 2008). Corresponding values are based on published data from Wells (1999) and Njeh et al. (1999). TAU-n generates an ultrasound wave and passes that wave through the jawbone. This wave is produced by an extra-oral transmitter and then detected and measured by a receiving unit that is positioned intra-orally. Both parts (the transmitter and receiving unit) are fixed in a parallel position using a single handpiece. The size of the TAU-n receiving unit is configured such that it can be easily placed inside the mouth of a patient. TAU-n uses 91 piezoelectric elements that are arranged hexagonally. The jawbone must be positioned between the two parts of the measuring unit. With respect to the parts of the measuring unit to be placed inside a patient's mouth, the acoustical coupling between those parts and the alveolar ridge is performed with the aid of a semi-solid gel (Qinno). The contact between the jawbone and both the extra-oral ultrasound

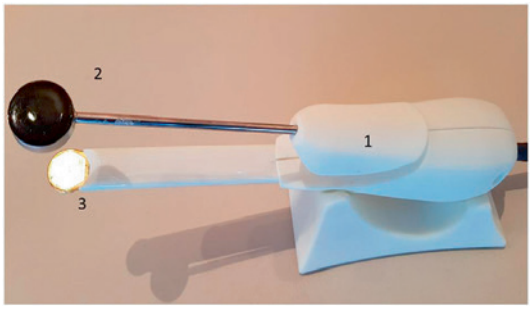

Fig. 3. Coplanar and fixed arrangement of the transmitter and receiver: (1) Handpiece with an ultrasound sender and receiver unit connected to a computer and screen. (2) Ultrasound transmitter. (3) Ultrasound receiver with 91 piezoelectric elements.

transmitter and intra-oral ultrasound receiver (Fig. 3) is optimized and individualized using a special ultrasound gel cushion that was developed for this purpose. The results are shown on a color monitor that displays different colors depending on the degree of attenuation. A semi-solid, single-use gel pad is used around the receiver for hygienic reasons (Fig. 4).

Color scale associated with TAU-n attenuation coefficients

Figure 5 presents the color scheme associated with the TAU-n attenuation coefficients. This scheme corresponds to an ultrasound signal-strength scale (top bar) and a color scale indicating the different degrees of bone density (lower bar). This color scale shows that the colors used to indicate different densities each represent a small part of the entire signal range. Logarithmic averaging broadens the range of bone-density measurements and increases the size of the area in green.

The representations of the measurements provided by the color-coding scheme are concerned with two functions. With the red/green color scale, the bone in the medically relevant area of conspicuousness is shown. The second color-coded scale shows structural differences, which serves as an orientation aid for the user in the placement of the measuring receiver. In this way, the orientation and position of the receiver may be monitored (via live display) while the measurement position is slowly adjusted before the relevant area is captured and stored.

The TAU-n display

The TAU-n display is able to capture the following physical structures in the dentoalveolar region (Fig. 6), with corresponding color variations of 91 color columns/cm^2: solid bone in the marginal cortical area (green or white/light blue); healthy medullary cancellous bone (green or white/light blue); chronic inflammatory medullary cancellous bone with fatty-degenerative components (red or black/dark blue); fatty nerve structures (yellow/light blue); and extremely dense and complex structures such as teeth, implants and crowns (green or white/light blue).

Numerical representation of TAU-n attenuation coefficients

The TAU-n software numerically represents the attenuation coefficients of the TAU-n measurement range. By a mouse click on one of the 91 sensor fields of a given measurement, the software marks the field and displays the measured value in a logarithmic evaluation. The sensor fields that show the highest attenuation values defined by TAU-n are marked in either red or black, and this indicates the bone density of an area of BMDJ/FDOJ. TAU-n computes the logarithmic average of the sum of the sensor elements with the lowest density unit as Average(log), displayed in red (Fig. 7, left panel). In the same way, the logarithmic average of the sensor elements with the highest density—equivalent to reduced attenuation by solid structures—is displayed in

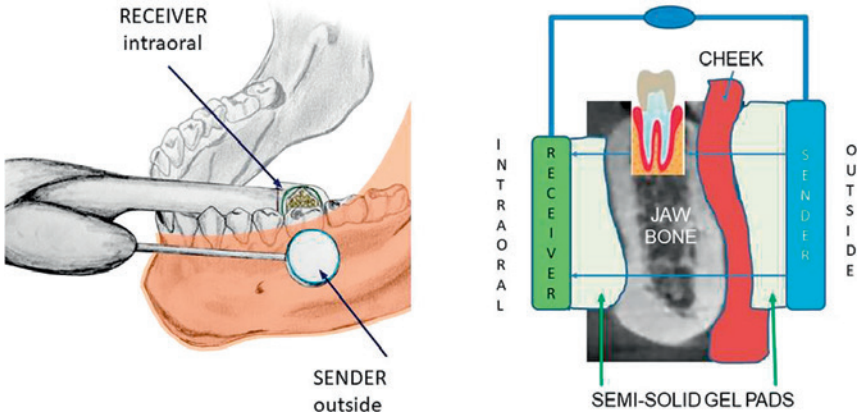

Fig. 4. Left: Positioning of the transmitter (*outside*) and receiver (*intra-oral*) in the lower jaw; the shaded area marks the cheek. Right: The transmitter (*in blue on the right*) and receiver (*in green on the left*) are in a fixed coplanar position (*a blue bar connects them*); semi-solid gel pads between the transmitter and the cheek on the outside of the mouth and between the receiver and the alveolar ridge in the intra-oral position; trans-alveolar ultrasonic impulse from the transmitter to the receiver (*blue arrows*).

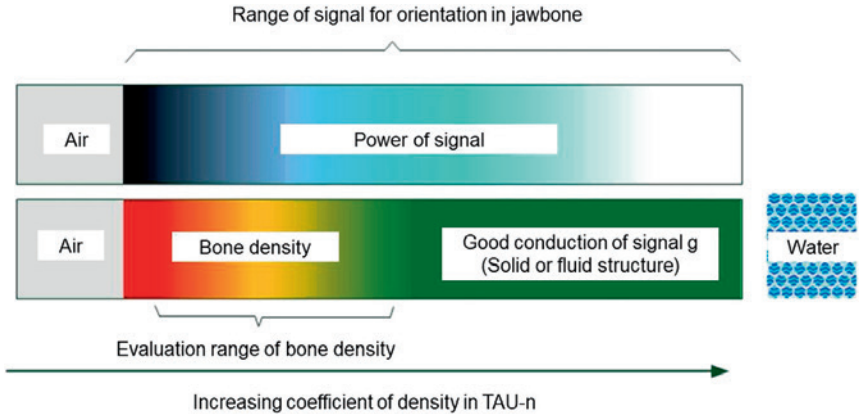

Fig. 5. The color scale is used by the TAU-n device to indicate different degrees of density; gray corresponds to air (*i.e.,* the far left of the scale), and blue area corresponds to water (*i.e.,* the far right of the scale). The signal strength received by the sensor (*top bar*) is displayed in blue and increases from dark to light with increasing density coefficients. Bone density (*lower bar*) is indicated by a color scale ranging from red to green, representing high attenuation of diminished bone density (*red*) and reduced attenuation with increasing density (*green*). TAU-n = new through-transmission alveolar ultrasonography.

Fig. 6. Example of the color-coding scheme associated with attenuation used by TAU-n in area 38. In the upper panel, the measurement of jaw areas 37 to 38/39 (*i.e.,* the retromolar area) is presented. TAU-n displays different degrees of mineralization, as highlighted by the various color patterns of 91 individual sensor fields that correspond to each jawbone area. Green indicates hard and dense structures that correspond to a higher degree of mineralization in spongial jawbone or cortical bone; it also denotes teeth, dental crowns or implants. Yellow indicates diminished bone density and also corresponds to the nerve canal in the lower jaw. Red indicates severely diminished bone density with a low degree of mineralization, corresponding to BMDJ/FDOJ areas. BMDJ/FDOJ = bone-marrow defects of the jaw/fatty-degenerative osteolysis/osteonecrosis of the jaw; TAU-n = new through-transmission alveolar ultrasonography.

green (Fig. 7, right panel). In the following sections and Table 1, the term "TAU-n log" is used to represent the values of Average(log) displayed by TAU-n.

Problems of acoustic coupling in TAU-n

Practical application of the transducer and receiver with fixed geometric positions to obtain intra-oral ultrasonic measurements (*i.e.,* within the mouth of a patient) with sufficient acoustical conductivity proved difficult. The ultrasonic gel, which was placed inside the patient's mouth, was shown to be the main obstacle in attempting to obtain signals from TAU-n in an easy and reproducible manner. The primary difficulty is ensuring that the ultrasonic gel is completely free of air bubbles, given its high viscosity. Air bubbles interfere with obtaining reliable and repeatable measurements. In addition, we found that the anatomical contour of the jawbone at the site of measurement and the plane surface of the intra-oral receiver did not adequately conform to one

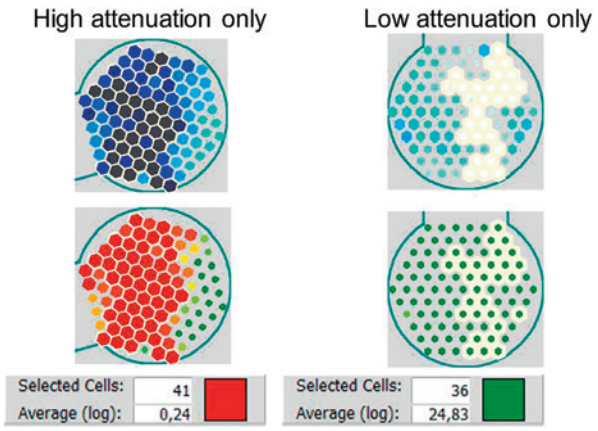

Fig. 7. Sensor elements. Numerical representation of the TAU-n attenuation coefficients for diminished bone density (*left*) and for dense material (*right*). Selected sensor cells (left panel: high attenuation; right panel: low attenuation) are indicated by a white border. The evaluation is presented in the window beneath for a number of selected sensor cells; the result is displayed as a logarithmic mean, which is associated with a corresponding color (*i.e.,* left: *red* = high attenuation; right: *green* = corresponds to low attenuation). TAU-n = new through-transmission alveolar ultrasonography.

Table 1. The four values measured to assess BMDJ/FDOJ

Participant	OPG	HU	Average (log)	R/C (pg/mL)
1	0.6	−29.0	1.35	8212.50
2	0.4	−96.0	1.41	2762.50
3	0.7	−533.0	0.67	5700.00
4	0.75	−326.0	4.49	3250.00
5	0.3	−316.0	0.3	3925.00
6	0.5	−591.0	0.33	3762.50
7	0.6	−295.0	0.36	2162.50
8	0.4	−93.0	0.44	2187.50
9	0.4	−250.0	0.84	2850.00
10	0.65	−745.0	1.58	722.50
11	0.55	−263.0	0.84	1825.00
12	0.5	−311.0	0.46	1787.50
13	0.45	89.0	0.67	1725.00
14	0.4	−300.0	1.37	5387.50
15	0.45	−340.0	0.87	992.50
16	0.5	−306.5	1.04	2512.50
17	0.3	−228.5	0.82	2362.50
18	0.65	11.5	0.9	3862.50
19	0.6	−58.5	0.64	457.50
20	0.5	−659.0	0.85	873.75
21	0.35	−447.0	0.31	706.25
22	0.4	−431.0	0.83	2825.00
23	0.4	−31.5	0.64	1165.00
24	0.55	−450.0	1.12	405.00
25	0.45	−565.0	0.69	146.25
26	0.4	−68.0	0.72	766.25
27	0.55	−647.0	2.58	5525.00
28	0.5	54.5	1.52	7275.00
29	0.6	−549.0	0.82	2112.50
30	0.4	−130.0	0.76	2575.00
31	0.65	120.5	0.94	5562.50
32	0.7	−345.0	0.95	1612.50
33	0.6	−77.5	0.58	205.00
34	0.65	72.5	1.85	2962.50
35	0.55	−173.0	1.07	1875.00
36	0.5	−249.0	0.66	267.50
37	0.4	−413.0	0.38	1750.00
38	0.7	−291.0	0.52	1887.50
39	0.6	−238.5	1.32	2000.00
40	0.6	−537.0	1.22	1337.50
41	0.65	−676.0	0.79	702.50
42	0.4	−62.0	0.54	846.25
43	0.4	−179.5	2.58	408.75
44	0.6	−243.0	1.26	810.00
45	0.4	−560.0	1.5	518.75
46	0.6	−494.0	0.84	486.25
47	0.55	−387.0	0.75	2875.00
48	0.6	−379.0	1.14	2737.50
49	0.4	−228.0	0.32	2425.00
50	0.5	−440.0	0.68	1078.75
51	0.6	−308.0	0.54	1800.00
52	0.6	−322.0	1.21	19,125.00
53	0.5	−589.0	2.29	645.00
54	0.55	−518.0	1.21	1575.00
55	0.45	−294.0	0.51	2187.50
56	0.55	−671.0	0.89	767.50
57	0.55	−244.0	1.89	580.00
58	0.3	−573.0	1.77	8062.50
59	0.65	−454.0	0.93	910.00
60	0.4	99.0	1.57	5025.00
61	0.2	−182.5	1.78	4562.50
62	0.6	−335.0	1.03	3725.00
63	0.4	−288.0	0.79	3587.50
64	0.5	−132.0	1.75	840.00
65	0.6	−202.0	1.03	2300.00
66	0.3	−418.0	0.81	5362.50
67	0.45	−290.0	1.38	1637.50
68	0.6	−41.0	0.96	636.25
69	0.4	−184.0	1.67	2200.00
70	0.5	−227.0	1.11	863.75
71	0.6	−198.0	1.38	1587.50
72	0.45	−261.0	1.65	3987.50
73	0.55	−543.0	1.01	3937.50
74	0.6	−363.0	1.19	1275.00
75	0.45	−268.0	0.32	10,150.00
76	0.55	−110.0	1.69	573.75
77	0.75	−248.0	1.61	1337.50
78	0.65	−142.0	1.28	611.25
79	0.35	−264.0	2.51	893.75
80	0.45	−301.0	0.86	2100.00
81	0.5	−654.0	1.05	866.25
82	0.75	−168.0	1.53	1775.00
83	0.4	146.0	0.79	1400.00
84	0.4	123.0	1.37	1800.00
85	0.4	−222.0	0.77	1925.00
86	0.6	−36.0	1.23	303.75
87	0.4	−5.0	1.15	1215.00
88	0.25	−213.0	1.52	412.50
89	0.5	88.0	1.24	495.00
90	0.25	−347.0	1.19	1600.00
91	0.45	45.0	1	1725.00
92	0.4	−38.0	0.47	527.50
93	0.5	160.0	1.28	3612.50
94	0.5	−313.0	0.82	1337.50
95	0.55	119.0	1.38	1192.50
96	0.4	−196.0	0.8	1246.25
97	0.55	−17.0	0.96	638.75
98	0.3	−457.0	0.47	6512.50
99	0.3	−373.0	0.7	456.25
100	0.5	−209.0	1.25	3275.00
101	0.4	−438.0	0.81	2262.50
102	0.5	−38.0	0.88	447.50
103	0.45	−404.0	0.47	746.25
104	0.35	−170.0	1.64	1400.00
105	0.4	126.0	1.07	436.25
106	0.55	103.0	1.05	588.75
107	0.4	96.0	0.84	1312.50
108	0.7	162.0	0.97	1500.00
109	0.6	−66.0	1.12	223.75
110	0.45	−105.0	1.21	373.75
111	0.5	−20.0	0.98	277.50
112	0.5	−208.0	1.58	705.00
113	0.6	−264.0	1.8	1912.50
114	0.6	−83.0	0.81	3962.50
115	0.6	−38.0	0.67	432.50
116	0.4	−348.0	1.33	1675.00
117	0.4	150.0	1.17	311.25
118	0.4	−166.0	1.35	1023.75
119	0.55	144.0	1.37	996.25
120	0.45	−94.0	1.71	498.75
121	0.5	41.0	2.67	3187.50
122	0.5	−157.0	1.4	417.50
123	0.45	−291.0	0.61	1325.00
124	0.6	77.0	1.17	917.50
125	0.35	−96.0	1.89	1687.50
126	0.4	4.0	0.98	228.75
127	0.25	−183.0	1.58	355.00
128	0.45	−43.0	1.18	407.50
129	0.4	−147.0	0.36	541.25
130	0.4	−145.0	0.73	408.75
131	0.4	−245.0	0.73	572.50

(*continued*)

Table 1 (***Continued***)

(*continued*)

Table 1 (***Continued***)

Participant	OPG	HU	Average (log)	R/C (pg/mL)
132	0.65	150.0	1.24	1600.00
133	0.4	−87.0	1.59	586.25
134	0.2	−138.0	1.38	1287.50
135	0.5	−27.0	1.09	945.00
136	0.35	−257.0	1.22	647.50
137	0.35	−120.0	0.31	267.50
138	0.35	−116.0	0.95	233.75
139	0.55	−30.0	1.38	572.50
140	0.4	150.0	1.57	673.75
141	0.6	−155.0	1.12	2862.50
142	0.55	157.0	1.11	691.25
143	0.5	−127.0	0.67	1650.00
144	0.3	−110.0	0.93	565.00
145	0.55	84.0	0.84	1137.50
146	0.45	−414.0	0.87	8087.50
147	0.45	−122.0	1.53	1217.50
148	0.4	−145.0	1.5	4075.00
149	0.6	170.0	0.67	562.50
150	0.5	97.0	0.97	1337.50
151	0.45	197.0	0.5	1875.00
152	0.6	−117.0	1.6	950.00
153	0.4	−363.0	1.95	1111.25
154	0.35	16.0	1.26	4437.50
155	0.55	−123.0	0.76	2750.00
156	0.4	23.0	1.58	370.00
157	0.35	52.0	1.48	370.00
158	0.35	320.0	0.58	518.75
159	0.4	−108.0	0.36	1475.00
160	0.6	−23.0	1.04	5175.00
161	0.4	−566.0	1.26	873.75
162	0.5	−55.0	1.28	2637.50
163	0.45	−305.0	0.85	486.25
164	0.5	93.0	1.9	460.00
165	0.55	42.0	0.75	457.50
166	0.5	59.0	1.46	1312.50
167	0.5	−175.0	0.96	5462.50
168	0.4	−450.0	1.07	11,437.50
169	0.5	107.0	1.66	1163.75
170	0.45	−8.0	1.86	650.00
171	0.6	192.0	1.56	1300.00
172	0.35	43.0	0.62	573.75
173	0.45	−120.0	0.73	190.00
174	0.6	−96.0	1.35	966.25
175	0.55	−58.0	1.09	3137.50
176	0.25	−69.0	0.77	3225.00
177	0.5	−420.0	0.94	978.75
178	0.4	−225.0	0.84	2675.00
179	0.35	123.0	0.89	2287.50
180	0.6	−115.0	0.7	1825.00
181	0.3	−63.0	1.31	1250.00
182	0.4	−175.0	1.57	1108.75
183	0.6	97.0	1.79	1425.00
184	0.5	2.0	1.56	1750.00
185	0.55	179.0	1.5	647.50
186	0.45	40.0	1.89	968.75
187	0.4	65.0	0.67	733.75
188	0.7	200.0	1.41	555.00
189	0.5	−44.0	1.23	1950.00
190	0.35	−58.0	1.44	631.25
191	0.4	−116.0	1.34	2362.50
192	0.35	−293.0	1.28	338.75
193	0.35	153.0	0.71	985.00
194	0.5	−316.0	1.32	1600.00
195	0.2	−231.0	0.35	4574.00
196	0.5	−162.0	1.09	3400.00
197	0.4	−94.0	0.73	1675.00
198	0.6	167.0	1.89	370.00
199	0.45	−62.0	1.25	324.00
200	0.55	−327.0	1.01	1132.00
201	0.6	−210.0	1.02	863.00
202	0.35	−197.0	1.42	2350.00
203	0.5	−550.0	1.88	1850.00
204	0.6	−290.0	0.32	863.00
205	0.5	−68.0	1.22	2887.00
206	0.3	−192.0	1.48	7912.00
207	0.5	63.0	1.56	1625.00
208	0.5	37.0	1.1	2237.00
209	0.45	−57.0	1.28	950.00
210	0.6	−154.0	0.73	661.00
	0.48	**−165.7**	**1.2**	**1950.38**

BMDJ/FDOJ = bone-marrow defects of the jaw/fatty-degenerative osteolysis/osteonecrosis of the jaw; DVT = digital volume tomography; HU = Hounsfield units; OPG = orthopantomogram; R/C = RANTES/CCL5; TAU-n = new through-transmission alveolar ultrasonography.

The mean value obtained pre-operatively for 2-D OPG was a relative bone density of 0.48; for 3-D DVT HU the value was −165.7 (normal ≥ 300), and for CaviTAU Average(log) the value was 1.2 (normal bone density > 2.0). For R/C expression, the mean was 1950.38 pg/mL (normal = 149.9 pg/mL). Pre-operative HU attenuation coefficients and corresponding TAU-n attenuation coefficients (Average(log); columns in gray) are compared with postoperatively measured levels of R/C expression from the samples obtained during surgical treatment for BMDJ/FDOJ (columns in blue). MV refers to the medium values obtained in the course of our research, and the final row compares the corresponding values of healthy jawbone found in the literature (HUs; Guglielmi and de Terlizzi 2009; Mah et al. 2010; Komar et al. 2019) and R/C levels (pg/mL; Klein et al. 2008; Lechner and Mayer 2010; Lechner and von Baehr 2013, 2015; Lechner, Huesker et al. 2017; Lechner, Schuett et al. 2017).

another. The distance between the surfaces of the receiver and the alveolar ridge was shown to vary widely.

As a solution, a semi-solid gel pad was placed between the receiver and the alveolar ridge of the patient. The sound velocity in the gel used should fall within the same range as that of soft tissue (*i.e.,* 1460−1615 m/s) and the gel should have a sound attenuation ranging from 0.3−1.5 dB/cm (1 MHz), so as not to impede the acoustical measurements in the jawbone. The haul-off speed for spontaneous resilience should not exceed 80 mm/s. The semi-solid property of the gel prevents it from evaporating or disappearing before or during measurement. To perform the measurements, inside the gel pad is a small pocket into which the receiver can be inserted. Following the elimination of any air bubbles between the receiver and the semi-solid gel, the measuring unit is ready for use.

Calibration of the TAU-n

The arrangement of the measuring unit in a defined geometry allows for easy calibration of the TAU-n. This functional test is performed with flexible gel pads covering both the transmitter and the receiver. Figure 8 illustrates the procedure—the full immersion of both parts into a vessel

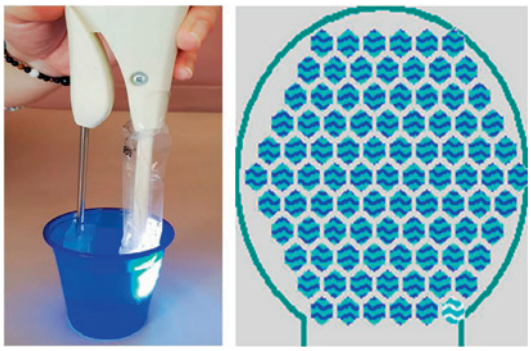

Fig. 8. Water test for calibration. Left: Transmitter and receiver must be completely submerged in water. Right: All sensor elements show watermarks with the exception of the lower right sensor element.

filled with water. The complete acoustic coupling is visible when all sensor elements show the watermark in the left image of the sensor on the computer display. This calibration in a water bath at constant conditions allows for compensation of possible deviation of the elements as a starting point for measurement. The calibration test ensures that no air pockets interfere in the arrangement of cushions, gel and sleeves and that no failure of elements or components leads to misinterpretation.

POST-OPERATIVE METHOD FOR DETERMINING BMDJ/FDOJ

Determining BMDJ/FDOJ with R/C expression

BMDJ/FDOJ cavitations contain degenerated adipocytes that exhibit a particular expression profile of the chemokine R/C (Lechner and Mayer 2010; Lechner and von Baehr 2013, 2015; Lechner, Huesker et al. 2017; Lechner, Schuett et al. 2017). Hence, BMDJ/FDOJ samples were also analyzed for expression of the inflammatory immune mediator R/C. Laboratory procedures used to define R/C expression levels in healthy jawbone and in BMDJ/FDOJ have been previously published; healthy jawbone showed R/C expression levels of 149 pg/mL, whereas a significant number of BMDJ/FDOJ samples (n = 301) among people with chronic disease (average age: 54.05 y; age range: 23−75 y; gender ratio: 89 women to 225 men) showed a 20-fold increase in R/C expression of 2940 pg/mL (Lechner and Mayer 2010; Lechner and von Baehr 2013, 2015; Lechner, Huesker et al. 2017; Lechner, Schuett et al. 2017). BMDJ/FDOJ is the only bone resorption process that shows R/C overexpression (Lechner et al. 2018). BMDJ/FDOJ also displays a reduction in expression of tumor necrosis factor-α and interleukin-6, whereas all other bone resorption-related diseases are characterized by overexpression of tumor necrosis factor-α and interleukin-6. In summary, the recent literature has shown that BMDJ/FDOJ not only is characterized by reduced mineralization and diminished bone density but also plays an important role in osteoimmunologic processes. Thus, R/C overexpression alone is involved in the characteristic and bone-degrading aspect of BMDJ/FDOJ (Lechner et al. 2018).

Based on findings in the literature (Lechner and Mayer 2010; Lechner and von Baehr 2013, 2015; Lechner, Huesker et al. 2017; Lechner, Schuett et al. 2017), it is known that an R/C expression level higher than 149 pg/mL indicates the presence of osteonecrosis or osteolysis which has resulted in diminished jawbone density. A control group of 19 participants volunteered to provide samples of healthy jawbone, which were removed using drill cores during dental implantation surgery. The inclusion criteria for this group were as follows: absence of distinctive radiologic features in 2-D OPG and 3-D DVT and inconspicuous TAU-n measurements of bone density in the implantation area. The use of bisphosphonate medication was the central exclusion criterion. The demographic data for the 19 participants in the BMDJ/FDOJ control group were average age, 51.4 y; age range, 33−72 y; gender breakdown, 10 women, 9 men.

Collection of pre-operative rel-JBD, HU and TAU-n values and post-operatively measured levels of R/C expression

In this study, a cohort of 210 participants who exhibited clinical evidence of BMDJ/FDOJ (*i.e.,* HU value, local R/C expression profile and TAU-n measurements) was identified

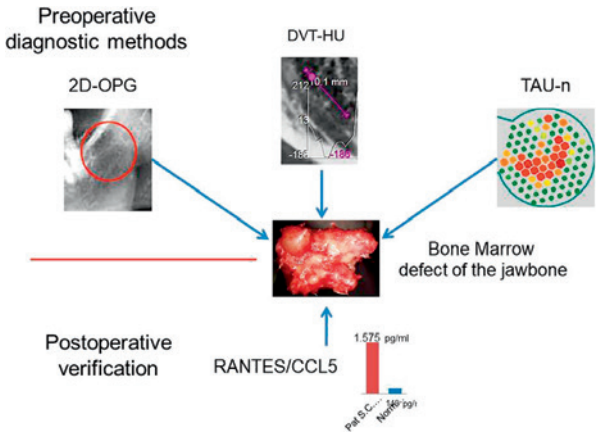

Fig. 9. The possible methods used to localize BMDJ/FDOJ. Pre-operative 2-D OPG is insufficient, but DVT with the possibility of HU measurement may provide a clear indication of BMDJ/FDOJ. The use of TAU-n as a novel, radiation-free measurement option is evaluated in this article. Post-operative multiplex analysis shows extreme R/C overexpression, providing evidence of inflammation. BMDJ/FDOJ = bone-marrow defects of the jaw/fatty-degenerative osteolysis/osteonecrosis of the jaw; DVT = digital volume tomography; HU = Hounsfield units; OPG = orthopantomogram; R/C = RANTES/CCL5; TAU-n = new through-transmission alveolar ultrasonography.

to investigate our research objective in a clinical setting. The schematic representation in Figure 9 illustrates the four validation parameters discussed and used in this study. Each of the participants in this group was assessed with TAU-n. To be included in this group, each participant was required to have the following with respect to the area of BMDJ/FDOJ investigated: positive pre-operative TAU-n measurements, low bone density (in HU values) and a post-operative evaluation of R/C expression. We compared the pre-operative TAU-n and HU values of the research group with the post-operatively obtained laboratory results of R/C expression of the corresponding jawbone areas of BMDJ/FDOJ.

Statistical analysis

The statistical analysis was conducted using the statistical software R version 3.5.1. The similarity between the HU and TAU-n methods was verified by means of the Spearman correlation coefficient.

RESULTS

Comparison of pre-operative TAU-n and HU values with post-operative evaluation of R/C expression

After evaluating the detection of BMDJ/FDOJ using TAU-n, we established clinical evidence of the TAU-n attenuation coefficients by comparing and verifying pre-operative HU and TAU-n values with the post-operatively determined R/C expression levels of corresponding BMDJ/FDOJ areas. The results are shown in Table 1. In Figure 9, we present three pre-operative methods and one post-operative method used to assess BMDJ/FDOJ. For this group of 210 participants, we carried out each of these four methods and compared the results, *i.e.,* (A) the OPG bone density; (B) the preoperative HU attenuation coefficients; (C) the corresponding TAU-n attenuation coefficients of BMDJ/FDOJ according to Average(log) in the TAU-n software (TAU-n Log in Table 1 = Average (log); see Fig. 7); and (D) the R/C expression levels in the fatty degenerated samples obtained during BMDJ/FDOJ surgery (Table 1).

Comparison of rel-JBD, HU and TAU-n values of healthy jawbone

To ensure that TAU-n generates significantly higher attenuation values in jawbone where BMDJ/FDOJ is not present, we measured rel-JBD, HU and TAU-n values in healthy jawbone. To obtain valid negative results, we focused on bone-marrow areas beneath healthy molar teeth. The process of determining rel-JBD and HU was already shown in Figure 1. The results obtained for healthy jawbone in 10 participants are presented in Table 2. We were unable to measure R/C values, because surgical intervention in areas of healthy jawbone was not possible for ethical reasons.

Table 2. Measurement of rel-JBD, HU and TAU-n values in healthy jawbone

Participant	Area	OPG	HU	TAU
1	37	0.55	272	7.02
2	37	0.5	599	8.49
3	47	0.55	97	4.46
4	37	0.45	193	7.14
5	36	0.55	678	6.89
6	37	0.45	271	11.51
7	36	0.35	744	6.71
8	46	0.6	306	10.51
9	47	0.4	329	6.16
10	37	0.4	315	9.79
Mean		0.48	380.4	7.868

HU = Hounsfield units; OPG = orthopantomogram; OPG: rel-JBD = relative bone density of the jawbone; TAU-n = new through-transmission alveolar ultrasonography.

Comparison of rel-JBD, HU and TAU-n values of healthy jawbone and BMDJ/FDOJ areas

The bone densities measured in healthy jawbone and BMDJ/FDOJ areas are compared as mean values. There is clear agreement in the rel-JBD values obtained with 2-D OPG (4.8 BMDJ/FDOJ, 4.8 healthy), whereas the HU values (−165 BMDJ/FDOJ, 380 healthy) and particularly TAU-n values (1.2 BMDJ/FDOJ, 7.8 healthy) differ significantly (Fig. 10).

DISCUSSION

Bone-marrow defects and 2-D OPG

To compare the results documented in Table 1 in terms of their clinical significance, we calculated 10 mean values of jawbone density measurements obtained with 2-D OPG from three different dental colleagues

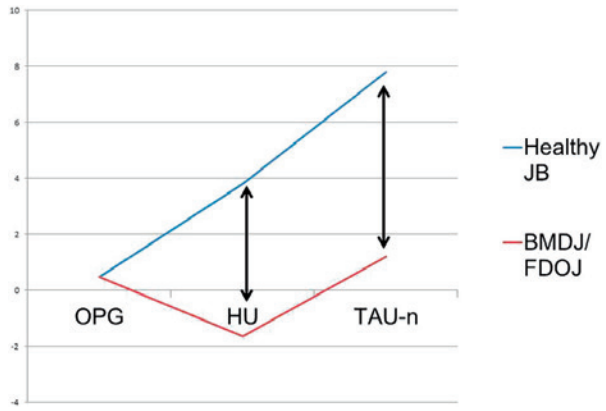

Fig. 10. Comparison of relative bone-density values determined with 2-D OPG, attenuation coefficients in HUs (1:100) and TAU-n values in healthy and BMDJ/FDOJ cohorts. BMDJ/FDOJ = bone-marrow defects of the jaw/fatty-degenerative osteolysis/osteonecrosis of the jaw; HU = Hounsfield units; OPG = orthopantomogram; TAU-n = new through-transmission alveolar ultrasonography.

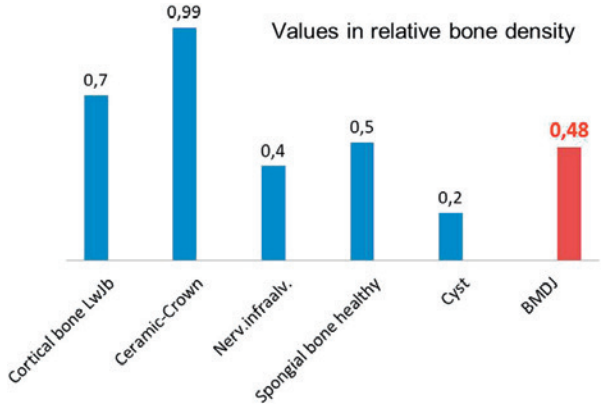

Fig. 11. Comparison of various density values with BMDJ/FDOJ values obtained using 2-D OPG. This shows that normal bone density measured in healthy spongial cancellous bone structure with a value of 0.5 is only slightly denser than the mean value of the 210 BMDJ/FDOJ areas we examine, with a medium value of 0.48. This explains in part why there is widespread doubt among dentists in the discussion about the actual existence of BMDJ/FDOJ. In summary, a critical detection of medullary bone density in BMDJ/FDOJ areas is not possible with 2-D OPG (Lechner 2014). BMDJ/FDOJ = bone-marrow defects of the jaw/fatty-degenerative osteolysis/osteonecrosis of the jaw; OPG = orthopantomogram.

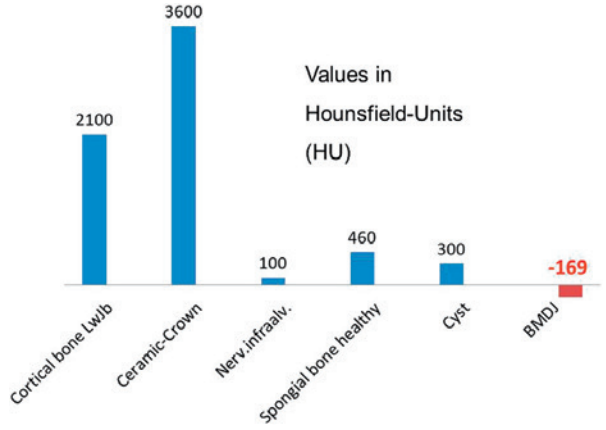

Fig. 12. Comparison of a wide variety of density values with BMDJ/FDOJ values obtained with 3-D DVT. This shows that the HU value of −169 produced by the reduced X-ray attenuation in the softened BMDJ/FDOJ areas is significantly less than the minimum value of 300 reported as healthy in the literature. A reliable assessment of the medullary bone density in areas of BMDJ/FDOJ is possible with the HU values derived using high-quality 3-D DVT (Loubele et al. 2009; Roberts et al. 2009). However, this method of examination requires a relatively high radiation exposure. Furthermore, DVT devices which provide the necessary HU measurement are costly. In our experience, inexpensive DVT units fail to achieve the requisite quality and lead to incorrect assessments based on purely subjective evaluation. BMDJ/FDOJ = bone-marrow defects of the jaw/fatty-degenerative osteolysis/osteonecrosis of the jaw; DVT = digital volume tomography; HU = Hounsfield units.

with available radiographs. The five control parameters comprised the following measurements: cortical bone on the mandibular branch, all-ceramic crown, the canal of the infra-alveolar nerve, cancellous bone normal, and cyst lumen. Figure 11 shows these values in blue. Bone-density values in areas of BMDJ/FDOJ collected from the cohort of 210 participants are presented in red.

Bone-marrow defects and 3-D DVT

As with the 2-D OPG radiographs, to compare the results documented in Table 1 in terms of their clinical significance we calculated 10 mean values of 3-D DVT measurements from three different dental colleagues with existing radiographs as before. Figure 12 shows these HU values in blue. The bone-density value of −169 HUs in the BMDJ/FDOJ areas collected from the cohort of 210 participants is presented in red.

Bone-marrow defects and TAU-n

When the TAU-n Average(log) values are compared with the DVT HU values determined in this study, both correspond to reduced bone density, which implies the presence of BMDJ/FDOJ. Further, the general correlation of HU and R/C multiplex analysis with the Average(log) values generated using the TAU-n software may be confirmed. In previous publications, light microscopy has also confirmed the reduction of bone density determined by the CaviTAU Average(log) values (Lechner et al. 2020).

The threshold for which TAU-n log indicates BMDJ/FDOJ

As shown in Table 1, the mean value of 210 TAU-n measurements in BMDJ/FDOJ areas is 1.2, with a range of 0.3 (#5) to 1.95 (#153). Accordingly, we defined the threshold for which a TAU-n log indicates diminished bone density corresponding to a BMDJ/FDOJ area at a TAU-n value of 2. TAU-n values of 4.49, 2.29 and 2.67 (participants 4, 53 and 123) were the only measurements determined beyond this threshold of 2; however, a 20-fold, 4-fold and 10-fold overexpression of R/C was also detected in these cases.

R/C expression in BMDJ/FDOJ

The values of R/C expression in the BMDJ/FDOJ samples analyzed post-operatively with multiplex methods in the laboratory average 1950.38 pg/mL, which is 13 times the normal value of 149.9 pg/mL found in healthy jawbone that we have previously published (Lechner and von Baehr 2013). First and foremost, the application of TAU-n allows for the use of low radiation levels in the stress-free detection of mineralization and

metabolic disorders in the medullary region of the jawbone. Medical devices that aim to measure specific phenomena must be able to consistently reproduce their results. In this respect, the measurements obtained with TAU-n are reliable and primarily free of operator error, as the TAU-n transmitter and receiver are positioned along a coplanar axis in a fixed arrangement. This ensures the necessary independence from the operator and the reproducibility of TAU-n measurements. Errors in acoustic coupling are avoided by displaying a gray sensor field, which is not associated with ultrasound transmission during the measurement process.

Limits in the comparability of the measured HU and TAU-n values

A 1:1 correlation of the measured values obtained with DVT in HUs and using TAU-n is not possible because both examination methods are physically different and thus measure different distances in the jaw. However, a general technical correlation may be made as follows: The measured HU values correspond to a selected cross-sectional slice of the jaw, whereas TAU-n penetrates through the entire distance from the transmitter to the sensor and thus reproduces the typical reflective and scattering properties of ultrasound. TAU-n is therefore unable to isolate particular sections within the jawbone. Furthermore, the attenuation coefficients of both methods behave in completely opposite ways. With HUs, the denser the irradiated object, the greater the positive attenuation coefficients and the lower the transmission. With TAU-n, the greater the density of the object to be examined, the lower the attenuation coefficients and, thus, the greater the sound transmission. A relationship between the two methods can still be established, however, as conspicuous areas assessed using HUs are also detectable with TAU-n and *vice versa*. To ensure that TAU-n is a reliable indicator of poor bone quality, this approach should be validated in people without BMDJ/FDOJ. Here we face an ethical obstacle, as people with HU values >300 and TAU-n log >2 are inappropriate candidates for jawbone surgery. Thus it is not possible to obtain R/C values in such cases. The study design we used is thus unable to fully answer the initial question posed in this study.

SUMMARY

The interest in the application of TAU-n lies in the decrease in bone density in BMDJ/FDOJ owing to osteolysis. The upper limit of DVT HU values of interest with respect to BMDJ/FDOJ is +300, as at this point there is a transition to healthy cancellous bone. Values over +300 HUs thus fall outside the necessary detection range of TAU-n. The HU values produced in this study (range: −680 to +150) indicate BMDJ/FDOJ in class 5 cases (Mah et al. 2010). The data presented here show that HU values demonstrate osteolysis and correspond to R/C overexpression in BMDJ/FDOJ areas (Lechner et al. 2018). When the data derived from both methods used to evaluate BMDJ/FDOJ (*i.e.,* HU values and R/C expression) are compared with the TAU-n results, there is a correlation between the attenuation coefficients of HUs and TAU-n. Thus, it may be assumed that TAU-n, which uses ultrasound waves, is able to provide an accurate representation of the degrees of mineralization and bone density in the jawbone area.

- Using the Average(log) values generated with TAU-n, we confirmed a general correspondence between HU values and R/C multiplex analysis in a cohort of 210 people with BMDJ/FDOJ patients.
- Table 1 shows two participants (#53 = 2.29 and #123 = 2.67) with an Average(log) value > 2 from the total of 210 participants.
- Here, HU values and post-operatively measured levels of cytokine expression confirm the reliability of TAU-n measurements with respect to displaying decreased bone density in cases of BMDJ/FDOJ.

LIMITATIONS

The limitations of this study include the sample size. Bias may also be present owing to the fact that not all parameters were validated in the cohort with healthy jawbone. For ethical reasons, surgical intervention and the measurement of R/C expression in healthy jawbone without any sign of BMDJ/FDOJ was not applicable.

CONCLUSION

A newly developed ultrasonography device (TAU-n) is able to detect and localize BMDJ/FDOJ caused by the fatty-degenerative dissolution of medullary trabecular structures in the jawbone. As other studies have confirmed (Guglielmi and de Terlizzi 2009; Komar et al. 2019), ultrasonography is a low-cost and efficient means of assessing jawbone health, and this was replicated with the use of the new TAU device presented here. This study established a new value using TAU-n which provides a reliable indicator of poor bone quality, rendering the device a useful tool for treatment-planning strategies in implantology as well as for fostering cooperation among professionals when assessing or treating osteoimmunologic diseases and linking such diseases with the immune system. TAU-n thus provides a non-harmful alternative to the use of X-ray irradiation, which is increasingly criticized (Brenner et al. 2001; Vañó et al. 2017), particularly in view of more stringent radiation protection laws (Strahlenschutzgesetz 1966).

TAU-n represents a novel type of imaging acquisition process in dentistry and offers the ability to non-invasively assess hidden BMDJ/FDOJ in the human jawbone. Further extensive clinical trials and multicenter comparative measurements examining TAU-n should be carried out to establish a new classification based on ultrasound and perform a reliability assessment.

Acknowledgments—English-language editing of this manuscript was provided by Journal Prep Services. Additional editing was provided by Natasha Gabriel. The practical measurements with the TAU-n were performed at our clinic by Gabriele Zidek and Tanja Scheller.

Conflict of interest disclosure—CaviTAU (Munich, Germany), the company that designed the new TAU-n apparatus and associated software, provided these tools without charge for the purposes of this study. The ultrasonography procedure was carried out at the Clinic for Integrative Dentistry (Munich, Germany). CaviTAU and the Clinic for Integrative Dentistry are engaged in ongoing discussions regarding numerous collaborative arrangements to further improve and verify the new TAU apparatus, CaviTAU, as it is introduced to the market. The corresponding author is the holder of a patent used in the CaviTAU.

REFERENCES

Al-Nawas B, Grötz KA, Kann P. Ultrasound transmission velocity of the irradiated jaw bone in vivo. Clin Oral Investig 2001;5:266–268.

Bouquot JE, Roberts AM, Person P, Christian J. Neuralgia-inducing cavitational osteonecrosis (NICO): Osteomyelitis in 224 jawbone samples from patients with facial neuralgia. Oral Surg Oral Med Oral Pathol 1992;73:307–319.

Brenner DJ, Elliston CD, Hall EJ, Berdon WE. Estimated risks of radiation-induced fatal cancer from pediatric CT. AJR Am J Roentgenol 2001;176:289–296.

Greenfield MA, Craven JD, Huddleston A, Kehrer ML, Wishko D, Stern R. Measurement of the velocity of ultrasound in human cortical bone in vivo: Estimation of its potential value in the diagnosis of osteoporosis and metabolic bone disease. Radiology 1981;138:701–710.

Guglielmi G, de Terlizzi F. Quantitative ultrasound in the assessment of osteoporosis. Eur J Radiol 2009;71:425–431.

Kaufman JJ, Einhorn TA. Ultrasound assessment of bone. J Bone Miner Res 1993;8:517–525.

Klein MO, Grötz KA, Manefeld B, Kann PH, Al-Nawas B. Ultrasound transmission velocity for noninvasive evaluation of jaw bone quality *in vivo* before dental implantation. Ultrasound Med Biol 2008;34:1966–1971.

Komar C, Ahmed M, Chen A, Richwine H, Zia N, Nazar A, Bauer L. Advancing methods of assessing bone quality to expand screening for osteoporosis. J Osteopath Med 2019;119:147–154.

Kumar VV, Sagheb K, Klein MO, Al-Nawas B, Kann PH, Kämmerer PW. Relation between bone quality values from ultrasound transmission velocity and implant stability parameters—an *ex vivo* study. Clin Oral Implants Res 2012;23:975–980.

Lechner J. Validation of dental X-ray by cytokine RANTES—comparison of X-ray findings with cytokine overexpression in jawbone. Clin Cosmet Investig Dent 2014;6:71–79.

Lechner J, Huesker K, Von Baehr V. Impact of RANTES from jawbone on Chronic Fatigue Syndrome. J Biol Regul Homeost Agents 2017;31:321–327.

Lechner J, Mayer W. Immune messengers in neuralgia inducing cavitational osteonecrosis (NICO) in jaw bone and systemic interference. Eur J Integr Med 2010;2:71–77.

Lechner J, Rudi T, von Baehr V. Osteoimmunology of tumor necrosis factor-alpha, IL-6, and RANTES/CCL5: A review of known and poorly understood inflammatory patterns in osteonecrosis. Clin Cosmet Investig Dent 2018;10:251–262.

Lechner J, Schuett S, von Baehr V. Aseptic-avascular osteonecrosis: Local "silent inflammation" in the jawbone and RANTES/CCL5 overexpression. Clin Cosmet Investig Dent 2017;9:99–109.

Lechner J, von Baehr V. Chemokine RANTES/CCL5 as an unknown link between wound healing in the jawbone and systemic disease: Is prediction and tailored treatments in the horizon?. EPMA J 2015;6:10.

Lechner J, von Baehr V. RANTES and fibroblast growth factor 2 in jawbone cavitations: Triggers for systemic disease?. Int J Gen Med 2013;6:277–290.

Lechner J, Zimmermann B, Schmidt M, von Baehr V. Ultrasound sonography to detect focal osteoporotic jawbone marrow defects: Clinical comparative study with corresponding Hounsfield units and RANTES/CCL5 expression. Clin Cosmet Investig Dent 2020;12:205–216.

Lee SC, Jeong CH, Im HY, Kim SY, Ryu JY, Yeom HY, Kim HM. Displacement of dental implants into the focal osteoporotic bone marrow defect: A report of three cases. J Korean Assoc Oral Maxillofac Surg 2013;39:94–99.

Lipani CS, Natiella JR, Greene GW, Jr. The hematopoietic defect of the jaws: A report of sixteen cases. J Oral Pathol Med 1982;11:411–416.

Loubele M, Bogaerts R, Van Dijck E, Pauwels R, Vanheusden S, Suetens P, Marchal G, Sanderink G, Jacobs R. Comparison between effective radiation dose of CBCT and MSCT scanners for dentomaxillofacial applications. Eur J Radiol 2009;71:461–468.

Mah P, Reeves TE, McDavid WD. Deriving Hounsfield units using grey levels in cone beam computed tomography. Dentomaxillofac Radiol 2010;39:323–335.

Mahmoud A, Cortes D, Abaza A, Ammar H, Hazey M, Ngan P, Crout R, Mukdadi O. Noninvasive assessment of human jawbone using ultrasonic guided waves. IEEE Trans Ultrason Ferroelectr Freq Control 2008;55:1316–1327.

Misch CE. Bone density: A key determinant for clinical success. In: Misch CE, ed. Contemporary implant dentistry. 2nd edition St Louis: CV Mosby; 1999. p. 109–118.

Njeh CF, Hans D, Fuerst T, Glüer CC, Genant HK. Quantitative ultrasound: Assessment of osteoporosis and bone status. London: Martin Dunitz; 1999.

Norton MR, Gamble C. Bone classification: An objective scale of bone density using the computerized tomography scan. Clin Oral Implants Res 2001;12:79–84.

Roberts JA, Drage NA, Davies J, Thomas DW. Effective dose from cone beam CT examinations in dentistry. Br J Radiol 2009;82:35–40.

Strahlenschutzgesetz (StrlSchG) Artikel 1 G. v. 27.06.2017 BGBl. I S. Strahlenschutzverordnung (StrlSchV) Artikel 1 V. v. 29.11.2018 BGBl. I S. 2034, 2036. Gesetz zur Neuordnung des Rechts zum Schutz vor der schädlichen Wirkung ionisierender Strahlung (StrlSchGEG) G. v. 27.06.2017 BGBl. I S. 1966. .

Swennen GRJ, Schutyser F. Three-dimensional cephalometry: Spiral multi-slice vs cone-beam computed tomography. Am J Orthod Dentofacial Orthop 2006;130:410–416.

Vañó E, Miller DL, Martin CJ, Rehani MM, Kang K, Rosenstein M, Ortiz-López P, Mattsson S, Padovani R, Rogers A. Authors on behalf of ICRP. ICRP publication 135: Diagnostic reference levels in medical imaging. Ann ICRP 2017;46:1–144.

Wells PNT. Ultrasonic imaging of the human body. Rep Prog Phys 1999;62:671.

Clinical, Cosmetic and Investigational Dentistry

Dovepress

open access to scientific and medical research

Open Access Full Text Article

ORIGINAL RESEARCH

Osteonecrosis of the Jaw Beyond Bisphosphonates: Are There Any Unknown Local Risk Factors?

This article was published in the following Dove Press journal:
Clinical, Cosmetic and Investigational Dentistry

Johann Lechner[1]
Volker von Baehr[2]
Bernd Zimmermann[3]

[1]Clinic for Integrative Dentistry, Munich, Germany; [2]Department of Immunology and Allergology, Institute for Medical Diagnostics, Berlin, Germany; [3]QINNO, Wessling, Germany

Introduction: Bisphosphonate (BP)-related osteonecrosis of the jaw (BRONJ) is a complication of intravenous (IV) BP therapy. BP therapy locally affects the dentoalveolar area, while systemic effects are associated with parenteral/IV BP use. Despite numerous publications, the pathogenesis of BRONJ is not fully understood, as only some patients receiving IV BPs develop BRONJ.

Purpose: Can impaired bone remodeling (found in aseptic-ischemic osteonecrosis of the jaw [AIOJ], bone marrow defects [BMD], or fatty-degenerative osteonecrosis of the jaw [FDOJ]) represent a risk factor for BRONJ formation?

Patients and Methods: A literature search clarified the relationship between AIOJ, BMD, FDOJ, and BRONJ, in which common characteristics related to signal cascades, pathohistology, and diagnostics are explored and compared. A case description examining non-exposed BRONJ is presented.

Discussion: Non-exposed BRONJ variants may represent one stage in undetected BMD development, and progression to BRONJ results from BPs.

Conclusion: Unresolved wound healing at extraction sites, where wisdom teeth have been removed for example, may contribute to the pathogenesis of BRONJ. With IV BP administration, persisting AIOJ/BMD/FDOJ areas may be behind BRONJ development. Therapeutic recommendations include IV BP administration following AIOJ/BMD/FDOJ diagnosis and surgical removal of ischemic areas. BPs should not be regarded as the only cause of osteonecrosis.

Keywords: bisphosphonates, bone marrow defects, osteonecrosis of the jaw, RANTES/CCL5, ultrasound sonography

Introduction

Recent literature reviews suggest that bisphosphonates (BPs) may contribute to the growing number of cases of osteonecrosis involving the maxilla and mandible that are associated with the pathogenesis of BP-related osteonecrosis of the jaw (BRONJ).[1] In the discussion concerning BRONJ, a distinction must be made between diseases featuring reduced osseous mineral content, which may be counteracted by BPs (such as those occurring during menopause or in cases of osteoporosis), and cases that present with indications for BPs (such as tumors). BPs have been used in the treatment of multiple myeloma, breast cancer, prostate cancer, and other tumors. In patients with metastatic breast cancer, the bones are affected in around two-thirds of cases. To protect patients from bone fractures and to reduce

Correspondence: Johann Lechner
Clinic for Integrative Dentistry, Gruenwalder Str. 10A, Munich 81547, Germany
Tel +49-89-6970129
Fax +49-89-6925830
Email drlechner@aol.com

submit your manuscript | www.dovepress.com
DovePress
http://doi.org/10.2147/CCIDE.S288603

pain, patients are often prescribed BPs or a special antibody that prevents the breakdown of, and subsequently stabilizes, affected bone. BRONJ is a newly emerging problem that is recognized as a serious complication of BP therapy, primarily following intravenous (IV) administration.[2]

The concern is that BPs affect the natural remodeling of bone tissues and delay the breakdown of older bone structures. BPs are potent inhibitors of bone resorption and have a chronic effect over a half-life of at least 5 years, possibly exerting their effects for more than 10 years. BRONJ is a seemingly "growing epidemic" associated with osteonecrosis of the jawbone (ONJ).[3–5] The long-term effects of oncological-related BP treatment on alveolar bone quality include the impact on BP-induced overexpression of alveolar bone remodeling. There are increased osteosclerotic properties in the alveolar bone that are associated with significantly greater bone volume and higher bone density.[6,7] The risk of BP therapy is divided into two categories: local and systemic risk factors; thus, a distinction must be made between oral and IV administration. Local oral risk factors for BRONJ in cancer patients include dentoalveolar surgery, dental extraction, and dental implant insertion.[8] Periodontal infections also significantly increase the risk of BRONJ in cancer patients.[9] In addition, there is a significant correlation between the use of removable prostheses, the administration of high-dose IV BPs, and an increased risk of BRONJ.[10] In patients receiving oral BP therapy for the treatment of osteoporosis, the prevalence of BRONJ only increased 0.21% from close to 0%. Systemically, however, there is a much higher risk associated with the IV injection of BPs. This is closely related to the frequent use of BPs in cancer patients who receive a significantly higher total dose over a longer duration.[11] The mean and minimum time for the development of ONJ is 1.8 years and 10 months, respectively.[12] The risk of BRONJ in cancer patients exposed to BP therapy is from 50–100 times higher than in cancer patients treated with a placebo. The BRONJ risk for the RANKL inhibitor denosumab was between 0.7% and 1.9%.[13,14] The risk of ONJ in cancer patients treated with high doses of IV BPs appears to be significantly higher: in the range of 1–10 per 100 patients (depending on therapy duration).[15] A recent review reported a wide-ranging BRONJ incidence of 0–27.5% that was associated with the IV administration of BPs, with an average incidence of 7%.[16] The cumulative frequency varied from 0.8–12.0% and was estimated to be up to 30.0% in some reports.[17,18] Despite numerous publications on the subject, the overall pathogenesis of BRONJ does not yet appear to be fully understood. In particular, the reasons why only a subset of patients (<30%) receiving IV BPs develop BRONJ remain unclear. Although most patients that develop BRONJ have a history of tooth extraction or injury, these factors do not fully explain the occurrence of BRONJ.[8] The development of BRONJ in edentulous areas in patients with no apparent history of injury suggests that pre-existing conditions, such as subclinical infections or potentially necrotic areas of the jawbone, may contribute to the conditions that lead to the development of BRONJ.

Research Question

Why does BRONJ develop in up to 30% of individuals following IV BP therapy and not the remaining 70%? This review raises the question of whether little-known or difficult-to-identify, pre-existing, impaired bone remodeling, such as that occurring in aseptic-ischemic osteonecrosis of the jaw (AIOJ), bone marrow defects (BMD), or fatty-degenerative osteonecrosis of the jawbone (FDOJ), represents a local risk factor in the development of BRONJ.

Materials and Methods

There is still a limited scientific understanding of the relationship between ONJ and BPs.[19] In order to clarify the research question and present the background and specific common characteristics of AIOJ/BMD/FDOJ and BRONJ, an extensive literature search was carried out in PubMed Central. In the literature, the terms "aseptic-ischemic osteonecrosis of the jaw" (AIOJ), 'bone marrow defects' (BMD), and "fatty-degenerative osteonecrosis of the jawbone" (FDOJ) are used to describe an intramedullary phenomenon with the same pathogenesis, morphology, and pathohistology.

The American Association of Oral and Maxillofacial Surgeons published four staging criteria ("at risk", Stage 0–3).[20] Stage 0 is of particular interest in our research as it refers to patients with "no clinical evidence of exposed bone, but presence of non-specific symptoms or clinical and/or radiographic abnormalities". The discussion concerning BRONJ is complicated by the fact that there are two clinical forms of BRONJ. The first presents as exposed bone in the maxillofacial region with clinically recognizable necrotic bone that is visibly exposed through the oral mucosa or facial skin, and present for more than 8 weeks, which is referred to as so-called exposed BRONJ.[15] The second form of BRONJ is particularly interesting for our investigation; it was recently

emphasized that BRONJ does not always appear with necrotic bone visible through a breech in the oral mucosa.[21] This form is referred to as "non-exposed BRONJ" (NE-BRONJ). In the absence of exposed bone, it is characterized by clinical features associated with the jaw, such as unexplained jawbone pain, fistulas/sinus tracts, loose teeth, and swelling.[22,23] Diagnosing NE-BRONJ is difficult, as other common jawbone diseases, such as odontogenic infections, may cause similar symptoms and must be excluded. The non-exposed variant may comprise up to one third of all BRONJ cases and is thus not uncommon;[24] however, this previously underestimated NE-BRONJ is difficult to accurately diagnose. Recently published papers emphasize that NE-BRONJ has received little attention so far and does not fulfill the current definition of BRONJ.[25] Nevertheless, NE-BRONJ belongs to the same disease as exposed BRONJ and should be identified as part of the full spectrum of BRONJ (see the section titled, "Case descriptions of AIOJ/BMD/FDOJ, non-exposed BRONJ, and Actinomyces colonization").[26]

Bisphosphonates and Antitumor Therapy

Our investigation requires the identification of the basic immune mechanisms associated with BP administration. Specifically, which mechanism is behind the anti-tumor activity of BPs in cancer patients?

Bisphosphonates and Mesenchymal Stem Cells

Various studies postulate that BPs change the bone microenvironment around cancer cells, which may prevent cancer cell survival and disease recurrence.[27] BPs may also reduce the appearance of disseminated tumor cells. The formation of metastases is complex; mesenchymal stem cells (MSCs) are predominantly found in the bone marrow.[28] MSCs may contribute to the formation of metastases through various mechanisms: (1) MSCs are recruited to develop breast tumors where they can enhance the metastatic potential of weakly tumorigenic breast cancer cells;[29] (2) MSCs and other bone marrow cells may form a pre-metastatic niche within the specific tissues to which tumor cells metastasize;[30] and (3) MSCs are able to maintain the growth and survival of cancer cells in the bone microenvironment where they may contribute to the formation of niches for dormant micrometastases that can later form distant metastases. BPs significantly reduce the ability of MSCs to migrate, thereby reducing the growth and survival of cancer cells.[31] Thus, the effects of BPs on MSCs in the bone marrow microenvironment contribute to anti-tumor activity by affecting the ability of MSCs to migrate and develop tumors in pre-metastatic niches. BPs disrupt the interaction between MSCs and breast cancer cells within the bone microenvironment, where BPs may also directly inhibit breast cancer cell growth.

Bisphosphonates and Antiangiogenesis

The antiangiogenic effect of BP administration in tumor patients also plays a role in therapy.[32] When administered systemically, BPs effectively inhibit angiogenesis. The pronounced antiangiogenic properties of BPs enhance their effectiveness in the treatment of malignant bone diseases. In addition to suppressing RANTES/CCL5 (R/C) expression in MSCs, BP administration plays a role in the treatment of tumor patients.[33] Similar to exogenous glucocorticoids and estrogen,[34] BPs are ischemic and hypoxia-related stressors of bone health that alter jawbone metabolism, thus leading to osteonecrosis. While tumor-associated BP therapy is currently the "heavy weight" for bone health, it may accelerate existing, chronic pathophysiological events within the microcirculation of bone marrow compartments in the jaw. BRONJ development is often characterized by a slow start and usually presents with infarcts and thrombosis of small vascular sections of the supplying artery within the medullary canal; these features also correspond to AIOJ/BMD/FDOJ. Myeloid elements (including fat marrow) liquefy and cancellous trabeculae are resorbed, so that individual bone spaces merge and gradually create larger cavities.

Osteoimmunological Parameters of AIOJ/BMD/FDOJ and BRONJ with the Same Impact in Response to BPs

If we compare the findings in the sections titled, "Bisphosphonates and mesenchymal stem cells" and "Bisphosphonates and antiangiogenesis" to pre-existing AIOJ/BMD/FDOJ, several strikingly common characteristics shared by BRONJ and AIOJ/BMD/FDOJ can be observed that help to answer our research question. In the sections following "Bisphosphonates and antitumor therapy", we present the foundations for the development of AIOJ/BMD/FDOJ and draw similarities with the development of BRONJ.

RANTES/CCL5: Overexpression as a Common Osteoimmunological Characteristic of BRONJ and AIOJ/BMD/FDOJ

The key function of proinflammatory chemokines R/C in the formation of breast cancer and its metastasis, as well as a possible connection with the intramedullary signaling of R/C overexpression from AIOJ/BMD/FDOJ areas, has been pointed out in previous studies.[35,36] The conspicuous overexpression of R/C in little-known BMDs, as found in AIOJ/BMD/FDOJ, has been reported.[37,38] R/C overexpression is a regulator of healthy bone metabolism in bone needing repair. The starting point for a typical AIOJ/BMD/FDOJ BMDs is the expression of R/C and its chemokine receptors (CCR5) in both osteoblasts (OBs) and osteoclasts (OCs). Ligands (CCL5) and receptors (CCR5) simultaneously activate autocrine and paracrine mechanisms in the bone.[39] One study examined the effects of BPs on human primary OBs and was able to show that the overexpression of proinflammatory R/C from BP-treated OBs also occurs in areas affected by BRONJ.[40] The secretion of proinflammatory cytokines interleukin (IL)-8 and R/C increased after 14 days of treatment with the highest dose of BPs.[40] The complexity of cytokine control becomes clear at this point. In contrast to the tumor, where BPs in the MSCs reduce R/C expression to such an extent that metastasis is prevented, R/C expression is increased by BPs in OBs. If AIOJ/BMD/FDOJ is already present, it may be assumed that the associated increased R/C secretion is thus further increased by BPs. Specifically, NE-BRONJ may develop as BPs increase the expression of IL-8 and R/C.[41] Other researchers have confirmed increases in the secretion of proinflammatory IL-8 and R/C from BP-treated OBs.[42] Combined with the lower proliferation rate of OBs and a decrease in their differentiation, higher doses or accumulations of BPs cause undesirable local changes in the bone by increasing the secretion of IL-8 and R/C from OBs. If these findings are applied to BP administration in the context of a chronic, pre-existing AIOJ/BMD/FDOJ area, then such areas may be expected to exhibit increased R/C secretion in response to BPs. This increase may result from the inhibition of OC activity, leading to the development of BRONJ. Figure 1 summarizes the effects of BP administration on the pre-existing physiological derailments associated with tumor and osteoporosis development.

Ischemia as a Common Osteoimmunological Characteristic of BRONJ and AIOJ/BMD/FDOJ

In the literature, the vascular composition of AIOJ/BMD/FDOJ is characterized by the fact that blood flow in the medullary canal is impaired by micro-infarcts, which leads to chronic marrow ischemia.[43] BRONJ also shows reduced vascularization in the medullary canal.[44] Several publications have shown that ischemic bone diseases such as AIOJ/BMD/FDOJ and BRONJ are of multifactorial origin and emphasize the "multiple stroke model" as the cause of ischemic bone diseases.[45,46] In the orthopedic literature, intensive research conducted on the development of ischemic bone disease in the early stages of the disease

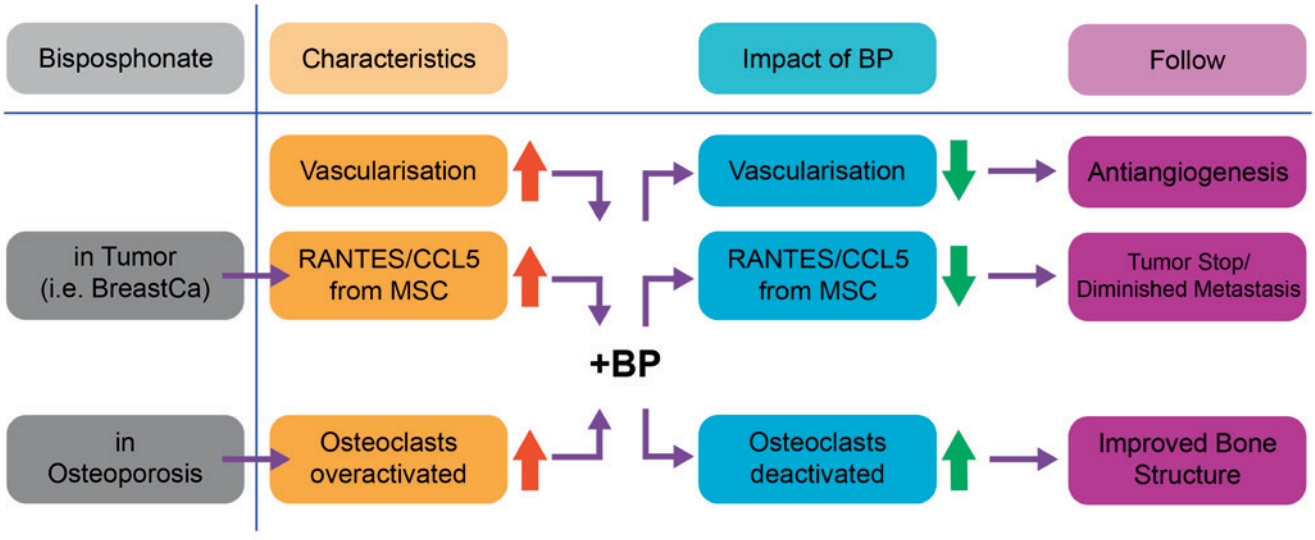

Figure 1 Comparison of the effects of BP administration (+BP) in the context of a tumor (upper part of Figure 1) and pre-existing osteoporosis (lower part of Figure 1).
Legend: The red arrows indicate overactivity; the green arrows show reversal following BP administration.

process is presented.[47] Our aim here is to apply this knowledge not only to extreme forms of the disease, such as osteoradionecrosis and BRONJ, but also to chronic, subclinical, and ischemic forms such as bone marrow edema and AIOJ/BMD/FDOJ, which often progress asymptomatically. Many of these forms are manifestations of both local and systemic risk factors that compromise circulation in the bone marrow, and may also impact on the homeostasis of bone resorption and formation, in addition to BP therapy. The importance of this multifactorial exposure to risk factors for ischemia – and the associated causal genetics that are very similar to those in cases of AIOJ/BMD/FDOJ – is shown by observing how bone that is exposed to BPs demonstrates minimal OC activity, followed by the deposition of newly formed, thicker bone with reduced vascular supply.[48] The resulting mosaic-like pattern of bone remodeling is strikingly similar to that found in Paget's disease, which tends to be associated with the development of osteomyelitis.[49] Similar to AIOJ/BMD/FDOJ, the remodeling induced by BPs leaves cavities, otherwise known as "cavitations", which leads to both necrosis and – unlike that which is found in AIOJ/BMD/FDOJ – subsequent infection by colonizing bacteria. Many patients with AIOJ/BMD/FDOJ have inherited prothrombotic tendencies, which is comparable to what is found in patients with idiopathic osteonecrosis of the femoral head (Paget's disease) and includes thrombophilia and hypofibrinolysis.[50–52] Although a consensus has been reached that ischemic marrow edema is not part of the pathogenesis of BRONJ,[53] it is regarded as a typical characteristic of AIOJ/BMD/FDOJ, serving as a precursor to BRONJ development. Systemic antibiotic therapy has limited access to these avascular zones and surgical debridement is usually necessary.

Osteoblast Activation as a Common Osteoimmunological Characteristic of BRONJ and AIOJ/BMD/FDOJ

The initial OB situation found in AIOJ/BMD/FDOJ is highly characteristic; under pathological conditions, OBs express R/C chemokines in a non-physiological manner.[54,55] The increasing frequency of ONJ and its possible association with high cumulative doses of BPs was investigated in one study, which concluded that high doses of BPs had both OC and OB effects, and thus bone remodeling was inhibited in vivo.[56] Other researchers have examined the proliferation, viability, expression, and secretion of bone markers and cytokines/chemokines from primary OBs following exposure to BPs.[42] Increased concentrations of proinflammatory cytokines were found in response to BPs. Similarly, increased R/C expression is present in AIOJ/BMD/FDOJ. Following treatment with the highest dose of BPs, the secretions of proinflammatory cytokines IL-8 ($P<0.001$) and R/C ($P<0.001$) were significantly increased after 14 days. In addition, the secretion of proinflammatory R/C from OBs exposed to BPs increased. It has also been determined that R/C plays a role in the etiology of the osteolytic changes that are present in AIOJ/BMD/FDOJ.[37,57] The aim of another study was to investigate the effect of BPs on human OBs in vitro, while considering RANKL and osteoprotegerin (OPG), both of which mediate OC differentiation.[40] OPG increased significantly in the group that received BPs at a dose of 10 μM, while RANKL expression decreased significantly with different concentrations of BPs. In summary, exposure to various BP concentrations had a positive effect on OB differentiation, but did not affect proliferation. In contrast, the BP-associated changes in RANKL and OPG production contributed to the suppression of osteoclastic bone resorption. Excess R/C leads to OC inhibition which, in our model, also leads to a disturbance in RANK/RANKL homeostasis (see Figure 2). The chain of reactions that arise from pre-existing AIOJ/BMD/FDOJ and BP administration result in the development of BRONJ in response to the subsequent OB depression; it also leads to increased OC apoptosis. In addition, bone densification takes place following BP administration as a result of increased OB activity. As such, osteonecrosis occurs in the jawbone when BPs are used parenterally. The reasons for these different reactions to BPs have not yet been clarified.

Osteoclast Deactivation as a Common Osteoimmunological Characteristic of BRONJ and AIOJ/BMD/FDOJ

The first step in tumor necrosis factor alpha (TNF-a)-induced OC genesis occurs in the bone marrow.[58] Although mature OCs erode the resorption of the bone as a focal point over the course of months to years, the lifespan of individual OCs is only a few weeks. Thus, mature OCs must be constantly replaced. With respect to OC formation, TNF-a directly stimulates the formation of mature OCs,[59,60] and supports and promotes the survival of mature OCs.[61] TNF-a increases the survival time of OCs to extend the duration of bone resorption. In the early stages of AIOJ/BMD/FDOJ, the situation for OCs is highly contradictory: the extremely low TNF-a values found in areas of AIOJ/BMD/FDOJ – as compared to the

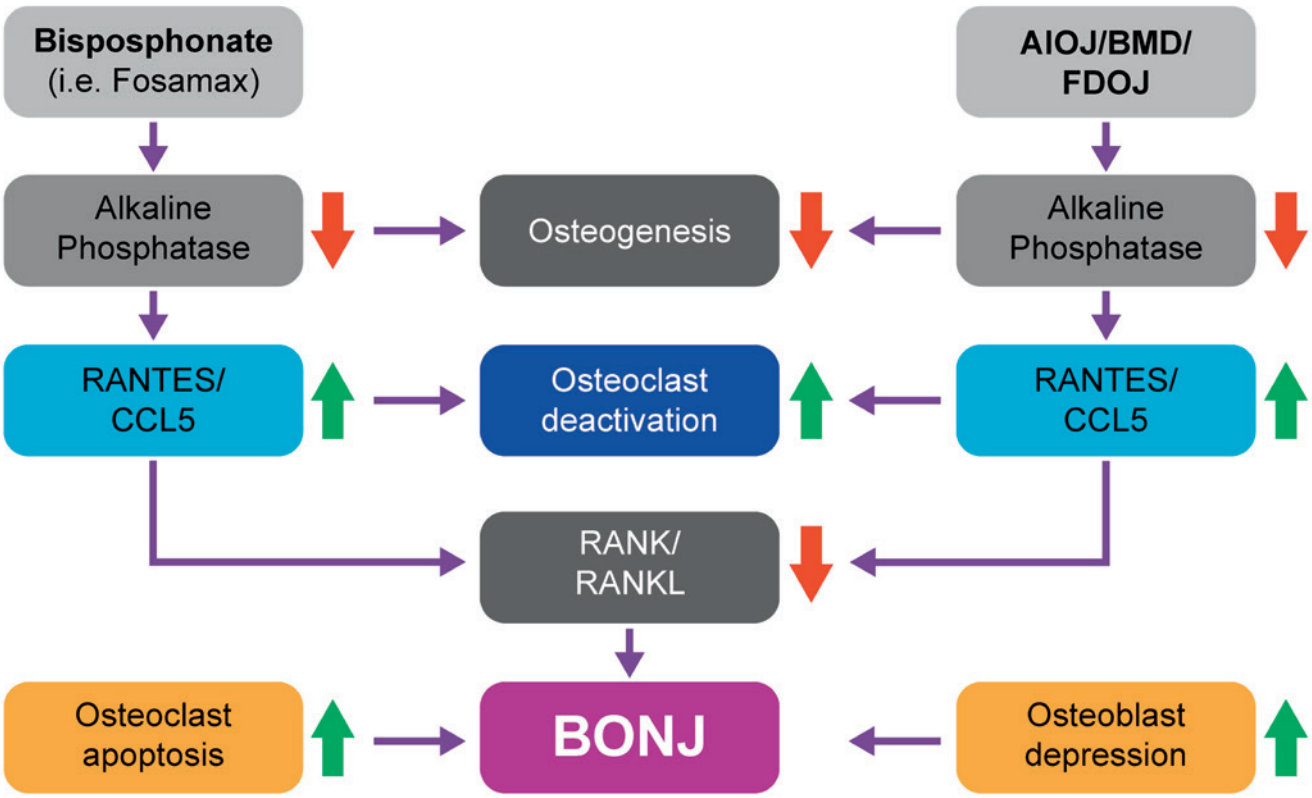

Figure 2 The effects of BP administration and the characteristics of AIOJ/BMD/FDOJ both include depressed alkaline phosphatase (AP) activity with subsequent R/C overexpression. On the one hand, this leads to OC inhibition and, on the other, to RANK/RANKL deactivation, which subsequently causes increased OC apoptosis and depressed OB activity resulting in BRONJ development. Legend: The red arrows indicate deactivation; the green arrows show a reversal of the effect following BP administration.

values in healthy jawbone samples (as documented in our previous studies) – indicate that any "inflammatory erosion" due to TNF-a supported OC formation is unlikely. Due to reduced TNF-a activation, OC formation in AIOJ/BMD/FDOJ is inhibited, which results in a fatty-degenerative morphology.[62]

In the same way, BPs inhibit the ability of OCs to resorb bone. They do so by suppressing farnesyl diphosphate synthetase activity, which inhibits OC recruitment and impacts the life expectancy of OCs through increased apoptosis. Where the OC function is excessively inhibited, dying OCs will not be replaced, and the capillary network of the bone will not be maintained, which leads to BRONJ.[19] The ability of BPs to regulate bone turnover by suppressing OC activity has led to its widespread use in the treatment of osteoporosis, Paget's disease, humoral hypercalcemia, and in tumors metastasizing to bone.[17,63] Several studies have shown the effectiveness of BPs in suppressing OC activity in arthritic bone erosions, which was comparable to the effects of OPG injections.[64]

Alkaline Phosphatase Reduction as a Common Osteoimmunological Characteristic of BRONJ and AIOJ/BMD/FDOJ

The initial alkaline phosphatase (AP) situation in AIOJ/BMD/FDOJ is as follows: AP has an optimum pH in the alkaline range. The pH level of AIOJ/BMD/FDOJ areas, however, is reduced as a consequence of the proinflammatory characteristics of R/C overexpression, resulting in a chronic inflammatory state. AP activity is thus inhibited within the increasingly acidic environment of such areas. Furthermore, BPs increase R/C secretion from OBs, and the acidity of areas affected by AIOJ/BMD/FDOJ, together with an excess of R/C, leads to OC inhibition.[65] At the same time, there is also reduced osteogenesis due to the suppression of AP activity,[66] as well as the overexpression of R/C that is present in AIOJ/BMD/FDOJ areas and also caused by BP administration. In our model, these two factors led to OC inhibition via disturbed RANK//RANKL homeostasis. In addition, depressed OB activity and increased OC apoptosis result in BRONJ development. While the skeletal bone consolidation that results from

BP administration occurs in response to increased OB activity, BRONJ develops in the jawbone when BP is administered parenterally. The reasons for these different responses to BPs have not yet been clarified. If we apply these considerations to an existing AIOJ/BMD/FDOJ area (as shown in Figure 2), then BRONJ and AIOJ/BMD/FDOJ both show suppressed AP activity with subsequent R/C overexpression.[67] This leads to OC inhibition and RANK/RANKL deactivation and, subsequently, increased OC apoptosis. Decreased OB activity may ultimately lead to the development of exposed BRONJ.

Osteoimmunological Parameters of AIOJ/BMD/FDOJ and BRONJ with Reversed Effects After BP Treatment

Despite the similarities detailed in the section titled "Osteoimmunological parameters of AIOJ/BMD/FDOJ and BRONJ with the same impact in response to BPs", BRONJ and AIOJ/BMD/FDOJ present two very different clinical pictures; different reactions to BP administration are also likely to occur.

RANKL Disorder as a Common Osteoimmunological Characteristic of BRONJ and AIOJ/BMD/FDOJ

The initial involvement of RANKL in AIOJ/BMD/FDOJ has been described in the literature as follows: pathological increases in levels of R/C and MCP-3 from activated OBs stimulate chemotactic recruitment and RANKL formation of resorptive OCs and aggravate local osteolysis. However, BP administration indirectly inhibits OC maturation by increasing OPG protein secretion and decreases transmembrane RANKL expression in human OBs. Several studies have shown that although BPs do not significantly affect RANKL gene expression, they reduce transmembrane RANKL protein expression in OBs.[68,69] This shows that BPs, in addition to directly inhibiting mature OCs, prevent OC recruitment and differentiation by splitting transmembrane RANKL into OBs. OC activation and RANKL activation in areas of AIOJ/BMD/FDOJ, and OC inhibition and RANKL inhibition in BRONJ distinguish these two forms of derailed bone metabolism and thus yield different clinical results. Specifically, imperceptible fatty osteolysis of the marrow structures in AIOJ/BMD/FDOJ and painful BRONJ sequestrum arise as a result. BPs have been shown to downregulate the expression of RANKL, the OC-differentiating factor produced by OBs.[70]

Osteoprotegerin Disorder as a Common Osteoimmunological Characteristic of BRONJ and AIOJ/BMD/FDOJ

The initial involvement of OPG in AIOJ/BMD/FDOJ is described in the literature. Since the TNF-a level found in AIOJ/BMD/FDOJ represents only 50% of the TNF-a level in healthy jawbone,[36,37] the OPG enzyme that belongs to the TNF family is deactivated. In the resulting osteolysis found in areas of AIOJ/BMD/FDOJ, this leads to reduced RANKL binding and thus results in OC activation. In conclusion, data from previously published studies have suggested that BPs modulate the production of OPG by normal OBs, which may contribute to the inhibition of OC bone resorption.[71] As the production of OPG increases with OB maturation, the amplification of OPG by BPs may be linked to OB differentiation via stimulatory BP effects. BPs have been shown to increase the gene expression for the decoy receptor, OPG, in human OBs.[71] OPG balance is disturbed in both AIOJ/BMD/FDOJ and BRONJ, albeit in opposite ways. However, the prior imbalance of OPG activity in AIOJ/BMD/FDOJ may increase the effects associated with BP administration.

Common Diagnostic Parameters of AIOJ/BMD/FDOJ and BRONJ

With respect to the exposed variant of BRONJ, radiographic procedures are required in order to determine the extent to which the degree of ossification has increased.[72] However, the existence of this variant of BRONJ is clinically evident. In contrast, the non-exposed BRONJ variant and AIOJ/BMD/FDOJ are associated with very similar problems in terms of diagnostic imaging. As with AIOJ/BMD/FDOJ, the prevalence of this variant of BRONJ is largely underestimated as the disease is often underdiagnosed and under-reported.[73] Studies have shown that almost a quarter of patients with BRONJ remain undiagnosed.[74]

Histopathology as a Common Feature of BRONJ and AIOJ/BMD/FDOJ

The initial histopathological presentation of AIOJ/BMD/FDOJ found in the literature is as follows: Bouquot describes these bone modeling disorders as ischemic osteonecrosis, which is a bone disease characterized by the degeneration and death of marrow and bone due to a slow or abrupt decrease in marrow blood flow.[75] Clumps of coalesced, liquefied fat (oil cysts) may be seen. Bone death is represented by a focal loss of OCs. Dark masses

of calcific necrotic detritus may often be present.[75] The histopathological features of AIOJ/BMD/FDOJ include necrotic adipocytes and fibrosis, but an almost complete absence of inflammatory cells.[76] Additional research has shown the role of aseptic necrosis following injury or drug therapy in the pathophysiology of BRONJ. Aseptic bone necrosis, as found in AIOJ/BMD/FDOJ, has been reported as a manifestation of selected systemic diseases and also documented following operations, trauma, and immunosuppressive therapy at the site of BRONJ.[77,78] The development of aseptic necrosis has been documented in the upper and lower jaw, particularly following osteotomies.[79,80] Researchers have observed a relationship between oral BP use and non-specific aseptic osteonecrosis among a cohort of older cardiovascular patients.[81] Other researchers have identified necrotic liquefaction, which often extend to large areas of the jaw, especially within BRONJ lesions of cancer patients, as shown using digital volume tomography (DVT)/cone beam computed tomography (CBCT).[82] Research has been published on BRONJ samples that were characterized by low to moderate inflammation.[83] This is in accordance with other reports of histopathological analyses of BRONJ samples.[48,78,84–86] Bone samples from BRONJ patients were investigated by microscopy and the presence of inflammatory infiltrates in the bone tissues was not observed.[87] These studies have demonstrated that aseptic necrosis, a lack of inflammatory reactions, and empty OC lacunae are common histopathological features of AIOJ/BMD/FDOJ and BRONJ.

Imaging Difficulties as a Common Feature of BRONJ and AIOJ/BMD/FDOJ

The diagnostic difficulties associated with BRONJ and AIOJ/BMD/FDOJ present another common feature. In order to diagnose BRONJ with imaging procedures, the Task Force Report of the American Society for Bone and Mineral Research highlights that the differential diagnosis of BRONJ should exclude other common intraoral diseases such as periodontitis, gingivitis, infectious osteomyelitis, osteoradionecrosis, neuralgia-inducing cavitational osteonecrosis ("NICO"), bone tumors, and metastases.[15] The authors of the report thus rule out an etiological equation for diagnosing "NICO" and BRONJ. The current review is focused on the potential role of imaging techniques in the diagnosis of the early stages of BRONJ. A combination of clinical and radiological symptoms suggest that, while not specific to BRONJ, they may collectively be more comprehensive and representative of the bone disease process.[2] The American Association of Maxillofacial Surgery accepts the use of imaging techniques when detecting BRONJ during presurgical evaluation.[72] It is important for the BRONJ patient that various imaging methods be examined critically prior to being adopted for the early detection and diagnosis of BRONJ.

(a) Panoramic X-rays (2D-OPG): Panoramic X-rays (2D-OPG) are routinely used in clinical dentistry to assess jawbone status. Pathological changes may be completely absent in 2D-OPG without pathognomonic findings indicating the presence of BRONJ.[88] The only radiological finding that is specific to BP therapy is that of "persistent alveolar socket"; even months following tooth removal or spontaneous tooth loss, the cortical walls of the alveolar bone remain intact without showing progressive destruction in response to osteolysis.[89] 2D-OPG may adequately differentiate between osteonecrosis and metastases, but is less useful when the lesion is osteolytic.[90] 2D-OPG is also helpful in cases where there is a mix of osteolysis and osteosclerosis; however, a significant loss of bone material (30–50%) is required before image acquisition is optimal.[91,92] This loss is unlikely to occur even in cases of NE-BRONJ before the lesion clinically manifests. 2D-OPG generates a 2D image showing significant overprojections that may hide important anatomical or pathological details. It is also difficult to delineate between the edges of necrotic and healthy bone, which often leads to overlooking early-stage lesions.[90] Given these known limitations, we have excluded 2D-OPG in the assessment of NE-BRONJ and, for the same reasons, in the assessment of AIOJ/BMD/FDOJ (see Figure 3). The medullary defects found in the latter present a similar diagnostic problem with respect to 2D-OPG as those in cases of NE-BRONJ.

(b) Computed tomography (CT): As a method of 3D reconstruction, CT has the potential to detect both cancellous and cortical bone infections.[93] CT can identify both osteosclerotic areas and areas of advanced BRONJ. However, CT scans are unable to provide additional information when compared to conventional X-ray

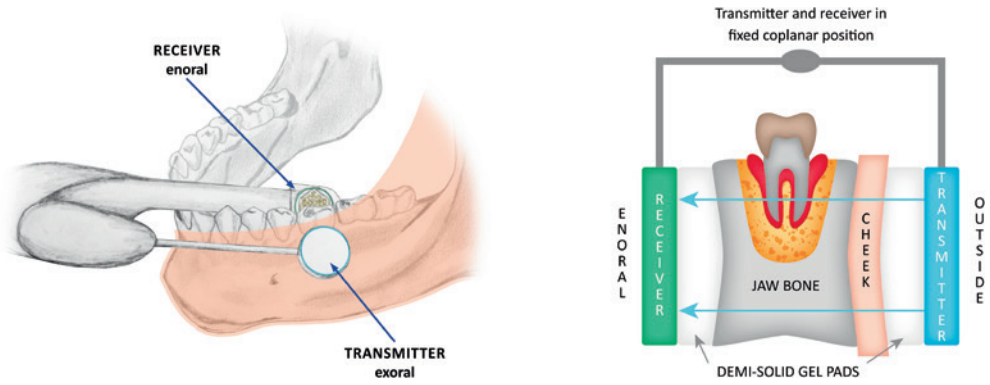

Figure 3 Left panel shows jawbone area 18; hematoxylin and eosin staining, magnification ×200. The lower half of the image illustrates eosinophilic bone substance with empty osteocyte cavities corresponding to devitalized bone sequestrum. Middle part of the left panel: Highly irregular trabecular surfaces with a wide edging comprised of Actinomyces colonies surrounded by a wall of leukocytes. Upper part of left panel: Fibrin particles and individual lymphocytes. Right panel: Actinomyces granules visualized in a PAS reaction; the red color represents a broad band of granules in the middle. The lower edge of the right panel images once again shows a bone sequestrum and typically empty osteocyte lacunae. Diagnosis: Aseptic bone necrosis with Actinomyces colonization.

diagnostics in asymptomatic patients with osteonecrosis.[88] As the differences between cortical and trabecular bone may be identified with a CT scan, this imaging modality may be used in the differential diagnosis of BRONJ.[92]

(c) Cone beam computed tomography/digital volume tomography (CBCT/DVT): CBCT/DVT is a technique that employs lower radiation exposure (<1/15 of that required for CT), but has a higher spatial resolution when compared with conventional CT and provides a superior image quality, especially with respect to cancellous bone features.[94,95] Although the ability of CBCT/DVT to differentiate between the quality of soft tissue is limited due to low contrast resolution, this modality is able to provide detailed information about cortical thickness and integrity, medullary abnormalities following tooth extraction, and cancellous bone density.[82]

Magnetic Resonance Imaging (MRI) and Positron Emission Tomography (PET)

The histopathological changes in necrotic bone may be visualized with MRI scans, as with CBCT/DVT. The images detect progressive cell death and the repair response (ie, edema). As the fat cells in normal bone marrow provide high signal intensity, it may be assumed that signal changes evident in the marrow are related to the death of fat cells. Necrotic adipocytes are a morphological characteristic of AIOJ/BMD/FDOJ.[76] Following the application of a contrast agent, areas of ischemia may be identified as non-enhancing regions. Cases in which fibrosis and sclerosis of the bone occur may also result in lower signal intensity. Nevertheless, the currently available data on MRI results for BRONJ are limited,[96] as are those related to AIOJ/BMD/FDOJ. Studies showed positron-emission tomography (PET) as a sensitive method for diagnosis of BRONJ. Thus, PET could be useful for evaluating the severity of BRONJ.[97]

Measurement of Bone Density with Transalveolar Ultrasound Sonography (TAU)

2D-OPG is used to identify osteopathies of the jawbone. However, this imaging technique fails to show AIOJ/BMD/FDJ areas, thus generating false-negative findings. As a result, AIOJ/BMD/FDOJ have been highly neglected in dentistry and medicine.[98] Therefore, transalveolar ultrasound sonography (TAU) appears to be necessary as an additional imaging technique in order to improve the diagnosis of AIOJ/BMD/FDOJ.[99,100] A newly developed TAU device (TAU-n) measures sound velocity attenuation when the bone marrow has been penetrated. An ultrasound transmitter is placed over the jaw area and a thumbnail-sized receiver is placed inside the mouth. To obtain reproducible results when measuring bone density, the transmitter and receiver are arranged in a coplanar and fixed position. The parts of the receiving unit are placed inside a patient's mouth, the acoustic coupling between those parts and the alveolar ridge is performed with the aid of a semi-solid gel (Figure 3). With the receiver containing 91 piezoelectric fields, sound waves are registered and converted into a color graph of the corresponding areas

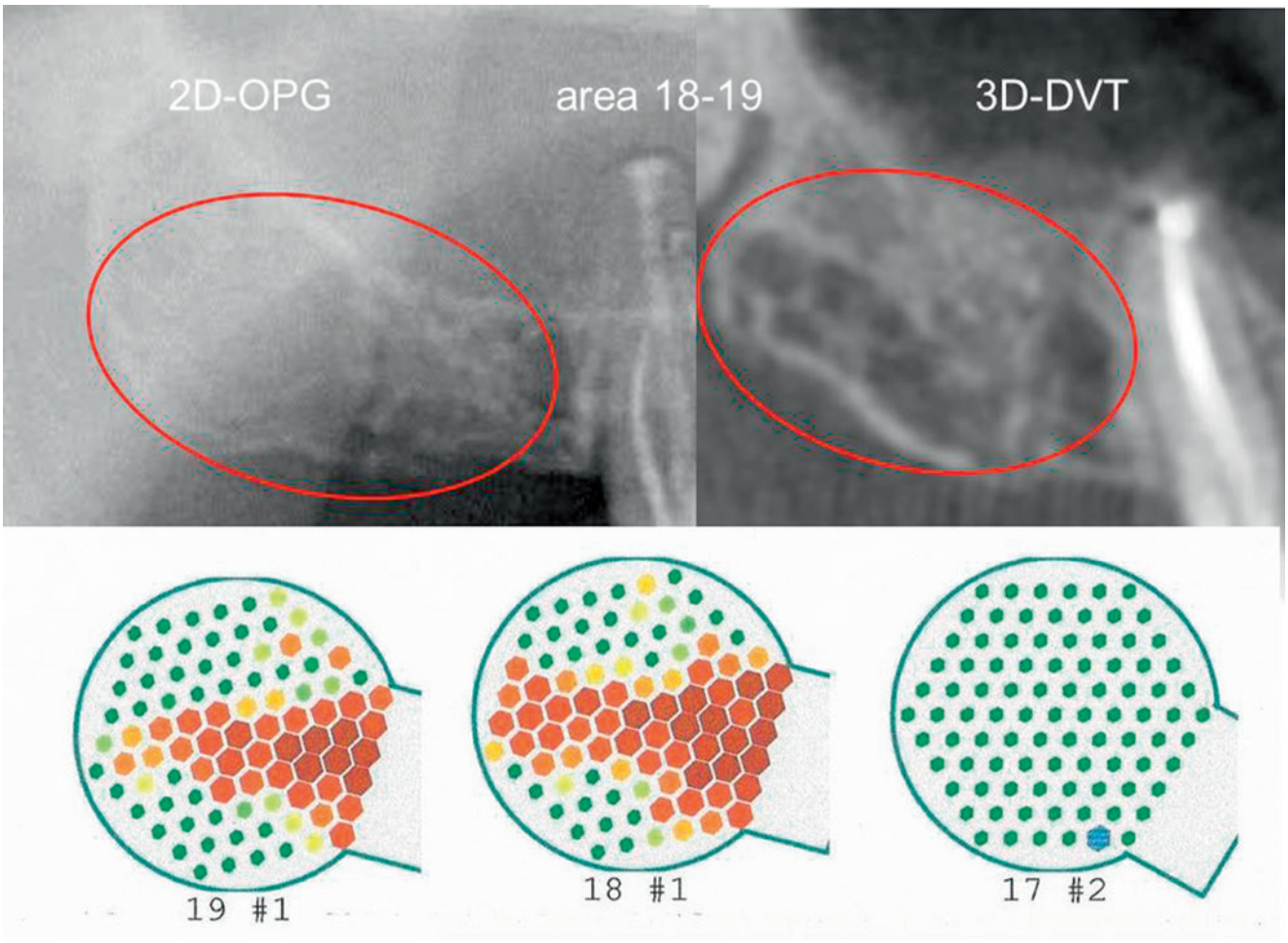

Figure 4 Left panel shows positioning of transmitter (outside) and receiver (enoral) in the lower jaw; the red band marks the cheek. Right panel shows the transmitter (in blue at the right) and receiver (in green at the left) in a fixed coplanar position (blue bar connecting the transmitter and receiver); semi-solid gel pads between the transmitter and the cheek on the outside of the mouth and between receiver and the alveolar ridge in the enoral position; trans-alveolar ultrasonic impulse from the transmitter to receiver (arrows in blue).

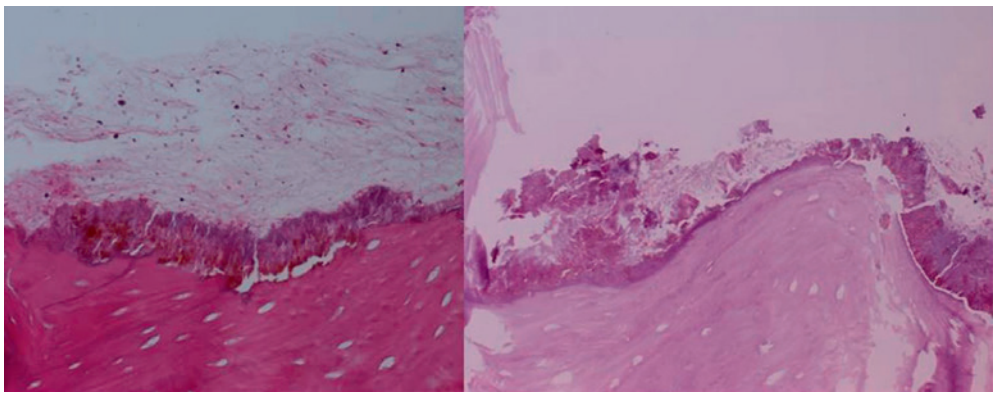

Figure 5 Inconspicuous 2D-OPG findings (left panel); suspected osteolytic processes in areas 17–19 in the sagittal section of the image using DVT (right panel). Lower panel: TAU measurement from region 17 to retromolar region 19. Legend: Green areas indicate normal bone density; yellow, orange, and red areas show decreasing bone density until complete osteolysis is reached.

of bone density (Figure 4).On the graphic visualization, green indicates healthy, dense, and solid bone, yellow indicates the presence of ischemic metabolism, and orange and red highlight areas of AIOJ/BMD/FDOJ presence.[101]

Case Descriptions of AIOJ/BMD/FDOJ, Non-Exposed BRONJ, and Actinomyces Colonization

A clinical case of a 55-year-old patient with prostate carcinoma who was treated with parenteral BPs received an X-ray diagnosis of non-exposed BRONJ with normal intraoral findings in the right upper jawbone from area 17 to retromolar area 19. While 2D-OPG of area 18/19 showed no suspicious findings, the CBCT/DVT image demonstrated ossification irregularities and partial cavities that resembled AIOJ/BMD/FDOJ. The development and progression of BRONJ could not be reliably determined by reference to these images and it was not possible to make a differential diagnosis. In contrast, TAU-n images clearly indicated osteolysis (see Figure 4, below). The postoperative light microscopy findings from area 18/19 showed marrow with adipose tissue, significant fibrillar and myxoid degeneration of adipocytes, individual lymphocytes, and mast cells; however, no florid inflammation was observed. These are the typical histological features of AIOJ/BMD/FDOJ.[76] It is worth noting, however, that there was a large bone sequestrum with empty OC cavities, highly irregular trabecular surfaces, and empty marrow spaces, with Actinomyces colonization (Figure 3).

Several reviews have indicated that light microscopy examinations were able to detect that 68.8% of BRONJ cases featured Actinomyces colonization.[32] Anaerobic Actinomyces has long been associated with necrotic bone findings in BRONJ lesions.[102] Actinomyces colonization is thus a top priority as a possible pathological trigger with respect to BRONJ. Since we have not identified bacterial colonization in areas of AIOJ/BMD/FDOJ in our own studies,[103] an accompanying secondary Actinomyces colonization seems to be an additional prerequisite for the development of BRONJ from an area of AIOJ/BMD/FDOJ in response to BP administration.

Selection of Manuscripts for Review

Table 1 displays all studies and their impact on the research question based on the inclusion and exclusion criteria in literature review.

Table 1 The Table Displays the Criteria for Inclusion of Specific Manuscripts in Our Research. Exclusion Criteria Were Unspecific Reviews Concentrating on Exposed BRONJ Only

Criteria PubMed Research	Number in References
1. risk of BP therapy/BRONJ new phenomenon	[1–19]
2. Staging BRONJ-Non-Exposed BRONJ	[20–26]
3. BP and antitumor therapy	[27–34]
4. BP impact on AIOJ/BMD/FDOJ and BRONJ	[35–71]
5. Diagnosis of AIOJ/BMD/FDOJ and BRONJ	[72–100]
5.1 X-ray techniques/MRI/PET	[72–97]
5.2 Transalveolar ultrasonography (TAU)	[98–101]

Discussion

Can hitherto little-known, yet – according to our clinical experience[37,76] – epidemiologically widespread AIOJ/BMD/FDOJ represent cofactors in the development of BRONJ? The development of biological processes takes place in different stages and during various phases of transition. This also seems to be the case for BRONJ, as the exposed form found in the maxillofacial region represents the final, late-stage form of the NE-BRONJ variant. The focus of our study is thus on the early stage of BRONJ (Stage 0) without exposed bone, as based on the recommendations of the American Association of Oral and Maxillofacial Surgeons.[5,20,104] Our hypothesis considers the NE-BRONJ variant as one stage of development featuring an unrecognized BMD that is characteristic of AIOJ/BMD/FDOJ and amplified by BP administration. The cumulative effects of BPs on pre-existing AIOJ/BMD/FDOJ support this premise. The relationship between AIOJ/BMD/FDOJ and the administration of BPs (as shown in Figure 6) leads, etiologically, to the non-exposed BRONJ variant, which is less clearly described in the literature than the late-stage form of BRONJ, and also results in considerable oral impairment.

As BPs and AIOJ/BMD/FDOJ exert the same effects, resulting in the hyperfunctioning of R/C expression, OB activity, hypoxia/ischemia, and the inhibition of OC activity, vascularization, and AP activity, AIOJ/BMD/FDOJ may be regarded as a prerequisite to the formation of BRONJ.

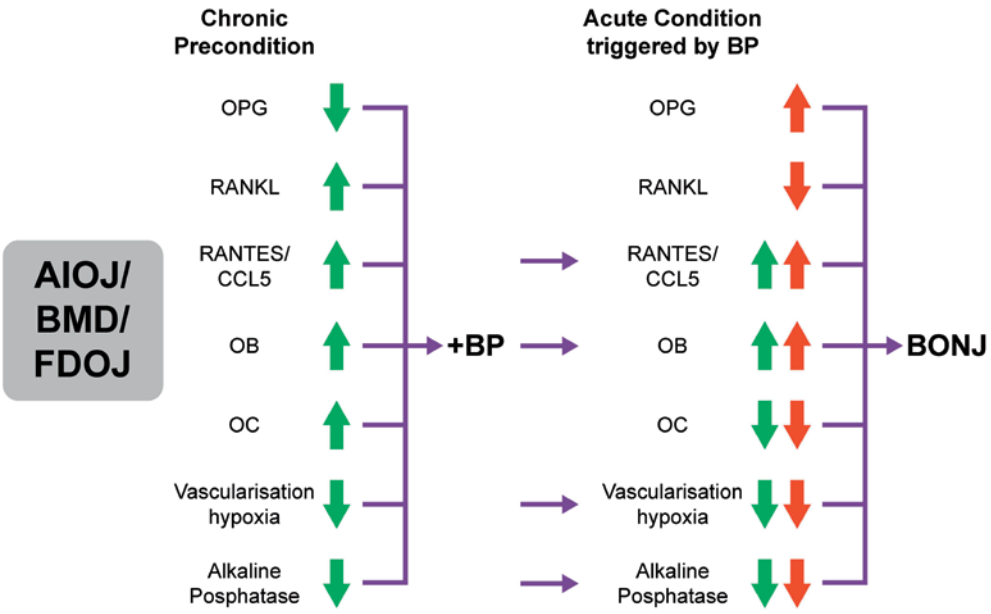

Figure 6 Overview of the individual osteoimmunological signal cascades present in AIOJ/BMD/FDOJ and their conversion or amplification following BP administration, resulting in the development of BRONJ. Legend: A pair of arrows, one red and one green, indicates the reinforcement or, in one instance, the reversal of the typical overexpression or inhibition found in AIOJ/BMD/FDOJ following BP administration.

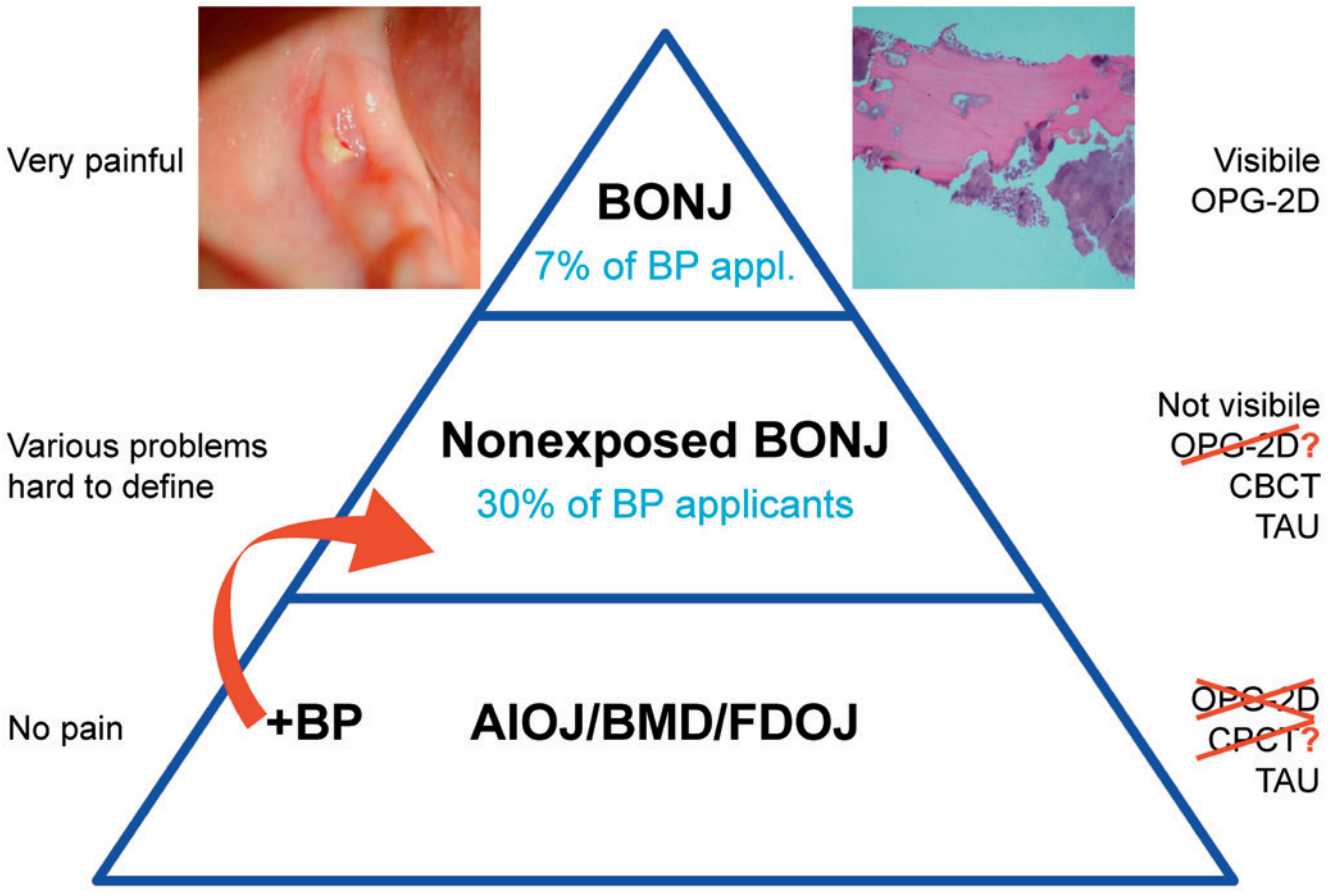

Figure 7 Three-step model for the development of BRONJ beginning with undetected AIOJ/BMD/FDOJ followed by the development of the NE-BRONJ variant, and finally by BRONJ.
Notes: Exposed bone BNOJ (left panel). Bony sequestrum BRONJ (right panel). Figure courtesy of Professor J Bouquot.

Changes in silent AIOJ/BMD/FDOJ processes, including strongly inhibited OC production, reduced RANKL activity, and increased OPG activity, appear to induce the occurrence of BRONJ. Figure 7 presents a hypothetical three-step model detailing the basic stages for the development of BRONJ at AIOJ/BMD/FDOJ areas. Regions with fatty-degenerative changes may be the focal point for the subsequent development of BRONJ, as such changes may constitute an additional risk factor. This is consistent with the hypothesis described in the literature, whereby bone necrosis precedes clinically evident ONJ that is exposed through the oral mucosa.[78,105] Regions featuring subclinical changes and necrotic bone may represent significant risk factors in the development of BRONJ.[104] Further, it is known that patients at each stage exhibit a very different bone composition.[104]

Conclusion

The prevention of BRONJ is of paramount importance and has been repeatedly emphasized.[106–108] Thus, BPs should not be regarded as the sole cause of osteonecrosis. The results of this study indicate that unresolved areas of wound healing at extraction sites – especially in former wisdom tooth areas – may directly contribute to the pathogenesis of BRONJ. Other research has already described the involvement of the jaw in BRONJ as opposed to other bone sites.[109] This may be because BPs are preferentially deposited in bones with high turnover rates such as the jawbone. The jawbone also presents with hidden conditions that – according to our hypothesis – share common characteristics with those found in AIOJ/BMD/FDOJ. Under the influence of BPs, areas of AIOJ/BMD/FDOJ may develop the pathological features of BRONJ. Efforts to prevent BRONJ, therefore, should not ignore the fact that BRONJ and AIOJ/BMD/FDOJ share similar osteoimmunological characteristics with respect to amplifying or reversing derailed signal cascades. Since AIOJ/BMD/FDOJ represent chronic, subclinical states, the sudden formation of BRONJ may be interpreted as a subsequent acute event. The early detection of BRONJ (as well as AIOJ/BMD/FDOJ) using X-ray techniques appears to be difficult. A new risk-benefit analysis should be considered: Patients should be screened for hidden oral risk factors, such as AIOJ/BMD/FDOJ. Thus, TAU may be used to measure bone density and fill this diagnostic gap. When parenteral BP therapy is administered, periodontal prophylaxis and tooth restoration should take precedence;[110,111] furthermore, AIOJ/BMD/FDOJ should be diagnosed first, preferably (and accurately) with TAU-n, and then surgically eliminated. The formation of difficult-to-treat BRONJ could be avoided in certain cases if the exacerbation of pre-existing areas of AIOJ/BMD/FDOJ is prevented before initiating anti-tumorigenic BP therapy. Surgical opening of the cortex, removal of ischemic marrow, and accompanying wound care represent the only way to address cases of AIOJ/BMD/FDOJ.[112] Consultation with an oncologist is mandatory, as the oncologist may insist on radiation therapy and the prevention of osteoradionecrosis of the jawbones via tooth restoration. To the best of our knowledge, we have highlighted, for the first time, the possible impact chains flowing from AIOJ/BMD/FDOJ and leading to the development of NE-BRONJ and further to exposed BRONJ. We also support the hypothesis presented herein with scientific data from the available literature. Due to the lack of clinical studies investigating these impact chains, multiple studies are necessary to elucidate the hypothesized relationships.

Abbreviations

AIOJ, aseptic-ischemic osteonecrosis of the jawbone; BMD, bone marrow defects; BRONJ, bisphosphonate (BP)-related osteonecrosis of the jaw; CBCT, cone beam computed tomography; CCL5, chemokine (C-C motif) ligand 5; DVT, digital volume tomography; FDOJ, fatty-degenerative osteonecrosis/osteolysis of the jawbone; HU, hounsfield units; OPG, orthopantomogram; R/C, RANTES/CCL5; RANTES, regulated on activation, normal T cell expressed and secreted; TAU, transalveolar ultrasonography; TAU-n, new transalveolar ultrasonography device.

Ethics and Consent Statement

Hereby we confirm that written informed consent has been provided by the patient to have the case details and any accompanying images published. The data were collected as part of the normal everyday medical care of the patients and evaluated retrospectively. Institutional approval was not required to publish the case details.

Acknowledgments

English language editing of this manuscript was provided by Journal Prep Services. Additional English language editing was provided by Natasha Gabriel.

Funding

This research did not receive any specific grant from funding agencies in the public, commercial, or not-for-profit sectors.

Disclosure

The corresponding author, Johann Lechner, is the holder of a patent used in the TAU-n apparatus and its associated software and reports a patent CaviTAU licensed to Dr. Johann Lechner. Bernd Zimmermann is an employee of QINNO. The authors report no other potential conflicts of interest for this work.

References

1. Ruggiero SL, Dodson TB, Fantasia J, et al. American Association of Oral and Maxillofacial Surgeons position paper on medication-related osteonecrosis of the jaw—2014 update. *J Oral Maxillofacial Surg*. 2014;72:1938–1956. doi:10.1016/j.joms.2014.04.031.
2. Khan A, Sandor G, Dore E, et al. Canadian consensus practice guidelines for bisphosphonate associated osteonecrosis of the jaw. *J Rheumatol*. 2008;35:1391–1397.
3. Marx RE. Pamidronate (Aredia) and zoledronate (Zometa) induced avascular necrosis of the jaws: a growing epidemic. *J Oral Maxillofacial Surg*. 2003;61:1115–1117. doi:10.1016/S0278-2391(03)00720-1.
4. Rosenberg T, Ruggiero S. Osteonecrosis of the jaws associated with the use of bisphosphonates. *J Oral Maxillofac Surg*. 2003;61:60. doi:10.1016/S0278-2391(03)00566-4
5. Wang J, Goodger NM, Pogrel MA. Osteonecrosis of the jaws associated with cancer chemotherapy. *J Oral Maxillofacial Surg*. 2003;61:1104–1107. doi:10.1016/S0278-2391(03)00328-8.
6. van Dessel J, Ferreira Pinheiro Nicolielo L, Huang Y, et al. Quantification of bone quality using different cone-beam CT devices: accuracy assessment for edentulous human mandibles. *Eur J Oral Implantol*. 2016;9:411–424.
7. Imada T, van Dessel J, Rubira-Bullen I, Santos P. Long-term effects of zoledronic acid on alveolar bone remodeling and quality in the jaw of an oncological rat model. *Dent Craniofacial Res*. 2018;1.
8. Marx RE, Sawatari Y, Fortin M, Broumand V. Bisphosphonate-induced exposed bone (osteonecrosis/osteopetrosis) of the jaws: risk factors, recognition, prevention, and treatment. *J Oral Maxillofacial Surg*. 2005;63:1567–1575. doi:10.1016/j.joms.2005.07.010.
9. Palomo L, Bissada N, Liu J. Bisphosphonate therapy for bone loss in patients with osteoporosis and periodontal disease: clinical perspectives and review of the literature. *Quintessence Int*. 2006;37:103–107.
10. Vahtsevanos K, Kyrgidis A, Verrou E, et al. Longitudinal cohort study of risk factors in cancer patients of bisphosphonate-related osteonecrosis of the jaw. *J Clin Oncol*. 2009;27:5356–5362. doi:10.1200/JCO.2009.21.9584.
11. Kyrgidis A, Vahtsevanos K, Koloutsos G, et al. Bisphosphonate-related osteonecrosis of the jaws: a case-control study of risk factors in breast cancer patients. *J Clin Oncol*. 2008;26:4634–4638. doi:10.1200/JCO.2008.16.2768.
12. Palaska PK, Cartsos V, Zavras AI. Bisphosphonates and time to osteonecrosis development. *Oncologist*. 2009;14:1154–1166. doi:10.1634/theoncologist.2009-0115.
13. Stopeck AT, Lipton A, Body JJ, et al. Denosumab compared with zoledronic acid for the treatment of bone metastases in patients with advanced breast cancer: a randomized, double-blind study. *J Clin Oncol*. 2010;28:5132–5139. doi:10.1200/JCO.2010.29.7101.
14. Lipton A, Fizazi K, Stopeck AT, et al. Superiority of denosumab to zoledronic acid for prevention of skeletal-related events: a combined analysis of 3 pivotal, randomised, Phase 3 trials. *Eur J Cancer*. 2012;48:3082–3092. doi:10.1016/j.ejca.2012.08.002.
15. Khosla S, Burr D, Cauley J, et al. Bisphosphonate-associated osteonecrosis of the jaw: report of a task force of the American Society for Bone and Mineral Research. *J Bone Min Res*. 2007;22:1479–1491. doi:10.1359/jbmr.0707onj.
16. Kühl S, Walter C, Acham S, Pfeffer R, Lambrecht JT. Bisphosphonate-related osteonecrosis of the jaws – a review. *Oral Oncol*. 2012;48:938–947. doi:10.1016/j.oraloncology.2012.03.028.
17. Bamias A, Kastritis E, Bamia C, et al. Osteonecrosis of the jaw in cancer after treatment with bisphosphonates: incidence and risk factors. *J Clin Oncol*. 2005;23:8580–8587. doi:10.1200/JCO.2005.02.8670.
18. Mavrokokki T, Cheng A, Stein B, Goss A. Nature and frequency of bisphosphonate-associated osteonecrosis of the jaws in Australia. *J Oral Maxillofacial Surg*. 2007;65:415–423. doi:10.1016/j.joms.2006.10.061.
19. Gutta R, Louis PJ. Bisphosphonates and osteonecrosis of the jaws: science and rationale. *Oral Surg Oral Med Oral Pathol Oral Radiol Endodontol*. 2007;104:186–193. doi:10.1016/j.tripleo.2006.12.004.
20. Ruggiero SL, Dodson TB, Assael LA, Landesberg R, Marx RE, Mehrotra B. American Association of Oral and Maxillofacial Surgeons position paper on bisphosphonate-related osteonecrosis of the jaws—2009 update. *J Oral Maxillofacial Surg*. 2009;67:2–12. doi:10.1016/j.joms.2009.01.009.
21. Patel S, Choyee S, Uyanne J, et al. Non-exposed bisphosphonate-related osteonecrosis of the jaw: a critical assessment of current definition, staging, and treatment guidelines. *Oral Dis*. 2012;18:625–632. doi:10.1111/j.1601-0825.2012.01911.x.
22. Yarom N, Fedele S, Lazarovici TS, Elad S. Is exposure of the jawbone mandatory for establishing the diagnosis of bisphosphonate-related osteonecrosis of the jaw? *J Oral Maxillofacial Surg*. 2010;68:705. doi:10.1016/j.joms.2009.07.086.
23. Mignogna MD, Sadile G, Leuci S. Drug-related osteonecrosis of the jaws: "Exposure, or not exposure: that is the question". *Oral Surg Oral Med Oral Pathol Oral Radiol*. 2012;113:704–705. doi:10.1016/j.oooo.2012.01.004.
24. Junquera L, Gallego L. Nonexposed bisphosphonate-related osteonecrosis of the jaws: another clinical variant? *J Oral Maxillofacial Surg*. 2008;66:1516–1517. doi:10.1016/j.joms.2008.02.012.
25. Fedele S, Porter SR, D'Aiuto F, et al. Nonexposed variant of bisphosphonate-associated osteonecrosis of the jaw: a case series. *Am J Med*. 2010;123:1060–1064. doi:10.1016/j.amjmed.2010.04.033.
26. Schiodt M, Reibel J, Oturai P, Kofod T. Comparison of nonexposed and exposed bisphosphonate-induced osteonecrosis of the jaws: a retrospective analysis from the Copenhagen cohort and a proposal for an updated classification system. *Oral Surg Oral Med Oral Pathol Oral Radiol*. 2014;117:204–213. doi:10.1016/j.oooo.2013.10.010.
27. Gnant M, Mlineritsch B, Stoeger H, et al. Adjuvant endocrine therapy plus zoledronic acid in premenopausal women with early-stage breast cancer: 62-month follow-up from the ABCSG-12 randomised trial. *Lancet Oncol*. 2011;12:631–641. doi:10.1016/S1470-2045(11)70122-X.
28. Deans RJ, Moseley AB. Mesenchymal stem cells. *Exp Hematol*. 2000;28:875–884. doi:10.1016/S0301-472X(00)00482-3.
29. Karnoub AE, Dash AB, Vo AP, et al. Mesenchymal stem cells within tumour stroma promote breast cancer metastasis. *Nature*. 2007;449:557–563. doi:10.1038/nature06188.
30. Psaila B, Lyden D. The metastatic niche: adapting the foreign soil. *Nat Rev Cancer*. 2009;9:285–293. doi:10.1038/nrc2621.
31. Gallo M, de Luca A, Lamura L, Normanno N. Zoledronic acid blocks the interaction between mesenchymal stem cells and breast cancer cells: implications for adjuvant therapy of breast cancer. *Ann Oncol*. 2012;23:597–604. doi:10.1093/annonc/mdr159.

32. Hinson AM, Smith CW, Siegel ER, Stack BC. Is bisphosphonate-related osteonecrosis of the jaw an infection? A histological and microbiological ten-year summary. *Int J Dent*. 2014;2014:1–7. doi:10.1155/2014/452737.
33. Wood J, Bonjean K, Ruetz S, et al. Novel antiangiogenic effects of the bisphosphonate compound zoledronic acid. *J Pharmacol Exp Ther*. 2002;302:1055–1061. doi:10.1124/jpet.102.035295.
34. Glueck CJ, McMahon RE, Bouquot JE, Triplett D. Exogenous estrogen may exacerbate thrombophilia, impair bone healing and contribute to development of chronic facial pain. *CRANIO®*. 1998;16:143–153. doi:10.1080/08869634.1998.11746052.
35. Gonzalez RM, Daly DS, Tan R, Marks JR, Zangar RC. Plasma biomarker profiles differ depending on breast cancer subtype but RANTES is consistently increased. *Cancer Epidemiol Biomarkers Prev*. 2011;20:1543–1551. doi:10.1158/1055-9965.EPI-10-1248.
36. Lechner J, von Baehr V. Hyperactivated signaling pathways of chemokine RANTES/CCL5 in osteopathies of jawbone in breast cancer patients-case report and research. *Breast Cancer*. 2014;8:89–96. doi:10.4137/BCBCR.S15119.
37. Lechner J, von Baehr V. Chemokine RANTES/CCL5 as an unknown link between wound healing in the jawbone and systemic disease: is prediction and tailored treatments in the horizon? *EPMA J*. 2015;6:10. doi:10.1186/s13167-015-0032-4.
38. Lechner J, von Baehr V. RANTES and fibroblast growth factor 2 in jawbone cavitations: triggers for systemic disease? *Int J Gen Med*. 2013;6:277–290. doi:10.2147/IJGM.S43852.
39. Lechner J, von B. RANTES and fibroblast growth factor 2 in jawbone cavitations: triggers for systemic disease? *Int J Gen Med*. 2013;277. doi:10.2147/IJGM.S43852.
40. Greiner S, Kadow-Romacker A, Lübberstedt M, Schmidmaier G, Wildemann B. The effect of zoledronic acid incorporated in a poly(D,L-lactide) implant coating on osteoblasts in vitro. *J Biomed Mater Res A*. 2007;80A:769–775. doi:10.1002/jbm.a.30950.
41. Troeltzsch M, Kriegelstein S, Messlinger K, Steiner T, Messlinger K, Troeltzsch M. Physiology and pharmacology of nonbisphosphonate drugs implicated in osteonecrosis of the jaw. *J Can Dent Assoc*. 2012;78:c85.
42. Krüger TB, Herlofson BB, Landin MA, Reseland JE. Alendronate alters osteoblast activities. *Acta Odontol Scand*. 2016;74:550–557. doi:10.1080/00016357.2016.1217041.
43. Bouquot J, McMahon R The histopathology of chronic ischemic bone disease (ON) – parameters and disease classification. Tucson, Arizona: Proceedings of the Annual Meeting of the American Association of Oral & Maxillofacial Pathology; 2010.
44. Assael LA. New foundations in understanding osteonecrosis of the jaws. *J Oral Maxillofacial Surg*. 2004;62:125–126. doi:10.1016/j.joms.2003.11.009.
45. Kenzora J, Glimcher M. Accumulative cell stress: the multifactorial etiology of idiopathic osteonecrosis. *Orthop Clin North Am*. 1985;16:669–679.
46. Schoutens A, Arlet J, Gardeniers J, Hughes S, editors. *Bone Circulation and Vascularization in Normal and Pathological Conditions*. New York, NY: Plenum Press; 1993.
47. Arlet J, Mazieres B. *Bone Circulation and Bone Necrosis*. Heidelberg, Germany: Springer-Verlag; 1990.
48. Favia G, Pilolli GP, Maiorano E. Histologic and histomorphometric features of bisphosphonate-related osteonecrosis of the jaws: an analysis of 31 cases with confocal laser scanning microscopy. *Bone*. 2009;45:406–413. doi:10.1016/j.bone.2009.05.008.
49. Paparella ML, Brandizzi D, Santini-Araujo E, Cabrini RL. Histopathological features of osteonecrosis of the jaw associated with bisphosphonates. *Histopathology*. 2012;60:514–516. doi:10.1111/j.1365-2559.2011.04061.x.
50. Gruppo R, Glueck CJ, Mcmahon RE, et al. The pathophysiology of alveolar osteonecrosis of the jaw: anticardiolipin antibodies, thrombophilia, and hypofibrinolysis. *J Lab Clin Med*. 1996;127:481–488. doi:10.1016/S0022-2143(96)90065-7.
51. Glueck CJ, McMahon RE, Bouquot J, et al. Thrombophilia, hypofibrinolysis, and alveolar osteonecrosis of the jaws. *Oral Surg Oral Med Oral Pathol Oral Radiol Endodontol*. 1996;81:557–566. doi:10.1016/S1079-2104(96)80047-3.
52. Glueck C, Freiberg R, Gruppo R. *Osteonecrosis: Etiology, Diagnosis, and Treatment*. Rosemont, IL: American Academy of Orthopaedic Surgeons; 1997.
53. Gabriel H, Fitzgerald SW, Myers MT, Donaldson JS, Poznanski AK. MR imaging of hip disorders. *RadioGraphics*. 1994;14:763–781. doi:10.1148/radiographics.14.4.7938767.
54. Votta BJ, White JR, Dodds RA, et al. CKbeta-8 [CCL23], a novel CC chemokine, is chemotactic for human osteoclast precursors and is expressed in bone tissues. *J Cell Physiol*. 2000;183:196–207. doi:10.1002/(SICI)1097-4652(200005)183:2<96::aid-jcp6>3.0.CO;2-8.
55. Lisignoli G, Toneguzzi S, Grassi F, et al. Different chemokines are expressed in human arthritic bone biopsies: IFN-γ and IL-6 differently modulate IL-8, MCP-1 AND RANTES production by arthritic osteoblasts. *Cytokine*. 2002;20:231–238. doi:10.1006/cyto.2002.2006.
56. Pozzi S, Vallet S, Mukherjee S, et al. High-dose zoledronic acid impacts bone remodeling with effects on osteoblastic lineage and bone mechanical properties. *Clin Cancer Res*. 2009;15:5829–5839. doi:10.1158/1078-0432.CCR-09-0426.
57. Kamalakar A, Bendre MS, Washam CL, et al. Circulating interleukin-8 levels explain breast cancer osteolysis in mice and humans. *Bone*. 2014;61:176–185. doi:10.1016/j.bone.2014.01.015.
58. Yao Z, Li P, Zhang Q, et al. Tumor necrosis factor-α increases circulating osteoclast precursor numbers by promoting their proliferation and differentiation in the bone marrow through up-regulation of c-Fms expression. *J Biol Chem*. 2006;281:11846–11855. doi:10.1074/jbc.M512624200.
59. Roodman GD. Cell biology of the osteoclast. *Exp Hematol*. 1999;27:1229–1241. doi:10.1016/S0301-472X(99)00061-2.
60. Kim N, Kadono Y, Takami M, et al. Osteoclast differentiation independent of the TRANCE–RANK–TRAF6 axis. *J Exp Med*. 2005;202:589–595. doi:10.1084/jem.20050978.
61. Zhang Q, Badell IR, Schwarz EM, et al. Tumor necrosis factor prevents alendronate-induced osteoclast apoptosis in vivo by stimulating Bcl-xL expression through Ets-2. *Arthritis Rheum*. 2005;52:2708–2718. doi:10.1002/art.21236.
62. Lechner J, Rudi T, von Baehr V. Osteoimmunology of tumor necrosis factor-alpha, IL-6, and RANTES/CCL5: a review of known and poorly understood inflammatory patterns in osteonecrosis. *Clin Cosmet Investig Dent*. 2018;10:251–262. doi:10.2147/CCIDE.S184498.
63. Oral complications of chemotherapy and head/neck radiation (PDQ®); 2006. Available from: http://www.cancer.gov/cancertopics/pdq/supportivecare/oral-complications/HealthProfessional. Accessed December 30, 2020
64. Sims NA, Green JR, Glatt M, et al. Targeting osteoclasts with zoledronic acid prevents bone destruction in collagen-induced arthritis. *Arthritis Rheum*. 2004;50:2338–2346. doi:10.1002/art.20382.
65. Jensen ED, Gopalakrishnan R, Westendorf JJ. Regulation of gene expression in osteoblasts. *BioFactors*. 2010;36:25–32. doi:10.1002/biof.72.
66. Vaisman DN, McCarthy AD, Cortizo AM. Bone-specific alkaline phosphatase activity is inhibited by bisphosphonates: role of divalent cations. *Biol Trace Elem Res*. 2005;104:131–140. doi:10.1385/BTER:104:2:131.

67. Klein B, Ben-Bassat H, Breuer E, Solomon V, Golomb G. Structurally different bisphosphonates exert opposing effects on alkaline phosphatase and mineralization in marrow osteoprogenitors. *Cell Biochem*. 1998;68:186–194. doi:10.1002/(SICI)1097-4644(19980201)68:2<186::AID-JCB5>3.0.CO;2-R
68. Pan B, Farrugia AN, To LB, et al. The nitrogen-containing bisphosphonate, zoledronic acid, influences RANKL expression in human osteoblast-like cells by activating TNF-α converting enzyme (TACE). *J Bone Min Res*. 2004;19:147–154. doi:10.1359/jbmr.2004.19.1.147.
69. Taylor KH, Middlefell LS, Mizen KD. Osteonecrosis of the jaws induced by anti-RANK ligand therapy. *Br J Oral Maxillofacial Surg*. 2010;48:221–223. doi:10.1016/j.bjoms.2009.08.030.
70. Mackie PS, Fisher JL, Zhou H, Choong PFM. Bisphosphonates regulate cell growth and gene expression in the UMR 106-01 clonal rat osteosarcoma cell line. *Br J Cancer*. 2001;84:951–958. doi:10.1054/bjoc.2000.1679.
71. Viereck V, Emons G, Lauck V, et al. Bisphosphonates pamidronate and zoledronic acid stimulate osteoprotegerin production by primary human osteoblasts. *Biochem Biophys Res Commun*. 2002;291:680–686. doi:10.1006/bbrc.2002.6510.
72. American Association of Maxillofacial Surgery. Parameters of care. Clinical practice guidelines for oral and maxillofacial surgery (AAOMS ParCare 2012). *J Oral Maxil Surg*. 2012;70.
73. Fusco V, Galassi C, Berruti A, et al. Osteonecrosis of the jaw after zoledronic acid and denosumab treatment. *J Clin Oncol*. 2011;29:e521–2. doi:10.1200/JCO.2011.35.1551.
74. Fedele S, Bedogni G, Scoletta M, et al. Up to a quarter of patients with osteonecrosis of the jaw associated with antiresorptive agents remain undiagnosed. *Br J Oral Maxillofacial Surg*. 2015;53:13–17. doi:10.1016/j.bjoms.2014.09.001.
75. Neville B, Damm D, Allen C, Bouquot J. *Oral and Maxillofacial Pathology*. 4th ed. Elsevier Health Sciences; 2008.
76. Lechner J, von Baehr V. Peripheral neuropathic facial/trigeminal pain and RANTES/CCL5 in jawbone cavitation. *Evid Based Complement Alt Med*. 2015;2015:1–9. doi:10.1155/2015/582520.
77. McCarthy E. Aseptic necrosis of bone: an historic perspective. *Clin Orthop*. 1982;216–221.
78. Lesclous P, Abi Najm S, Carrel J-P, et al. Bisphosphonate-associated osteonecrosis of the jaw: a key role of inflammation? *Bone*. 2009;45:843–852. doi:10.1016/j.bone.2009.07.011.
79. Lanigan DT, West RA. Aseptic necrosis of the mandible: report of two cases. *J Oral Maxillofacial Surg*. 1990;48:296–300. doi:10.1016/0278-2391(90)90397-K.
80. Lanigan DT, Hey JH, West RA. Aseptic necrosis following maxillary osteotomies: report of 36 cases. *J Oral Maxillofacial Surg*. 1990;48:142–156. doi:10.1016/S0278-2391(10)80202-2.
81. Etminan M, Aminzadeh K, Matthew IR, Brophy JM. Use of oral bisphosphonates and the risk of aseptic osteonecrosis: a nested case-control study. *J Rheumatol*. 2008;35:691–695.
82. Barragan-Adjemian C, Lausten L, Ang DB, Johnson M, Katz J, Bonewald LF. Bisphosphonate-related osteonecrosis of the jaw: model and diagnosis with cone beam computerized tomography. *Cells Tissues Organs*. 2009;189:284–288. doi:10.1159/000151451.
83. Cardemil C, Thomsen P, Larsson Wexell C. Jaw bone samples from bisphosphonate-treated patients: a pilot cohort study. *Clin Implant Dent Relat Res*. 2015;17:e679–91. doi:10.1111/cid.12307.
84. Hansen T, Kirkpatrick CJ, Walter C, Kunkel M. Increased numbers of osteoclasts expressing cysteine proteinase cathepsin K in patients with infected osteoradionecrosis and bisphosphonate-associated osteonecrosis—a paradoxical observation? *Virchows Archiv*. 2006;449:448–454. doi:10.1007/s00428-006-0261-y.
85. Hoefert S, Schmitz I, Tannapfel A, Eufinger H. Importance of microcracks in etiology of bisphosphonate-related osteonecrosis of the jaw: a possible pathogenetic model of symptomatic and non-symptomatic osteonecrosis of the jaw based on scanning electron microscopy findings. *Clin Oral Investig*. 2010;14(3):271–284. doi:10.1007/s00784-009-0300-6.
86. Carmagnola D, Canciani E, Sozzi D, Biglioli F, Moneghini L, Dellavia C. Histological findings on jaw osteonecrosis associated with bisphosphonates (BRONJ) or with radiotherapy (ORN) in humans. *Acta Odontol Scand*. 2013;71:1410–1417. doi:10.3109/00016357.2013.765592.
87. Perrotta I, Cristofaro MG, Amantea M, et al. Jaw osteonecrosis in patients treated with bisphosphonates: an ultrastructural study. *Ultrastruct Pathol*. 2010;34:207–213. doi:10.3109/01913121003729806.
88. Stockmann P, Hinkmann FM, Lell MM, et al. Panoramic radiograph, computed tomography or magnetic resonance imaging. Which imaging technique should be preferred in bisphosphonate-associated osteonecrosis of the jaw? A prospective clinical study. *Clin Oral Investig*. 2010;14:311–317. doi:10.1007/s00784-009-0293-1.
89. Groetz KA, Al-Nawas B. Persisting alveolar sockets—a radiologic symptom of BP-ONJ? *J Oral Maxillofacial Surg*. 2006;64:1571–1572. doi:10.1016/j.joms.2006.05.041.
90. Store G, Larheim T. Mandibular osteoradionecrosis: a comparison of computed tomography with panoramic radiography. *Dentomaxillofac Radiol*. 1999;28:295–300. doi:10.1038/sj.dmfr.4600461
91. Store G, Boysen M. Mandibular osteoradionecrosis: clinical behaviour and diagnostic aspects. *Clin Otolaryngol Allied Sci*. 2000;25:378–384. doi:10.1046/j.1365-2273.2000.00367.x.
92. Chiandussi S, Biasotto M, Dore F, Cavalli F, Cova M, Di Lenarda R. Clinical and diagnostic imaging of bisphosphonate-associated osteonecrosis of the jaws. *Dentomaxillofacial Radiol*. 2006;35:236–243. doi:10.1259/dmfr/27458726.
93. Taguchi A, Akiyama H, Koseki T, Shimizutani K. Recognition of bisphosphonate-related osteonecrosis of the jaw among oral and maxillofacial radiologists: results from a questionnaire-based survey in Japan. *Oral Radiol*. 2013;29:98–104. doi:10.1007/s11282-012-0114-0.
94. Schulze D, Blessmann M, Pohlenz P, Wagner K, Heiland M. Diagnostic criteria for the detection of mandibular osteomyelitis using cone-beam computed tomography. *Dentomaxillofacial Radiol*. 2006;35:232–235. doi:10.1259/dmfr/71331738.
95. Guerrero ME, Jacobs R, Loubele M, Schutyser F, Suetens P, van Steenberghe D. State-of-the-art on cone beam CT imaging for preoperative planning of implant placement. *Clin Oral Investig*. 2006;10:1–7. doi:10.1007/s00784-005-0031-2.
96. Bisdas S, Chambron Pinho N, Smolarz A, Sader R, Vogl TJ, Mack MG. Biphosphonate-induced osteonecrosis of the jaws: CT and MRI spectrum of findings in 32 patients. *Clin Radiol*. 2008;63:71–77. doi:10.1016/j.crad.2007.04.023.
97. Wilde F, Steinhoff K, Frerich B, et al. Positron-emission tomography imaging in the diagnosis of bisphosphonate-related osteonecrosis of the jaw. *Oral Surg Oral Med Oral Pathol Oral Radiol Endodontol*. 2009;3:107. doi:10.1016/j.tripleo.2008.09.019
98. Kumar VV, Sagheb K, Klein MO, Al-Nawas B, Kann PH, Kämmerer PW. Relation between bone quality values from ultrasound transmission velocity and implant stability parameters - an ex vivo study. *Clin Oral Implants Res*. 2012;23:975–980. doi:10.1111/j.1600-0501.2011.02250.x.
99. Al-Nawas B, Grötz KA, Rose E, Duschner H, Kann P, Wagner W. Using ultrasound transmission velocity to analyse the mechanical properties of teeth after in vitro, in situ, and in vivo irradiation. *Clin Oral Investig*. 2000;4:168–172. doi:10.1007/s007840000068.

100. Bouquot J, Shankland WI, Margolis M. Through-transmission alveolar ultrasonography (TAU) - new technology for evaluation of bone density and desiccation. Comparison with radiology of 170 biopsied alveolar sites of osteoporotic and ischemic damage. *Oral Surg Oral Med Oral Pathol Oral Radiol Endod*. 2002;93:413–414.
101. Lechner J, Zimmermann B, Schmidt M, von Baehr V. Ultrasound sonography to detect focal osteoporotic jawbone marrow defects: clinical comparative study with corresponding hounsfield units and RANTES/CCL5 expression. *Clin Cosmet Investig Dent*. 2020;12:205–216. doi:10.2147/CCIDE.S247345.
102. Tsurushima H, Kokuryo S, Sakaguchi O, Tanaka J, Tominaga K. Bacterial promotion of bisphosphonate-induced osteonecrosis in Wistar rats. *Int J Oral Maxillofac Surg*. 2013;42:1481–1487. doi:10.1016/j.ijom.2013.06.011.
103. Lechner J, Schuett S, von Baehr V. Aseptic-avascular osteonecrosis: local "silent inflammation" in the jawbone and RANTES/CCL5 overexpression. *Clin Cosmet Investig Dent*. 2017;9:99–109. doi:10.2147/CCIDE.S149545.
104. Ruggiero SL, Fantasia J, Carlson E. Bisphosphonate-related osteonecrosis of the jaw: background and guidelines for diagnosis, staging and management. *Oral Surg Oral Med Oral Pathol Oral Radiol Endodontol*. 2006;102:433–441. doi:10.1016/j.tripleo.2006.06.004.
105. Mawardi H, Treister N, Richardson P, et al. Sinus tracts—an early sign of bisphosphonate-associated osteonecrosis of the jaws? *J Oral Maxillofacial Surg*. 2009;67:593–601. doi:10.1016/j.joms.2008.09.031.
106. Bagán J, Blade J, Cozar JM, et al. Recommendations for the prevention, diagnosis, and treatment of osteonecrosis of the jaw (ONJ) in cancer patients treated with bisphosphonates. *Med Oral Patol Oral Cir Bucal*. 2007;12:E336–40.
107. Cossío PI, Macián AC, Pérez Ceballos JL, Nicas JP, Gutiérrez Pérez JL. Bisphosphonate-related osteonecrosis of the jaw in patients with multiple myeloma. *Med Oral Patol Oral Cir Bucal*. 2008;13:E52–7.
108. Yip RML. Bisphosphonates and osteonecrosis of the jaw. *Hong Kong Bull Rheum Dis*. 2008;8:19–25.
109. Ruggiero SL, Drew SJ. Osteonecrosis of the Jaws and Bisphosphonate Therapy. *J Dent Res*. 2007;86:1013–1021. doi:10.1177/154405910708601101.
110. Dimopoulos MA, Kastritis E, Bamia C, et al. Reduction of osteonecrosis of the jaw (ONJ) after implementation of preventive measures in patients with multiple myeloma treated with zoledronic acid. *Ann Oncol*. 2009;20:117–120. doi:10.1093/annonc/mdn554.
111. Bramati A, Girelli S, Farina G, et al. Prospective, mono-institutional study of the impact of a systematic prevention program on incidence and outcome of osteonecrosis of the jaw in patients treated with bisphosphonates for bone metastases. *J Bone Miner Metab*. 2015;33:119–124. doi:10.1007/s00774-014-0566-x.
112. Hjørting-Hansen E. Decortication in treatment of osteomyelitis of the mandible. *Oral Surg Oral Med Oral Pathol*. 1970;29:641–655. doi:10.1016/0030-4220(70)90259-8.

International Medical Case Reports Journal

Dovepress

open access to scientific and medical research

Open Access Full Text Article

CASE REPORT

Chronic Fatigue Syndrome and Bone Marrow Defects of the Jaw – A Case Report on Additional Dental X-Ray Diagnostics with Ultrasound

Johann Lechner
Fabian Schick

Clinic for Integrative Dentistry, Munich, Germany

Purpose: This paper aims to demonstrate the additional benefit of ultrasound in the diagnosis of chronic osteolysis and osteonecrosis (bone marrow defects) of the jaw shown in a clinical case report.

Patients and Methods: A case of chronic fatigue syndrome (CFS) in a young man presenting the typical, ambiguous symptoms, which were accompanied by headaches and tinnitus. X-ray techniques, namely panoramic radiographs (OPG) and cone beam computed tomography (DVT/CBCT), failed to produce any remarkable findings of bone marrow defects (BMDJ) in the jawbone. However, the measurement of bone density using trans-alveolar ultrasound (TAU) indicated a possible bone marrow defect in the lower left jawbone.

Results: Surgery was undertaken at the conspicuous area. Additional to softened, ischemic, fatty tissue, a black area was revealed, which was surprisingly subsequently identified as aspergillosis by histopathological analysis. In addition, the excessive local RANTES/CCL5 expression found in the affected area confirmed the necessity for surgical debridement and additional findings of TAU.

Conclusion: In contrast to radiography, complementary TAU imaging of the BMDJ revealed chronic inflammatory signaling RANTES/CCL5 pathways and fungal colonization. This case report supports the need for additional diagnostic techniques beyond radiographic modalities, which can help to elucidate the diagnostic composition and knowledge of the bone manifestations of systemic diseases.

Keywords: chronic fatigue syndrome, radiographic diagnostics, bone marrow defect, osteonecrosis, RANTES/CCL5, trans-alveolar ultrasonography

Introduction

With the increasing complexity of various systemic diseases, it is necessary to determine their underlying pathogenesis. Autonomic dysfunction with poorly defined multisystem disorders frequently presents a clinical challenge for medical practitioners.[1,2] In the absence of an identifiable cause, and given the insufficient research available on this increasingly common phenomenon, presentations of "idiopathic multimorbidity" are often assumed to be of psychogenic origin, and pharmacological interventions such as psychoactive medications are most commonly prescribed.[3,4] A case report from our clinic supports the need for expanded diagnostic techniques, which can help elucidate the pathogenesis associated with systemic dysregulation. A common dysregulation today is the Chronic Fatigue Syndrome, as in the case report presented here.

Correspondence: Johann Lechner
Clinic for Integrative Dentistry,
Gruenwalder Street 10A, Munich, 81547, Germany
Tel +49 89 697 0129
Fax +49 89 692 5830
Email drlechner@aol.com

Clinical Case

Here we describe a case of Chronic Fatigue Syndrome (CFS) in a young man presenting with typical, ambiguous symptoms that are characteristic of this syndrome and which were accompanied by headaches and tinnitus. Given the unclear etiology of this patient's presentation, we associated this case in our clinic with avascular, aseptic-osteolytic, and inflammatory bone marrow defects (BMDJ) in the jawbone, collectively referred to as "silent inflammation".[5] The patient, 28 years of age, had been suffering from CFS for approximately four years. His symptoms included dizziness, the inability to work, impaired concentration, and depression. Previous treatment approaches, which were primarily psychologically oriented, showed no significant improvement. As a last resort, it was recommended that interference fields caused due to teeth and jawbone be investigated. The patient thus sought treatment at our clinic. The patient provided his written informed consent to participate in this report and to have the case details and any accompanying images published. Institutional approval was not required to publish the case details. The patient was given clear information that not all additional examination methods and surgical techniques have been generally accepted scientifically to date.

Clinical Investigations and Findings

The patient received the expert diagnosis of CFS after immunological and serological examinations and accompanying psychological counseling. In addition to taking the patient's full medical history and bimanual palpation of the bilateral lymph nodes, the radiographic exam was performed to determine whether previously undetected inflammation was present. In addition to the radiographs, a newly developed trans-alveolar ultrasound (TAU) device was used.

Radiographic Findings with 2D-OPG and DVT/CBCT

A two-dimensional orthopantomogram (OPG) and digital volume tomogram (DVT) combined with cone beam computed tomography (CBCT) were performed to provide a panoramic image of the patient's mouth (DVT/CBCT). Conventional OPG failed to show any abnormal findings in the wisdom tooth and retromolar region at area 38/39 (left panel, Figure 1). With the use of DVT/CBCT, it is possible to depict the medullary structures in the area of a bone marrow defect in the jawbone (BMDJ) with greater reliability.[6] However, the sectional image of the patient's jaw obtained using DVT/CBCT (right panel, Figure 1) also failed to show any further resolution of the bony trabecular structures at area 38and retromolar area. Based on these radiographic findings, an inflammatory process in the jaw area would be ruled out, and, accordingly, maxillofacial surgery determined not to be required. Currently, magnetic resonance imaging (MRI) is the method of choice for assessing osteonecrosis, which was not available in this case.

Trans-Alveolar Ultrasound Bone Density Measurement

In an earlier publication,[7] we demonstrated the fundamental problem associated with the use of diagnostic radiography when attempting to identify osteonecrosis and inflammatory osteolysis in cancellous bone. To supplement potentially unreliable X-ray findings, we used a radiation-free method known as trans-alveolar ultrasound (TAU) measurement, which determines the bone density in the jaw.[8] TAU devices in dentistry and their usefulness to measure bone density were described earlier in the scientific literature.[9,10] TAU measurements are based on ultrasonic principles where sound is best conducted through solid material, more weakly in aqueous environments, and slowest through the air. When the measurement is obtained, the ultrasonic pulse is attenuated; solid structures are able to attenuate sound to a weaker degree than fatty or aqueous structures. In order to indicate both physical and structural changes, the TAU device creates digital (two- and three-dimensional) images with corresponding color coding (Figure 2). The TAU device consists of an ultrasonic transmitter that is placed on the skin over the specific tooth and jaw area to be measured. A receiver, which is the size of a thumbnail, is also placed intraorally over the specific dental area to be assessed. Interference-free acoustic coupling is achieved with a gel cushion that is placed intraorally and extra orally (Figure 3). Each dental area is measured individually. The receiver has 91 piezoelectric fields that register the trans-alveolar sound waves. These sound waves are converted into a colored pulse via a computer unit whereby sound waves of varying speeds are represented in different colors. The TAU monitor displays the various structures detected based on mineralization density using two- and three-dimensional graphic representations of bone density.[9–12]

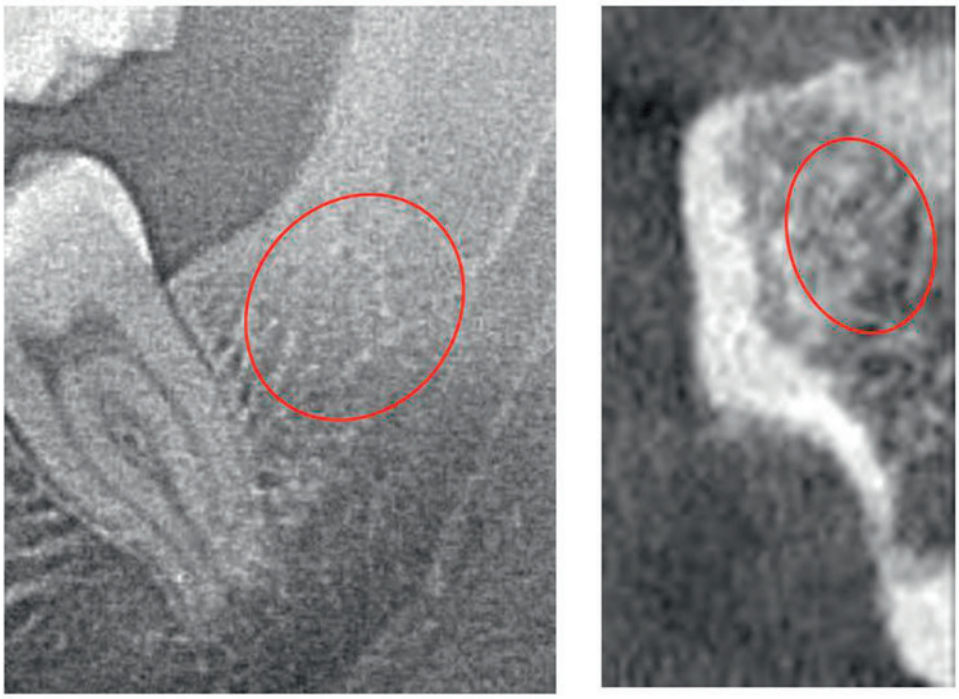

Figure 1 Panoramic radiograph OPG and sectional DVT/CBCT image.
Notes: Left panel: panoramic 2D-OPG image shows no abnormal findings at area 38 and retromolar area (39). Significance of the red circles: The red circles show the radiographically inconspicuous areas of the bone medulla, where OPG and DVT/CBCT failed to show any abnormal findings in the wisdom tooth and retromolar area. Right panel: sectional 3D-DVT image also shows no resolution of the bony trabecular structures at area 38/39.
Abbreviations: 2D-OPG, two-dimensional orthopantomogram; 3D-DVT, three-dimensional digital volume tomogram.

Surgical Repair of Area 38 and Retromolar Area

The findings of the TAU measurement performed on the patient indicated that there was a possible bone marrow defect (BMDJ) at area 38. As such, we decided to surgically debride area 38, extending beyond into so-called "area 39". Local anesthesia was administered from areas 37 to retromolar area 39, and, following this, a mucoperiosteal flap was created and folded down. The cortical bone of the jaw at area 38/39 was over-supplied with blood and removed at the retromolar area. With the intraosseous region now visible, the area was curetted (Figure 4), and the findings identified in the medullary cavity were surprising (Figure 5). Platelet-rich fibrin was applied to promote tissue healing.

Postoperative Diagnosis Following Oral Surgical Debridement of Left Lower Molar/Retromolar Area

Bone Marrow Defect Morphology

Throughout the entire medullary area spanning from region 38 to retromolar area 39, spongiose tissue had degenerated into fatty, ischemic tissue and did not indicate any healing tendencies. (Figure 3). This connective tissue was easily scooped out and collected as a sample. The left panel of Figure 5 shows a black mass that had formed along with typical fatty-degenerative, ischemic cancellous bone.

Histological Findings

The histopathological findings of the excised mass from area 38/39 was described as follows:

> Amorphous, nucleus-free substance, which showed fungal hyphae at the margin, and included hyphae that had recently started sprouting. This fungus may be Candida, but early-stage Aspergillus is also possible. Scar tissue with considerable cellular inflammation was present, whereby lymphocytes, plasma cells, and fibroblasts, as well as multinucleated giant cells of the foreign-body type and plenty of foam-cell macrophages, were identified. The extent of chronic inflammation, which was predominant, was quite considerable. An apparently devitalized bone fragment, with adipose tissue originating from the bone marrow cavity, also demonstrates chronic inactive inflammation, as well as colonization with small fungal spores.

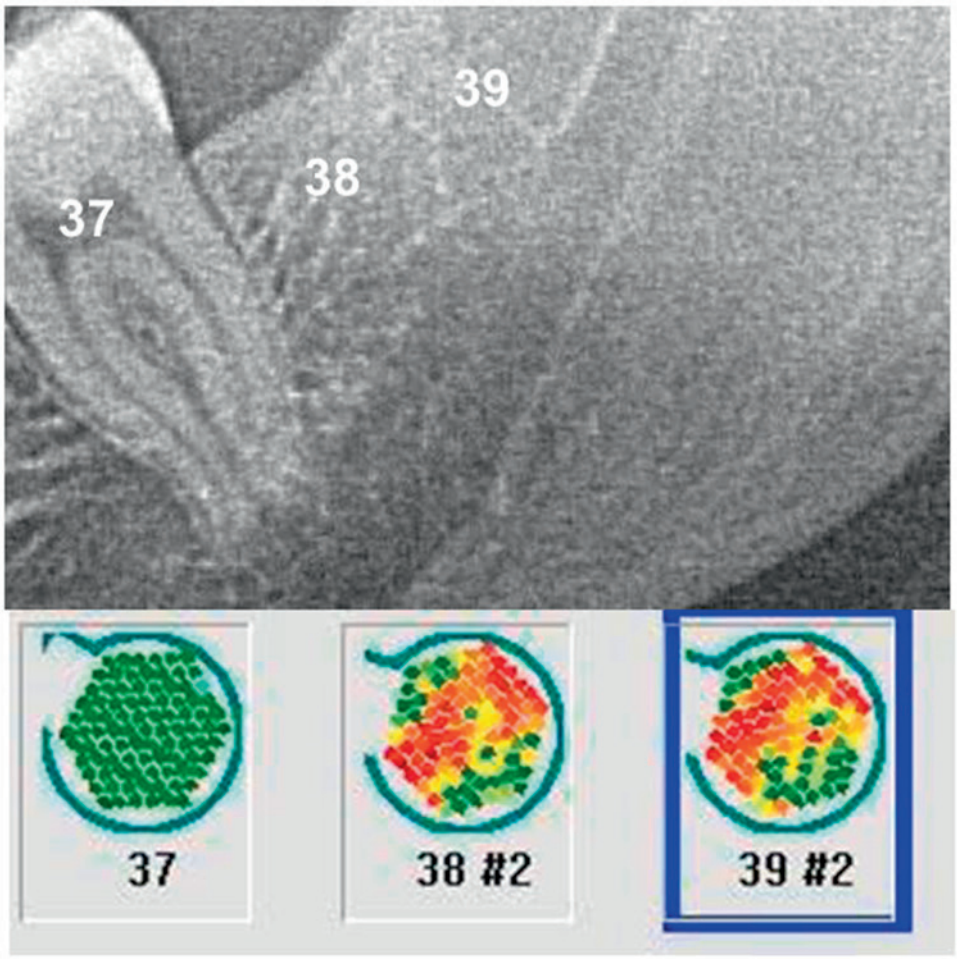

Figure 2 Comparison of panoramic radiograph (OPG) and TAU measurement which shows specific via green dense, inconspicuous structures) and red (low-density, conspicuous structures) resolution.

Notes: In contrast to the panoramic radiograph and DVT/CBCT images, the TAU measurements with respect to the edentulous retromolar area 38/39 clearly indicated the suspicion of osteolysis of the jaw This finding was a result of increased attenuation of the ultrasound beam due to fatty degeneration of the dense medullary cancellous bone. This may be compared to the finding for the area at healthy tooth 37 which showed a solid bone structure and bone density in green.

Abbreviations: OPG, two-dimensional panoramic radiograph; TAU, trans-alveolar ultrasound; DVT, three-dimensional digital volume tomogram; CBCT, cone beam computed tomography.

Local Hyperactivation of Immune Mediator Chemokine RANTES/CCL5 in the Osteolytic Jawbone

In the fatty tissue samples obtained from the softened region of the patient's jaw at area 38 and retromolar area 39, the multiplex analysis of the laboratory showed 6218 pg/mL of the proinflammatory chemokine RANTES/CCL5 (R/C), representing a nearly 40-fold overexpression; the normal finding for R/C in healthy medullary maxillary spongial bone is 149.9 pg/mL (average age, 51.4 years; range, 33–72 years; gender (female/male): 10/9) (Figure 6).[13,14] In a previous case report, we demonstrated the immunological connection between the local overexpression of R/C found in fatty degenerative osteonecrosis of the jawbone (FDOJ) and systemic disease.[15]

Discussion

Panoramic Radiograph and DVT/CBCT

Previous radiographs of the jaw failed to yield any remarkable findings in the patient (Figure 1). This is in coincidence with our hypothesis that the most common dental diagnostic tool, the panoramic radiograph OPG, is unsuitable for detecting BMDJ/FDOJ. This problem of radiographic imaging contributes to the widespread misjudgment of BMDJ/FDOJ as pathological and - via chronic local R/C overexpression - pathogenetic structural changes of the jawbone.[6,11] The DVT/CBCT performed in this case also failed to indicate the presence of intraosseous pathology (Figure 1).

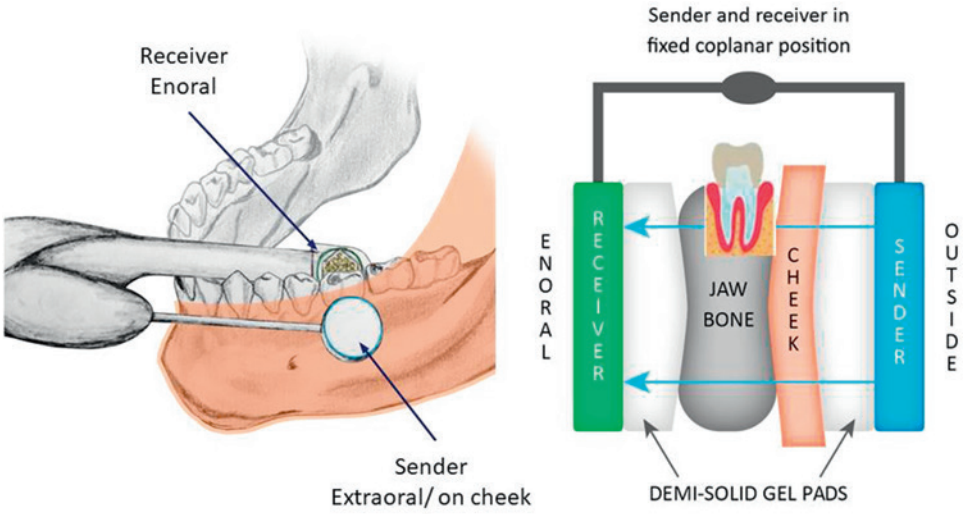

Figure 3 TAU measurement of jawbone density using a TAU device.
Note: Individual adjustments of the measuring unit are made in response to different jaw conditions by means of specially designed gel cushions.[11]
Abbreviation: TAU, trans-alveolar ultrasound.

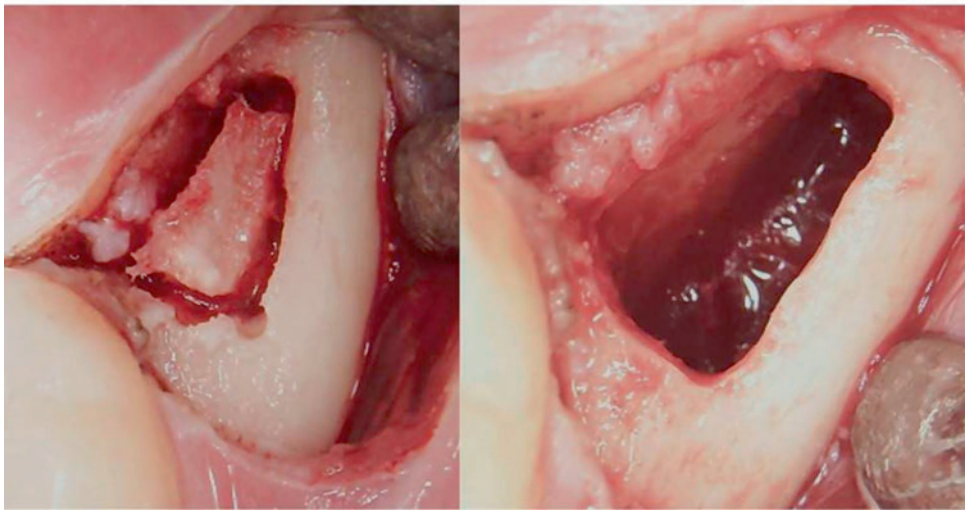

Figure 4 Surgical procedure for a retromolar BMDJ/FDOJ.
Notes: Left panel: after folding down the mucoperiosteal flap, a bone window was formed in the cortex. Right panel: curetted medullary cavity.
Abbreviations: BMDJ, bone marrow defect in jawbone; FDOJ, fatty degenerative osteonecrosis of the jawbone.

TAU Measurement of Bone Density

In contrast to the inconspicuous X-ray images of the patient's jaw, the TAU measurements showed extensive areas of softened and necrotic cancellous bone, often referred to as "cavitations." As in this case, cavitations may often be completely asymptomatic. In our efforts to close the diagnostic gap due to the limitations associated with standard X-ray methods, the application of TAU may be considered a major step forward in the detection of BMDJ/FDOJ.

RANTES/CCL5

With the analysis of RANTES expression in morphologically and histologically conspicuous jawbone samples, we are entering new territory.[13–15] Chemokine RANTES/CCL5 (R/C) is a recognized inflammatory agent in medical research. The progression of chronic inflammatory diseases is often hidden beneath the surface as a result of an immune system that is chronically activated by excess cytokines. These chemokines also stimulate other signaling pathways, the expression of which we have identified

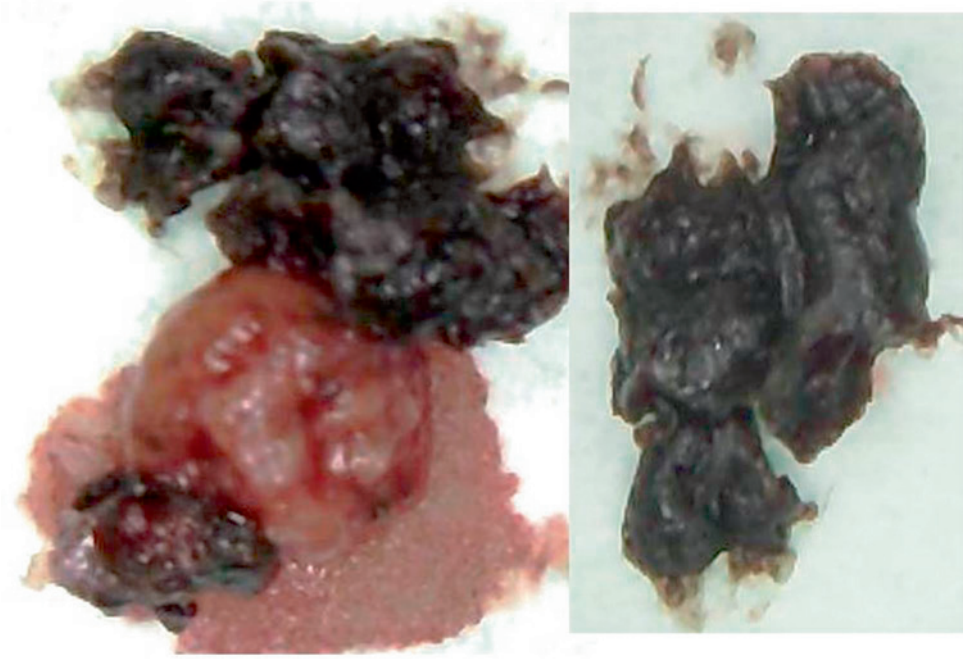

Figure 5 Aspergilloma removed from the cancellous medullary cavity in edentulous jaw area 38/39.
Note: Within the cancellous medullary cavity in the edentulous jaw area 38/39, an aspergilloma ("fungal ball") formed a large, spherical colony of mold together with a fungal network that also contained a mixture of inflammatory cells (see the "Histological Findings" section).

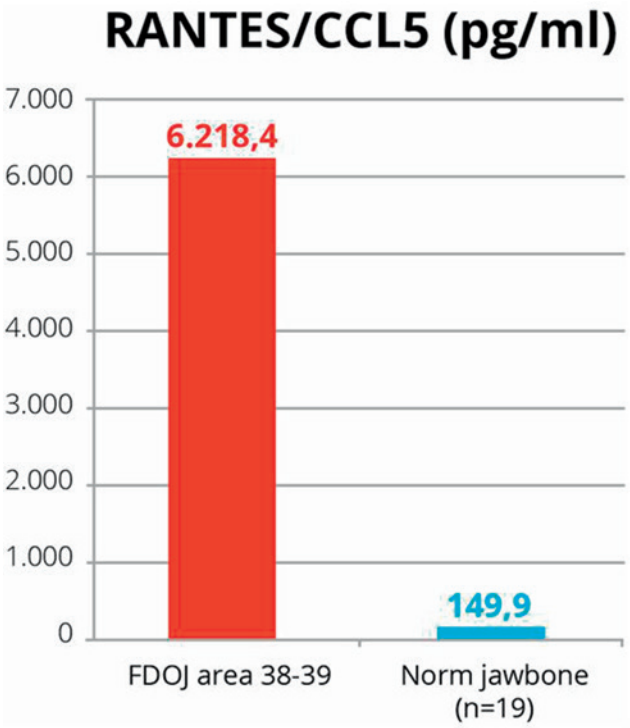

Figure 6 RANTES/CCL5 expression levels in BMDJ/FDOJ and normal jawbone areas.
Notes: The red column corresponds to the local RANTES/CCL5 expression (in pg/mL) found in BMDJ/FDOJ area 38/39. The blue column corresponds to the RANTES/CCL5 expression (in pg/mL) found in healthy cancellous bone.
Abbreviations: BMDJ, bone marrow defect in jawbone; FDOJ, fatty degenerative osteonecrosis of the jawbone.

in BMDJ/FDOJ,[13–15] including in the specific case presented here.[16] The striking result arising from the multiplex analysis of the BMDJ/FDOJ area indicated the marked elevation of the chemokine R/C.

Since there is little known about the direct clinical relationship between R/C signaling pathways detected in BMDJ/FDOJ and an organic-specific or systemic disease, the increased R/C level found in BMDJ/FDOJ may provide insights into possible causal pathways.[14,17] As in this case of CFS, for which the etiology is unclear, the possibility of BMDJ/FDOJ involvement was raised even though the patient did not present with obvious signs or symptoms, as numerous scientific publications demonstrate a relationship between R/C and central nervous system disorders.[18,19]

Fungal Toxins

This case of morphologically and histologically confirmed aspergilloma that was found broadens the discussion concerning causal pathways to include fungal toxins and their relationship to cases of CFS. Aspergillus is known to produce toxic compounds called mycotoxins, primarily aflatoxin and gliotoxins. These mycotoxins, which are formed by pathogenic Aspergillus, may contribute to the development of potentially serious and difficult-to-detect

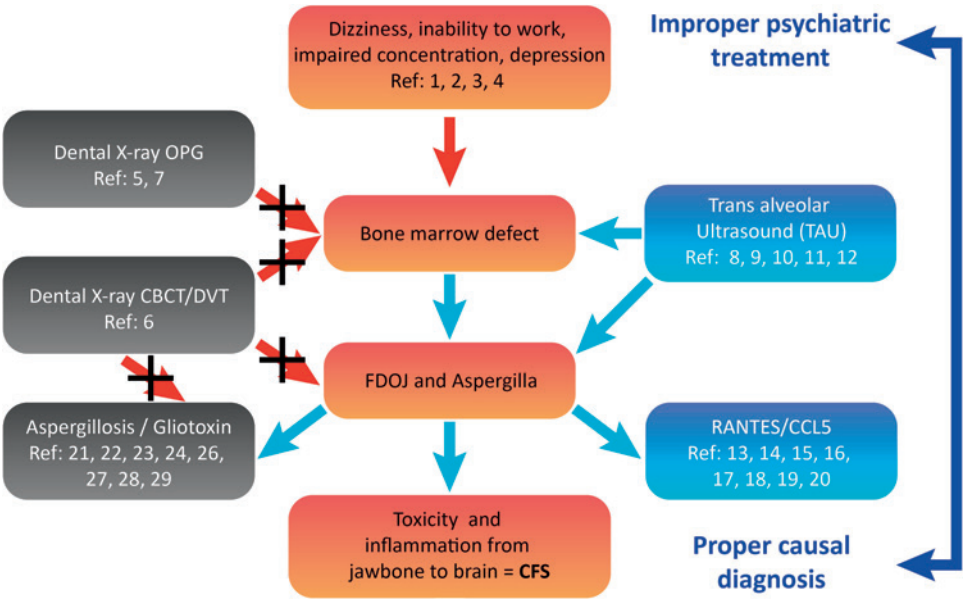

Figure 7 Case report overview including corresponding references.
Notes: Top: at the top of the graph are the disorders of the patient's state of mind that have so far been treated by unsuccessful psychotherapy. Left row: both OPG and CBCT/DVT do not lead to the detection of the bone marrow defect (center) and the FDOJ area (center, red arrows). In contrast, additional TAU examination leads to the detection of these bone marrow defects (right row, blue arrows). Postoperatively, the chronically overexpressed proinflammatory RANTES/CCL5 signaling pathways and aspergillosis can now be diagnosed in the bone marrow defects (blue arrows). Bottom: for the patient's CFS, this enables aproper causal diagnosis via the link of toxicity and inflammation from jawbone to brain.
Abbreviations: OPG, orthopantomogram; TAU, trans-alveolar ultrasound; DVT, digital volume tomogram; CBCT, cone beam computed tomography; FDOJ, fatty degenerative osteonecrosis of the jaw; CFS, chronic fatigue syndrome.

diseases. Aflatoxins have acute hepatotoxic effects at concentrations of ~10 µg/kg of body weight, but are carcinogenic at even lower concentrations and particularly when exposed to repeatedly.[20,21] In the case described, had the aspergillosis not been eliminated, the fungal toxins may have penetrated further into other tissues, involving one or more organs beyond the affected area of the jawbone.

Gliotoxin is a toxic agent that is produced by pathogenic yeasts and fungi. This compound is an active sulfur reagent of fat-soluble thiol alcohol and is an antiphagocytic and immunomodulating substance.[22,23] The structure of gliotoxin is decisive for toxicological analysis: gliotoxin reacts with a sulfhydryl group on active enzyme proteins and deactivates the enzyme. This also applies to the mitochondrial enzymes in the respiratory chain.[24,25] Due to this affinity for binding, there are intensive biochemical and medically relevant interactions of gliotoxin: Gliotoxin suppresses the immune system,[26] thereby causing DNA damage.[27] Gliotoxin also causes oxidative damage to the plasmid and cellular DNA.[28] As an immunomodulating substance, gliotoxin causes genomic DNA fragmentation.[28]

Summary

In this case report, the cause of the patient's systemic symptoms appears to be caused by possible irritations of the central nervous system due to R/C overexpression.[16,18,19] The problem associated with BMDJ/FDOJ begins when local, acute inflammation present in the jaw at the initial stage of the wound healing process transitions to a sub-chronic stage. The osteolytic BMDJ/FDOJ area in association with chemokine R/C overexpression may induce numerous unspecific symptoms and diseases.[18,19] At the same time, the mycotoxins formed in the medullary cavity of the jawbone may strongly contribute to the onset and maintenance of a chronic inflammatory condition that may favor the CFS (Figure 7). The histologically confirmed findings in area 38 and retromolar area of the patient's jaw indicate that the innate capacity for wound healing, without prior surgical debridement, was significantly impaired, which not only lead to an R/C overexpression in this case but also, in this case to a highly toxic fungal contamination.

Conclusion

The clinical examination and radiographic imaging performed by our team demonstrated that, X-ray diagnostics alone would not have identified a potential contributing cause of the patient's health condition. Neither OPG nor DVT/CBCT detected any lesions that would have provided a medical indication that necessitated oral surgical intervention. It is only with the additional TAU diagnostic methods that we were able to verify the previously undiscovered phenomenon of BMDJ/FDOJ preoperatively by imaging and postoperatively by histopathological investigations. Without complementary TAU measurement indicating possible medullary osteolysis in the distal and retromolar jaw (area 38/39), neither the chronic inflammatory signaling pathways (as identified via R/C expression) nor the extensive fungal colonization found in this area of the patient's jaw would have been recognized or eliminated. It is recommended that the results presented herein are used to guide further research, in particular, the demonstrated measuring of inflammatory cytokines found in bone tissue and visualize diminished bone density in bone marrow defects by TAU. The limitation of TAU lies in not displaying a detailed picture of bone structures but of only measuring bone density. Our findings in this case report of chronic fatigue syndrome clearly demonstrates the strong need of further examinations of BMDJ/FDOJ.

Acknowledgments

English-language editing of this manuscript was provided by Natasha Gabriel.

Disclosure

CaviTAU® (Munich, Germany), the company that designed the new TAU apparatus and associated software, provided this equipment without charge for the purposes of this report. The ultrasonography procedure was carried out at the Clinic for Integrative Dentistry (Munich, Germany). CaviTAU® and the Clinic for Integrative Dentistry are engaged in ongoing discussions to further improve and verify the new TAU apparatus, CaviTAU®, as it is introduced to the market. The author is the holder of a patent PTC/EP2018/084199 used in the CaviTAU®. The authors report no other conflicts of interest in this work.

References

1. Hawkes N. Better training is needed to deal with increasing multimorbidity. *BMJ*. 2012;344:e3336. doi:10.1136/bmj.e3336
2. Barnett K, Mercer SW, Norbury M, Watt G, Wyke S, Guthrie B. Epidemiology of multimorbidity and implications for health care, research, and medical education: a cross-sectional report. *Lancet*. 2012;380(9836):37–43. doi:10.1016/S0140-6736(12)60240-2
3. Smith SM, Soubhi H, Fortin M, Hudon C, O'Dowd T. Interventions for improving outcomes in patients with multimorbidity in primary care and community settings. *Cochrane Database Syst Rev*. 2012;4: CD006560.
4. Jakovljevic M, Reiner Z, Milicic D, Crncevic Z. Comorbidity, multimorbidity and personalized psychosomatic medicine: epigenetics rolling on the horizon. *Psychiatr Danub*. 2010;22(2):184–189.
5. Lechner J, Schuett S, von Baehr V. Aseptic-avascular osteonecrosis: local "silent inflammation" in the jawbone and RANTES/CCL5 overexpression. *Clin Cosmet Investig Dent*. 2017;9:99–109. doi:10.2147/CCIDE.S149545
6. Guerrero M, Jacobs R, Loubele M, Schutyser F, Suetens P, van Steenberghe D. State-of-the-art on cone-beam CT imaging for preoperative planning of implant placement. *Clin Oral Investig*. 2006;10:1–7. doi:10.1007/s00784-005-0031-2
7. Lechner J. Validation of dental X-ray by cytokine RANTES – comparison of X-ray findings with cytokine overexpression in jawbone. *Clin Cosmet Investig Dent*. 2014;6:71–79. doi:10.2147/CCIDE.S69807
8. Bouquot J, Martin W, Wrobleski G. Computer-based thru-transmission sonography (CTS) imaging of ischemic osteonecrosis of the jaws - a preliminary investigation of 6 cadaver jaws and 15 pain patients. *Oral Surg Oral Med Oral Pathol Oral Radiol Endod*. 2001;92:550.
9. Al-Nawas B, Grotz KA, Kann P. Ultrasound transmission velocity of the irradiated jaw bone in vivo. *Clin Oral Invest*. 2001;5(4):266–268. doi:10.1007/s00784-001-0133-4
10. Klein MO, Grotz KA, Manefeld B, Kann PH, Al-Nawas B. Ultrasound transmission velocity for non-invasive evaluation of jaw bone quality in vivo prior to dental implantation. *Ultrasound Med Biol*. 2008;34:1966–1971. doi:10.1016/j.ultrasmedbio.2008.04.016
11. Lechner J, Zimmermann B, Schmidt M, von Baehr V. Ultrasound sonography to detect focal osteoporotic jawbone marrow defects: clinical comparative report with corresponding Hounsfield units and RANTES/CCL5 expression. *Clin Cosmet Investig Dent*. 2020;12:205–216. doi:10.2147/CCIDE.S247345
12. Lechner J, von Baehr V, Zimmermann B. Osteonecrosis of the jaw beyond bisphosphonates: are there any unknown local risk factors? *Clin Cosmet Investig Dent*. 2021;13:21–37. doi:10.2147/CCIDE.S288603
13. Lechner J, Mayer W. Immune messengers in neuralgia inducing cavitational osteonecrosis (NICO) in jaw bone and systemic interference. *Eur J of Integrative Med*. 2010;2:71–77. doi:10.1016/j.eujim.2010.03.004
14. Lechner J, von Baehr V. RANTES and fibroblast growth factor 2 in jawbone cavitations: triggers for systemic disease? *Int J Gen Med*. 2013;6:277–290. doi:10.2147/IJGM.S43852
15. Lechner J, von Baehr V. Hyperactivated signaling pathways of chemokine RANTES/CCL5 in osteopathies of jawbone in breast cancer patients—case report and research. *Breast Cancer (Auckl)*. 2014;8:89–96. doi:10.4137/BCBCR.S15119
16. Lechner J, Huesker K, von Baehr V. Impact of RANTES from jawbone on chronic fatigue syndrome. *J Biol Regul Homeost Agents*. 2017;31(2):321–327.
17. Lechner J, von Baehr V. Chemokine RANTES/CCL5 as an unknown link between wound healing in the jawbone and systemic disease: is prediction and tailored treatments in the horizon? *EPMA J*. 2015;6(1):10. doi:10.1186/s13167-015-0032-4
18. Bolin LM, Murray R, Lukacs NW, et al. Primary sensory neurons migrate in response to the chemokine RANTES. *J Neuroimmunol*. 1998;81(1–2):49–57. doi:10.1016/S0165-5728(97)00158-6
19. Luo Y, Berman MA, Zhai Q, et al. RANTES stimulates inflammatory cascades and receptor modulation in murine astrocytes. *Glia*. 2002;39(1):19–30. doi:10.1002/glia.10079

20. Frisvad JC, Thrane U, Samson RA, Pitt JI. Important mycotoxins and the fungi which produce them. *Adv Exp Med Biol*. 2006;571:3–31.
21. Yamada A, Kataoka T, Nagai K. The fungal metabolite gliotoxin: immunosuppressive activity on CTL-mediated cytotoxicity. *Immunol Lett*. 2000;71(1):27–32. doi:10.1016/S0165-2478(99)00155-8
22. Shah DT, Jackman S, Engle J, Larsen B. Effect of gliotoxin on human polymorphonuclear neutrophils. *Infect Dis Obstet Gynecol*. 1998;6(4):168–175. doi:10.1155/S1064744998000349
23. Sutton P, Warig P, Mullbacher A. Exacerbation of invasive aspergillosis by the immunosuppressive fungal metabolite, gliotoxin. *Immunol Cell Biol*. 1996;74(4):318–322. doi:10.1038/icb.1996.57
24. Sutton P, Newcombe NR, Waring P, Mullbacher A. In vivo immunosuppressive activity of gliotoxin, a metabolite produced by human pathogenic fungi. *Infect Immun*. 1994;62(4):1192–1198. doi:10.1128/IAI.62.4.1192-1198.1994
25. Eichner RD, Al Salami M, Wood PR, Mullbacher A. The effect of gliotoxin upon macrophage function. *Int J Immunopharmacol*. 1986;8(7):789–797. doi:10.1016/0192-0561(86)90016-0
26. Mullbacher A, Eichner RD. Immunosuppression in vitro by a metabolite of a human pathogenic fungus. *Proc Natl Acad Sci U S A*. 1984;81(12):3835–3837. doi:10.1073/pnas.81.12.3835
27. Wang JS, Groopman JD. DNA damage by mycotoxins. *Mutat Res*. 1999;424(1–2):167–181. doi:10.1016/S0027-5107(99)00017-2
28. Zhou X, Zhao A, Going G, Hirszel P. Gliotoxin-induced cytotoxicity proceeds via apoptosis and is mediated by caspases and reactive oxygen species in LLC-PK1 cells. *Toxicol Sci*. 2000;54(1):194–202. doi:10.1093/toxsci/54.1.194